University of Alberta
Department of Civil Engineering

Structural Engineering Report No. 144

COMBINED FLEXURE AND TORSION OF I-SHAPED STEEL BEAMS

by

Robert G. Driver

and

D.J. Laurie Kennedy

March 1987

Structural Engineering Report 144

COMBINED FLEXURE AND TORSION OF I-SHAPED STEEL BEAMS

by

Robert G. Driver

and

D.J. Laurie Kennedy

Department of Civil Engineering

University of Alberta

Edmonton, Alberta

March 1987

ABSTRACT

Little analytical and experimental work on combined flexure and torsion of I-shaped steel beams in the inelastic region has been done. In particular, a comprehensive method for determining the ultimate capacity, as is required in limit states design standards, is not available.

Four tests were conducted on class 1 cantilever beams with varying loading eccentricities. It was established that the torsional behaviour has two distinct phases, with the second dominated by second order geometric effects. This second phase is non-utilizable because the added torsional restraint developed is load path dependent and if lateral deflections had been prevented, would not have been significant. Based on first phase behaviour, a normal and shearing stress distribution on the cross-section has been proposed for resisting flexural and torsional loads. From this, a moment-torque ultimate strength interaction diagram is developed applicable to a number of different end and loading conditions. This ultimate limit state interaction diagram and a serviceability limit state based on first yield provide a comprehensive design approach for these members.

ACKNOWLEDGEMENTS

This research was completed under the supervision of Dr. D.J.L. Kennedy. His helpful guidance and generous allocation of time to the project are greatly appreciated.

I would also like to acknowledge the technical assistance of L. Burden and R. Helfrich while conducting the experimental program. Summer students R. Selby and G. Mah, working under the direction of Dr. Kennedy, were also of great help.

Finally, I wish to thank M. Schmidt for cheerfully, patiently, and willingly typing a seemingly endless string of revisions and updates.

Funding for this research was provided by the Natural Sciences and Engineering Research Council in the form of a postgraduate scholarship and research grant 5833, through Dr. Kennedy.

Table of Contents

List of Tables

List of Figures

List of Symbols

a = length along beam in which warping restraint is effectively dissipated = $\sqrt{EC_w/GJ}$

b = width of flange

b_1 = length of rectangular element

B = flange bi-moment

B_p = plastic flange bi-moment

C_w = warping torsional constant = $I_y(d-t)^2/4$

d = overall depth of beam

e = eccentricity

E = modulus of elasticity

E_{st} = strain hardening modulus

G = shear modulus of elasticity

h = distance between flange centroids = $d-t$

I_y = moment of inertia about weak axis

J = St. Venant torsional constant

K = warping factor ($T_{wp}=Kb^2t(d-t)\sigma_y/L$)

L = length of beam

M = bending moment

M_f = lateral flange moment, factored bending moment

M_{fp} = plastic lateral flange moment

M_p = plastic bending moment

M_{pf} = plastic bending moment (flanges only)

M_{pw} = plastic bending moment (web only)

M_r = lateral torsional buckling moment resistance

M_y = yield bending moment

M_{yw} = yield bending moment (web only)

P = vertical load

S = flexural section modulus

S_w = warping statical moment = $b^2h/16$

t = thickness of flange

t_ℓ = peak torsional moment intensity (linearly varying torque)

t_{max} = thickness of thickest rectangular element

t_u = torsional moment intensity (uniformly distributed torque)

t_1 = thickness of rectangular element

T = torsional moment

T_f = factored torsional moment

T_p = total plastic torsional moment

T_{sh} = sand heap torsional moment

T_{shu} = ultimate sand heap torsional moment

T_{sv} = St. Venant torsional moment

T_u = total ultimate torsional moment

T_w = warping torsional moment

T_{wp} = plastic warping torsional moment

T_{wu} = ultimate warping torsional moment

T_{wy} = yield warping torsional moment

T_y = total torsional moment that causes first yield

u,v,w = displacements in x,y,z directions

V = coefficient of variation

V_f = lateral flange shear

w = width of web

W_n = normalized unit warping of cross-section = $bh/4$

x,y,z = co-ordinate axes

$\bar{x}$ = statistical mean

z = distance along longitudinal axis

Z = plastic section modulus

Z_{sh} = sand heap modulus

Z_w = plastic warping modulus

a = ratio of normal yield stress to shear yield stress ($a=\sqrt{3}$ for von Mises-Hencky yield criterion)

ϵ_f = strain at fracture

ϵ_{st} = strain at onset of strain hardening

ϵ_y = yield strain

σ_u = ultimate stress

σ_w = normal stress due to warping torsion

σ_y = yield stress

σ_{ys} = static yield stress

σ_{yu} = upper yield stress

τ_{sv} = shear stress due to St. Venant torsion

τ_w = shear stress due to warping torsion

τ_y = shear yield stress

ϕ = angle of rotation of beam, resistance factor

ϕ' = first derivative of angle ϕ

ϕ'' = second derivative of angle ϕ

ϕ''' = third derivative of angle ϕ

1. INTRODUCTION

1.1 General

I-shaped steel beams are widely used as structural elements because of their efficiency in flexure about the strong axis. They may also be subjected to torsional loads when the loads are applied eccentrically. Whenever the line of action of a load does not pass through the shear centre of the beam, a torque results.

CSA Standard CAN3-S16.1-M84 (CSA, 1984) requires that beams subjected to torsion be designed for strength to satisfy Section 15.11.1, which reads:

> "Beams and girders subjected to torsion shall have sufficient strength and rigidity to resist the torsional moment and forces in addition to other moment or forces. The connections and bracing of such members shall be adequate to transfer the reactions to the supports."

The designer must decide how this requirement is to be met.

Other codes, such as British Standard 5950 (BSI, 1985) and the American Institute of Steel Construction specification (AISC, 1978), do not give provisions for torsional design. Therefore, a need exists for more detailed requirements in the design of steel members for eccentric loading.

1.2 Objectives and Scope

The objective of this research was to develop a simple limit states procedure for the design of I-shaped beams subjected to both flexural and torsional loading. The procedure was to encompass all commonly occurring sets of flexural and torsional end conditions consisting of pinned-pinned, fixed-fixed, pinned-fixed, and fixed-free, and deal with both concentrated and uniformly distributed loads. Procedures for other conditions could be developed similarly. In addition, as a practical design approach, a limiting eccentricity below which torsional effects could be considered insignificant was to be defined quantitatively.

The design method is substantiated by tests conducted as part of this study and by other researchers. All test data are limited to class 1 beams. These sections have width-thickness ratios such that local buckling is precluded before the fully plastic moment is reached and sufficient hinge rotation has occurred to develop a plastic mechanism. The effects of manufacturing tolerances, such as initial out-of-straightness, have not been considered.

While attention is focused primarily on ultimate strength considerations, serviceability criteria have also been examined.

2. LITERATURE REVIEW

2.1 General

Almost all the literature describing the behaviour of beams subjected to combined flexural and torsional loads deals with elastic behaviour only. No simple, functional approach with a solid theoretical basis has been presented that takes into account inelastic behaviour and attempts to predict ultimate member strength.

Many researchers make an effort to simplify the problem by the use of approximate equations or a series of tables or graphs. These methods, although vastly simpler to use than closed form solutions, may remain cumbersome and often neglect aspects of the behaviour that could affect a sound design. Even with compensating design factors, most methods do not take into account the interaction of the two loading mechanisms.

2.2 Elastic Torsion Theory

Present day torsion theory is based on the classical approach developed by the French engineer Adhémar Jean Barré de Saint-Venant (1797-1886) and presented to the French Academy of Sciences in 1853 (Salmon and Johnson, 1980). Perhaps St. Venant's most significant contribution, from a structural engineering point of view, was the observation that prismatic beams of non-circular cross-section have a tendency to warp when subjected to torsional loads as shown

in Fig. 2.1. Previously, the simplifying assumption was made that the cross-section of a beam remains plane after a rotational deformation, as was proposed by Jakob Bernoulli (1654-1705) in the development of the elementary bending theory (Hamilton, 1952) and as was extended to torsion theory by Louis Marie Henri Navier (1785-1836) (Westergaard, 1964). Inherent in St. Venant's realization of the significance of warping is the observation that any form of warping restraint induces longitudinal normal stresses in the cross-section of the beam. The normal stresses are negligible in beams with rectangular or elliptical cross-sections but can be appreciable in I-shaped beams (Ugural and Fenster, 1979).

When a torque is applied to an I-shaped beam causing a rotation, ϕ (Fig. 2.2), the beam resists the load by two distinct mechanisms. The first is St. Venant or pure torsion. This mechanism induces shear stresses that are distributed over the cross-section as shown in Fig. 2.3. In 1903, Ludwig Prandtl showed that these stresses could be determined by using the membrane or soap film analogy (Timoshenko, 1983). This analogy states that an elastic membrane, placed over an opening with the same shape as the cross-section of a beam and subjected to uniform pressure, deforms in such a way that the slope of the membrane is proportional to the shear stress that would be present at that point when the beam is subjected to a torsional load. Also, the total St. Venant torque that can be carried by the

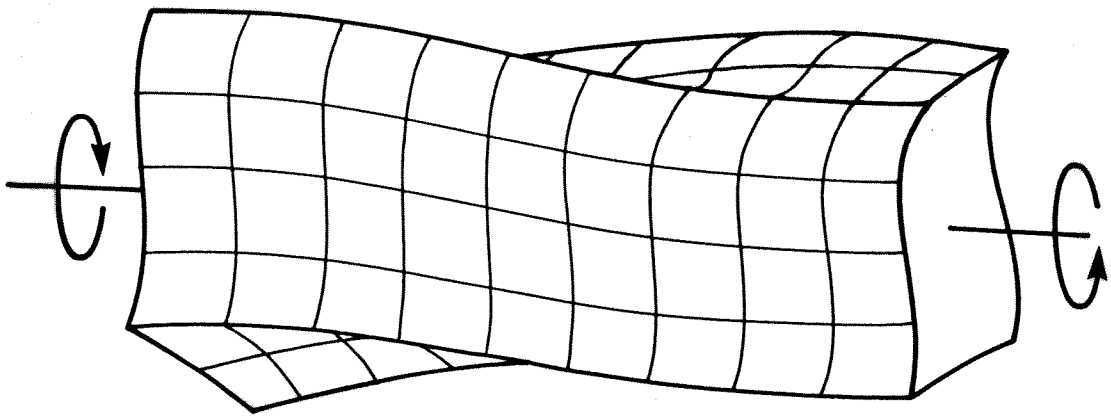

Figure 2.1 Warping of member with non-circular cross-section (after Ugural and Fenster, 1979)

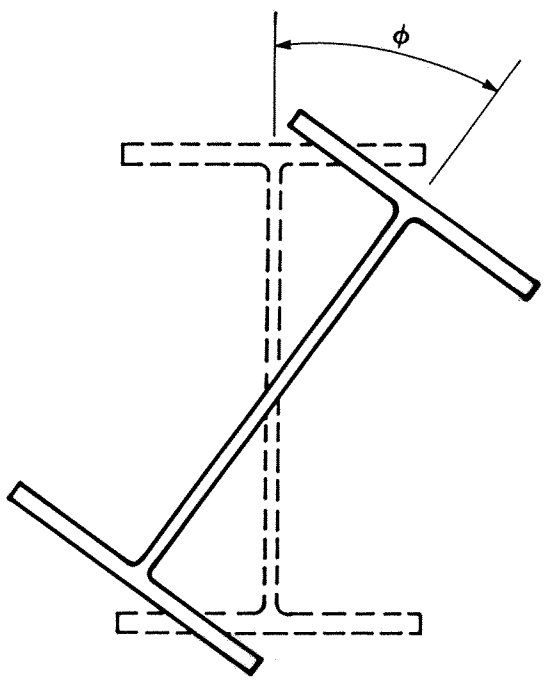

Figure 2.2 Rotation of I-shaped cross-section

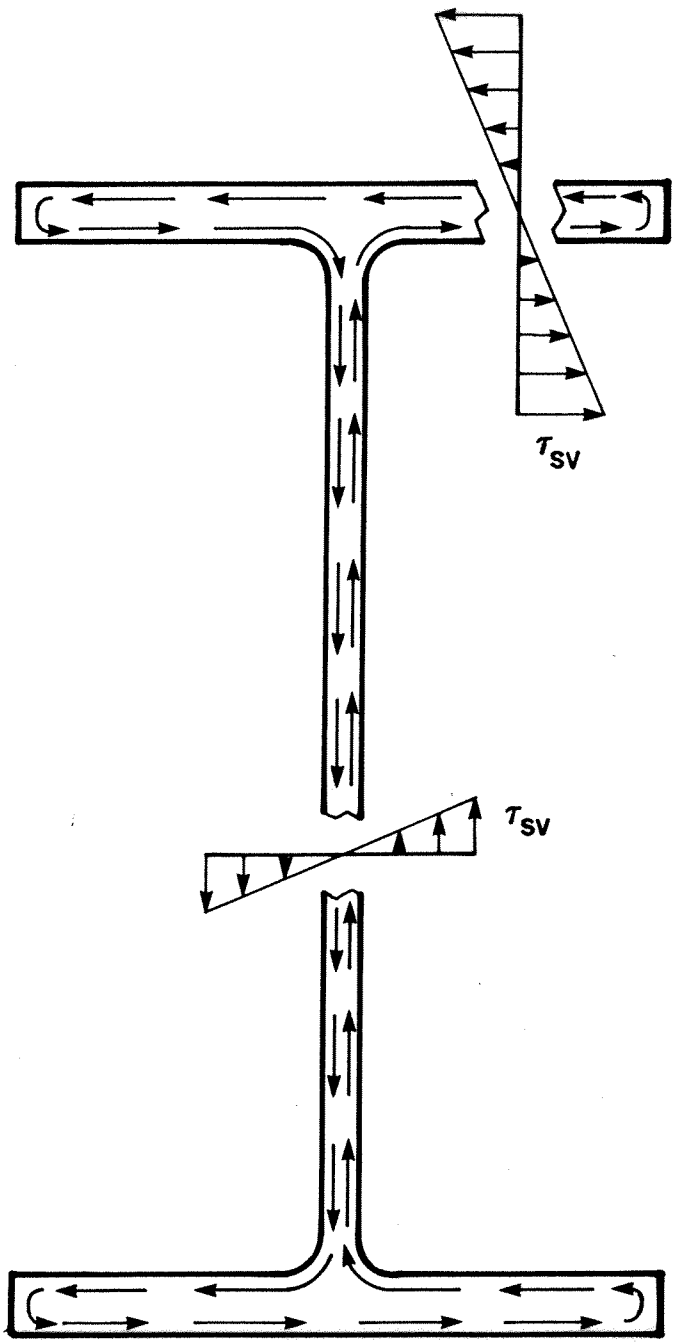

Figure 2.3 St. Venant shear stress distribution

(after Heins and Seaburg, 1963)

cross-section is proportional to the volume under the elastic membrane. It can be shown (e.g. Galambos, 1968; Heins, 1975; Trahair, 1977) that for an open cross-section made up of rectangles, the maximum shear stress due to St. Venant torsion can be expressed as

[2.1] $$\tau_{sv} = Gt_{max}\phi'$$

The total St. Venant torsional resistance is

[2.2] $$T_{sv} = GJ\phi'$$

Salmon and Johnson (1980) indicate that J can be closely approximated by

[2.3] $$J = \sum_{1}^{n} \frac{1}{3} b_1 t_1^3$$

where n is the number of rectangular elements. St. Venant originally provided a reduction term in the expression for J to account for end effects (Lyse and Johnston, 1936) but this correction is small and is partially offset by the increased resistance due to the fillets at the web-flange junctions (Seely and Putnam, 1936). Other authors, such as Goldberg (1953) and Darwish and Johnston (1965), suggest the use of stress concentration factors to account for the fact that the stresses are higher at internal corners.

The second mechanism by which torsional loads are resisted in I-shaped beams is warping torsion. As a torque is applied, the flanges can be visualized as rectangular beams being deformed laterally in flexure as seen in the plan view of Fig. 2.4. The shears that develop as the flanges are being bent in opposite directions create an internal couple that resists the applied torque (Fig. 2.5). The lateral bending produces tensile and compressive normal stresses in the flanges as shown in Fig. 2.6. Shear stresses in the web and vertical shear stresses in the flanges do exist as a product of warping restraint, but are small and may be neglected (Goldberg, 1953).

The value of the warping shear and normal stresses in the flanges can be calculated as (Heins, 1975)

[2.4] $$\tau_w = -ES_w\phi'''$$

[2.5] $$\sigma_w = -EW_n\phi''$$

The total warping torsional resistance is

[2.6] $$T_w = -EC_w\phi'''$$

Equations [2.2] and [2.6] give the contributions to torsional resistance of the St. Venant and warping components, respectively. Therefore, the overall differential equation describing the resisting torque is

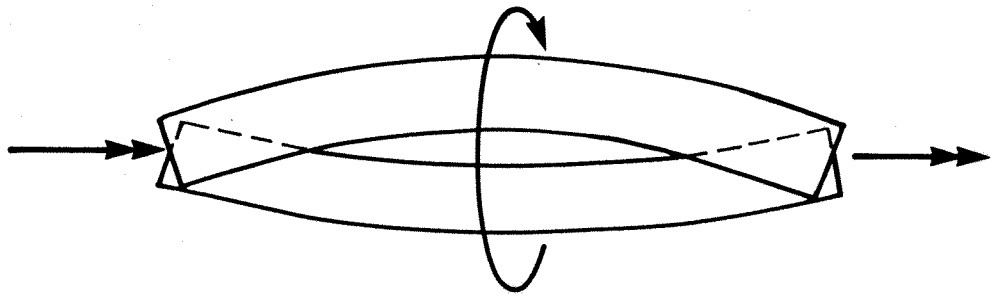

Figure 2.4 Warping of flanges

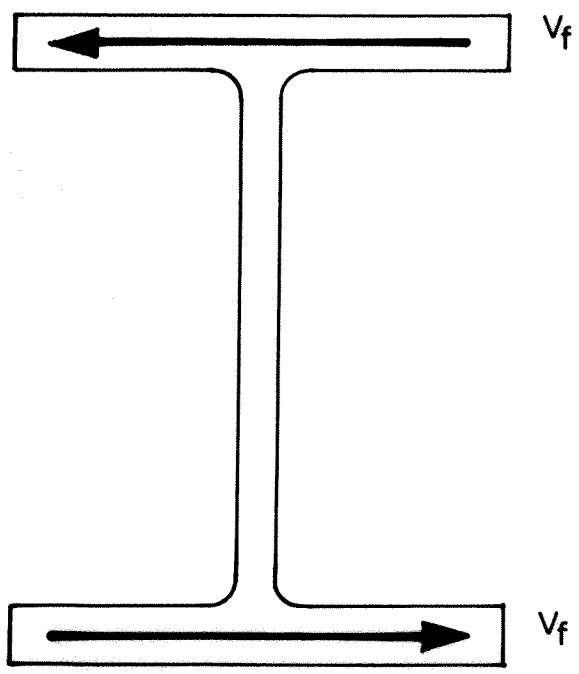

Figure 2.5 Flange shears in I-shaped beams

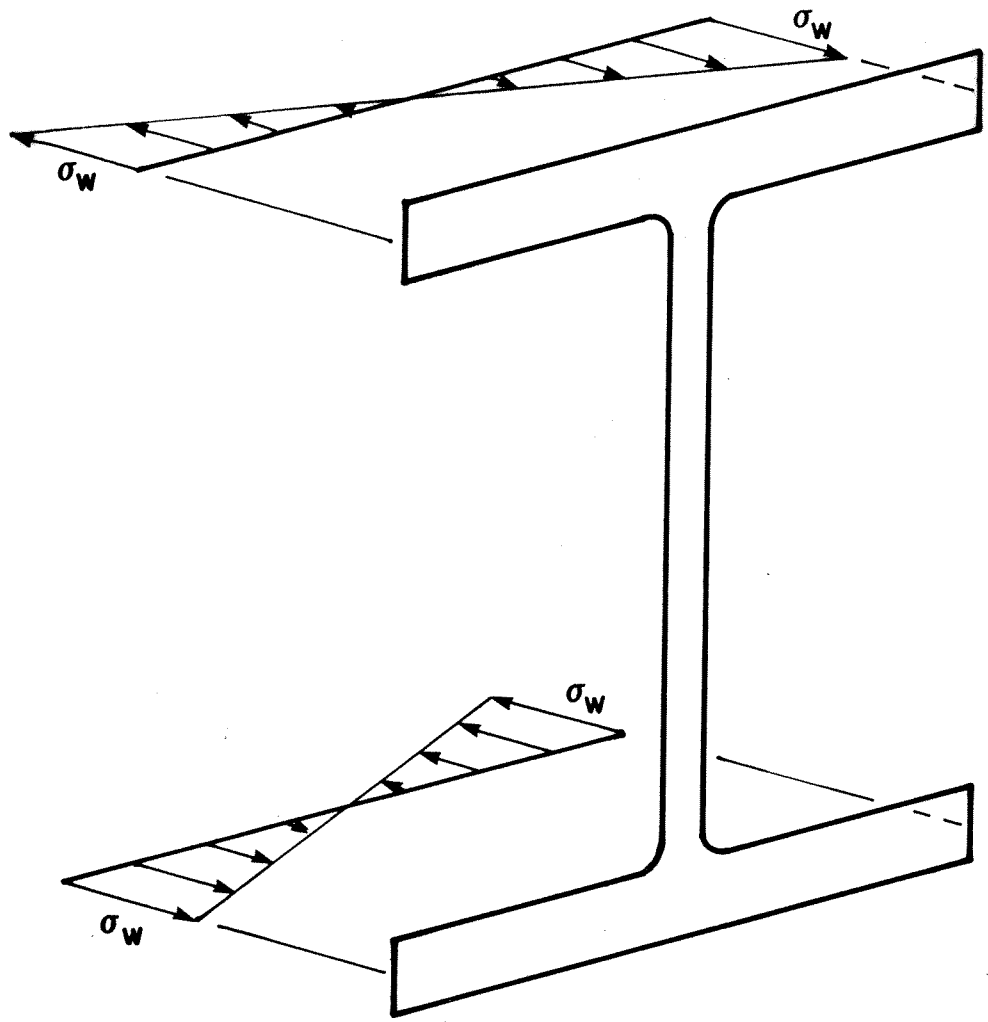

Figure 2.6 Lateral bending stresses in flanges

(after Heins and Seaburg, 1963)

[2.7] $$T = GJ\phi' - EC_w\phi'''$$

Equation [2.7] has the general solution

[2.8] $$\phi = A + B\cosh\frac{z}{a} + C\sinh\frac{z}{a} + \frac{Tz}{GJ}$$

for a concentrated torque,

[2.9] $$\phi = A + Bz + C\cosh\frac{z}{a} + D\sinh\frac{z}{a} - \frac{t_u z^2}{2GJ}$$

for a uniformly distributed torque, and

[2.10] $$\phi = A + Bz + C\cosh\frac{z}{a} + D\sinh\frac{z}{a} - \frac{t_\ell z^3}{6GJL}$$

for a linearly varying torque, where z is the distance along the longitudinal axis. The constants of integration are evaluated to comply with the torsional end conditions. The stresses in the beam may then be determined according to [2.1], [2.4], and [2.5]. Fig. 2.7 shows the distribution between St. Venant torque and warping torque for a torsionally pin-ended beam. It can be seen that at the centreline, where warping is fully restrained, the torque is carried entirely by the warping mechanism. Where the flanges are free to warp, the torque is resisted primarily by the St. Venant warping mechanism.

An important assumption made in the development of [2.7] is that the web remains undeformed during rotation.

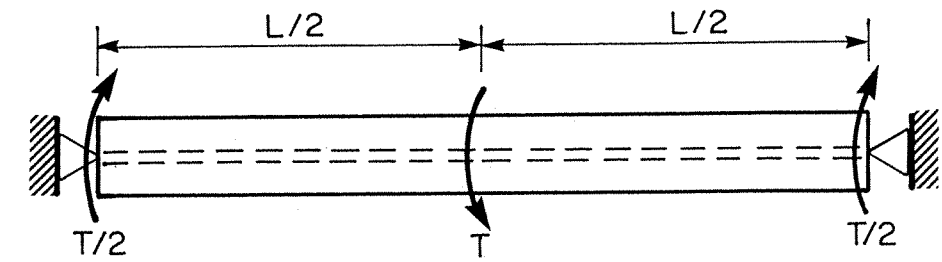

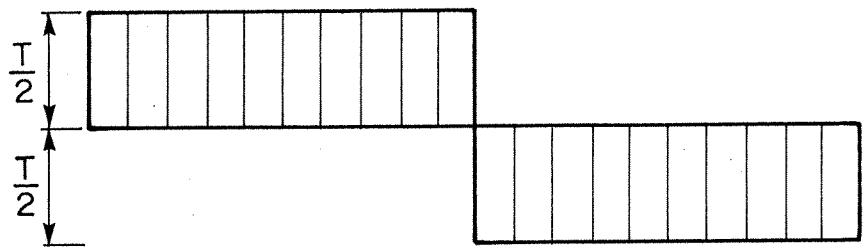

(a) Total torque

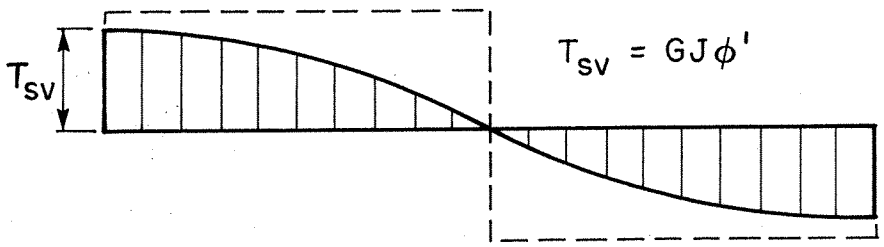

(b) St. Venant torque

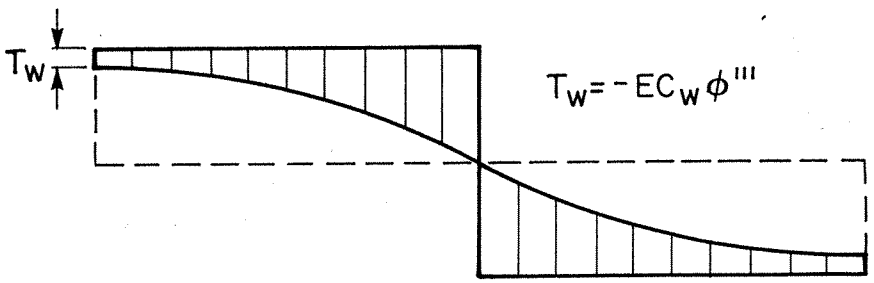

(c) Warping torque

Figure 2.7 Torque diagrams for a pin-ended beam (after Salmon and Johnson, 1980)

Although this is not strictly true, as shown in Fig. 2.8, it has been shown by Kubo, Johnston and Eney (1956) that except for unstiffened plate girders, it provides a good approximation (Salmon and Johnson, 1980).

2.3 Elastic Design Methods

Many different methods have been proposed for the design of beams under flexural and torsional loads, most of which are based on summing the stresses caused by the two types of loads. However, the method of superposition is valid only when bending moments are small and becomes very unconservative as the bending moment approaches the lateral torsional buckling value and interaction becomes significant, as discussed subsequently. In fact, when bending stresses approach 66% of yield (the maximum flexural stress allowed by the AISC specification (AISC, 1978)), rotation and stresses may be 50% higher than those predicted for simply supported beams and 80% higher for cantilevers (Chu and Johnson, 1974).

Two types of interaction occur that lead to unconservative solutions. First, if the torque is applied in the form of an eccentric vertical load acting on the top flange, the eccentricity increases as the section rotates as shown in Fig. 2.9 (Sourochnikoff, 1951). Second, a vertical load applied to a rotated section causes bending about both principal axes. Therefore, the stresses caused by flexure are larger than those predicted when neglecting the

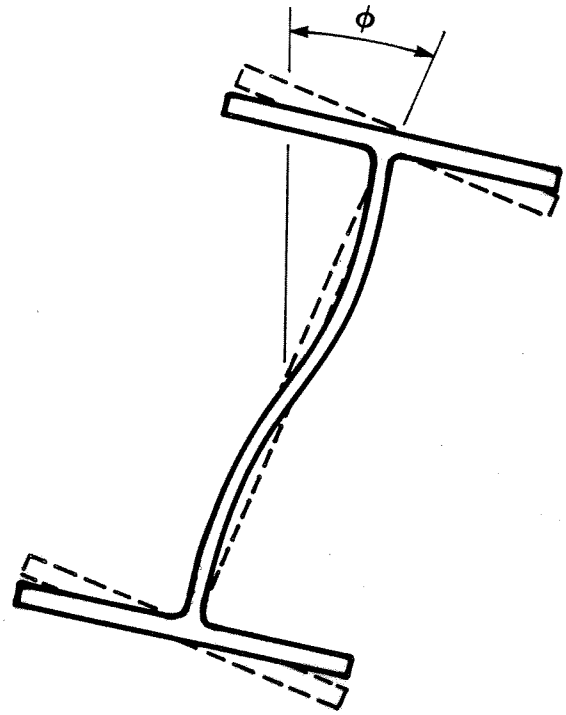

Figure 2.8 Distortion of web under torsional load

(after McGuire, 1968)

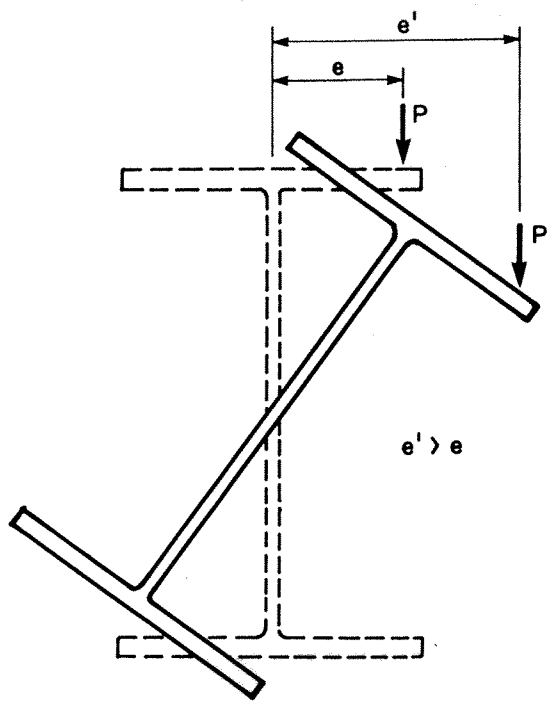

Figure 2.9 Increasing eccentricity as cross-section rotates

interaction (Pastor and DeWolf, 1979). Some authors have attempted to address this situation by using more complex differential equations (Chu and Johnson, 1974) or by introducing design factors to reduce the predicted strength of the beam (Pastor and DeWolf, 1979).

One approach to designing beams subjected to torsional loads is to use the exact solution to [2.7], which is facilitated by the use of graphs such as those published by the Bethlehem Steel Corporation (Heins and Seaburg, 1963). Johnston (1982) presented a similar set of graphical design aids. Superposition of stresses is then used to combine the effects of bending and torsion.

A very simple approach that often leads to overly conservative designs, is the flexural analogy. The torque is replaced by a couple acting on the two flanges, as shown in Fig. 2.10. The flanges are then treated as rectangular beams bent laterally in simple flexure. As the entire torque is assumed to be resisted by the shear forces in the flanges, these forces as well as the corresponding lateral flange moments and resulting normal stresses are over-estimated. As in most cases, normal stresses rather than shear stresses are critical, and therefore the solution is conservative (Salmon and Johnson, 1980).

The flexural analogy may be used with the "β-modifier" to achieve more economical designs. The β-modifier is a reduction factor applied to the flange moment calculated from the flexural analogy design method. The value of the

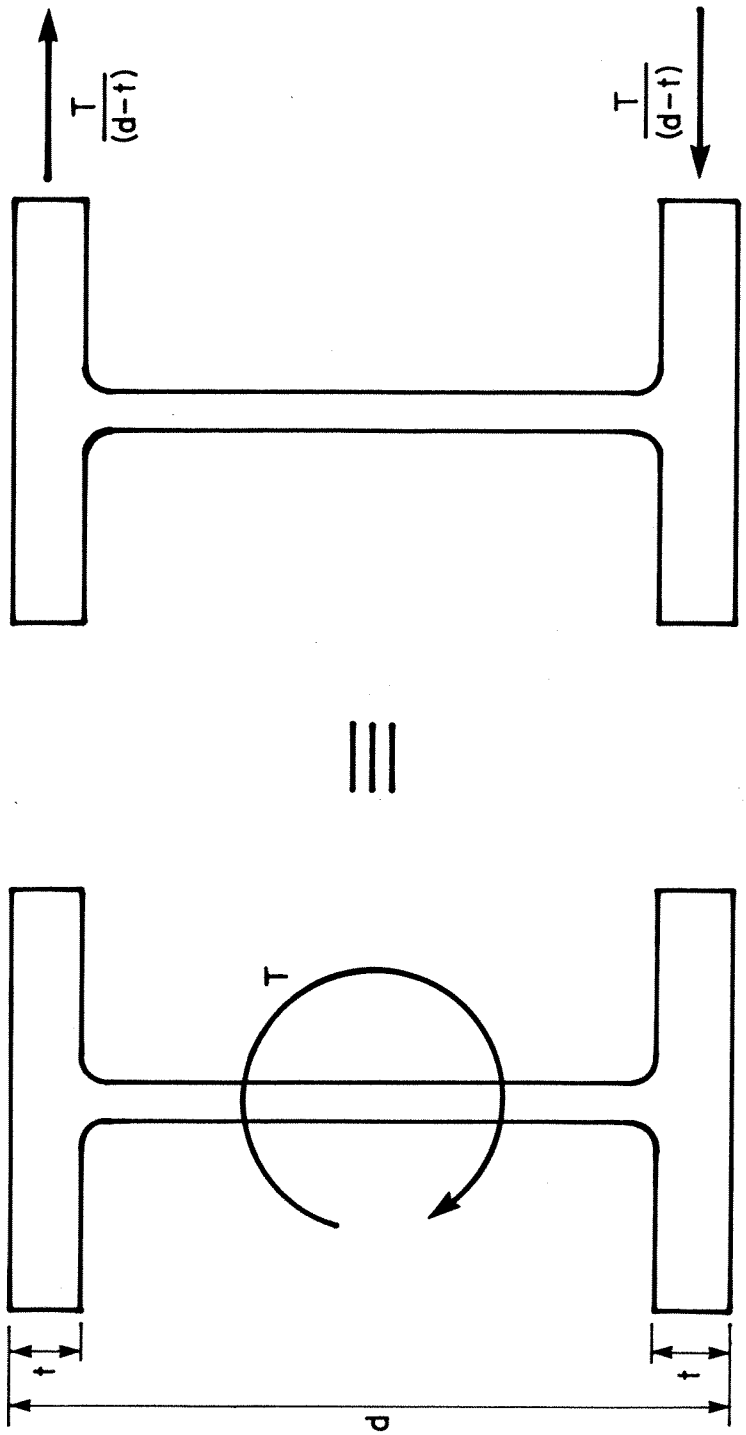

Figure 2.10 Flexural analogy for applied torque

β-modifier is dependent upon the end and loading conditions, and the length and section properties of the beam. A solution of this type requires the use of tables such as those presented by Lin (1977).

Walker (1975) also suggested an approach similar to the flexural analogy except that solutions are in terms of bi-moments, B, so termed by Vlasov (1961), where

$$B = M_f h \qquad [2.11]$$

This is an approximate method which requires a series of graphs of bi-moment and rotation correction factors to account for the difference between the approximate and the exact solutions. Once again, when stresses from torsion and bending are added, no reduction in strength due to interaction is incorporated.

Johnston, Lin and Galambos (1980) presented a design method whereby flange moments are calculated using fairly simple approximate formulae. From these, warping normal stresses and the corresponding shear stresses are determined. For short beams, the equations are identical to those of the flexural analogy method, that is, the torque is assumed to be resisted entirely by warping torsion. For intermediate and long beams, some modifications are incorporated to reflect the fact that the effect of warping restraint is dissipated in a distance from the restrained location approximately equal to a, where

[2.12] $$a = \sqrt{\frac{EC_w}{GJ}}$$

provided the members behave elastically.

2.4 Limit States Research

Although the behaviour of I-shaped beams subjected to both flexural and torsional loads has been described by many different authors, few have carried the analysis to a fully plastic condition. With the advent of limit states design standards such as Standard CAN3-S16.1-M84 (CSA, 1984), one of the ultimate limit states conditions of concern is the attainment of the full strength of the cross-section.

Boulton (1962) proposed a limit states method for the design of beams subject to torsional loads based on an equilibrium equation relating flange moments to flange shears. A portion of the sand heap torsional stresses are added to the warping stresses so that every point on each cross-section reaches the yield stress. This method results in complex equations that are not suitable for design standards. The generalized form of the theory can be used for beams under combined bending and torsion.

Boulton tested beams under torsion only and observed that the beams carried torques beyond the theoretical fully plastic torque that continued to increase with large angles of twist. He attributed this increased resistance to what has become known as the helix effect. With large rotations, the top and bottom flanges describe a helical shape. The

tension that develops along the helices has a component normal to the axis of the beam that resists the applied torque.

Dinno and Gill (1964) have summarized several different torsion theories including those of Boulton (1962) and Merchant (similar to Dinno and Merchant (1965)). They provide test results, but only for beams under torsion alone.

Dinno and Merchant (1965) presented a very simple design method based on the full plastification of the fixed end of a cantilever beam subjected to a concentrated torque at the free end. The method is extended to other end conditions by the use of effective length factors. It is assumed that the sand heap torque (the fully plastic St. Venant torque as described by Nadai (1931)), as shown in Fig. 2.11, can be carried at any section, regardless of the presence of warping stresses. In the absence of flexure, the flanges are assumed to have a fully plastified normal stress distribution at the fixed end, as shown in Fig. 2.12. A compatible flange shear distribution forms the warping torsional restraint. Therefore,

[2.13] $$T_p = T_{sh} + V_f h$$

The largest torque that can be carried is that based on a constant flange shear over the length of the cantilever. If the flanges are fully plastified at the fixed end,

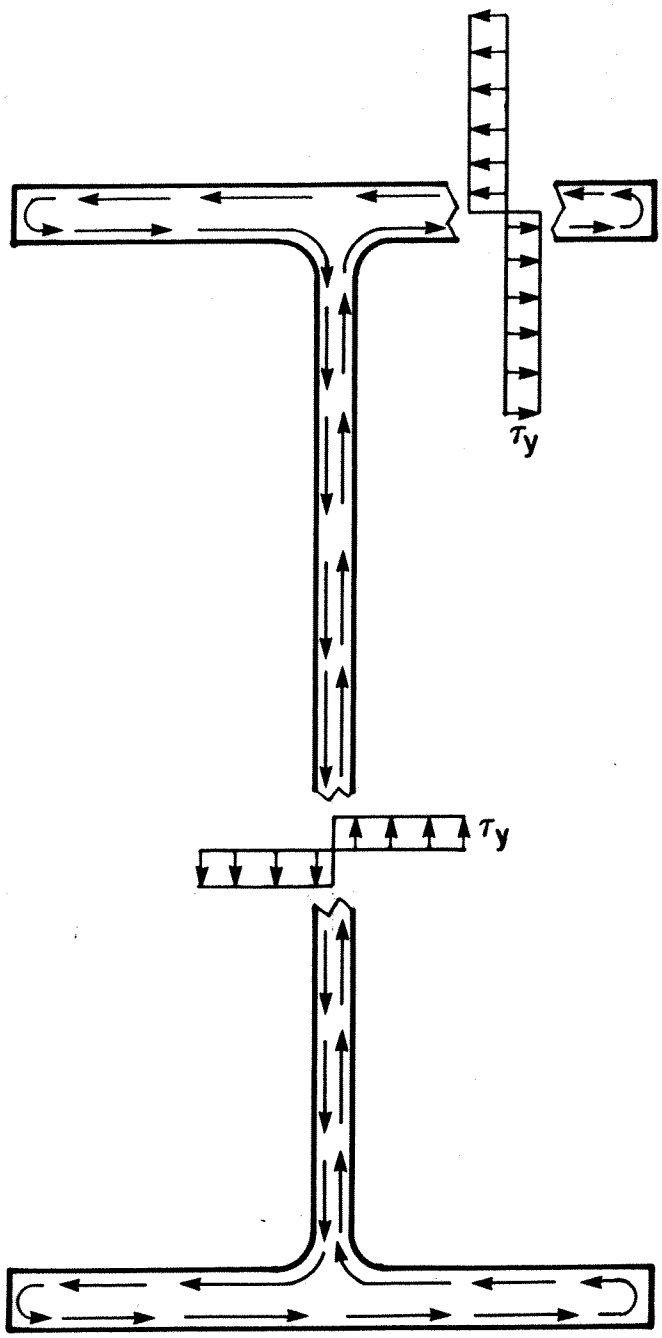

Figure 2.11 Sand heap shear stress distribution

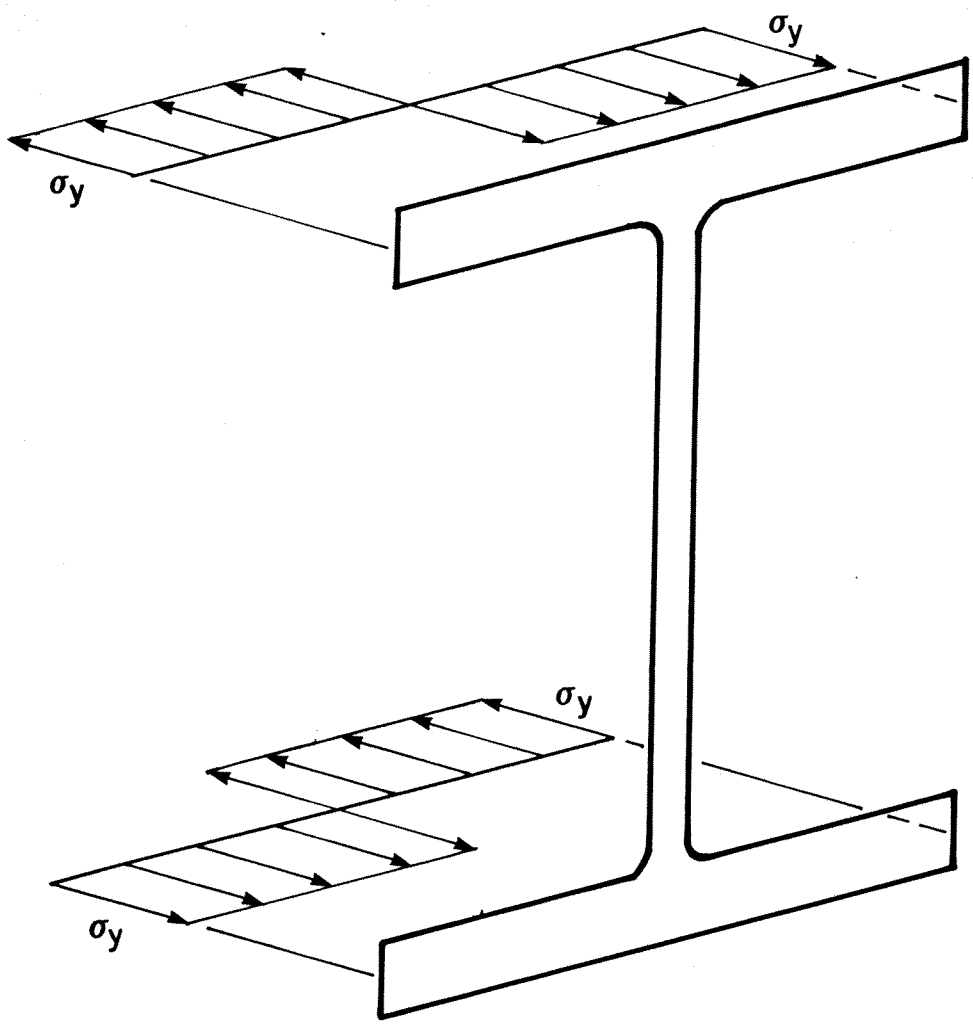

Figure 2.12 Fully plastic warping normal stresses

[2.14] $$V_f L = M_{fp} = \frac{\sigma_y t b^2}{4}$$

Combining [2.13] and [2.14] gives

[2.15] $$T_p = T_{sh} + \frac{\sigma_y t b^2 h}{4L} = T_{sh} + T_{wp}$$

Based on a derivation by Hodge (1959), they proposed the interaction curve for combined bending and torsion given by

[2.16] $$\left[\frac{M}{M_p}\right]^2 + \left[\frac{T}{T_p}\right]^2 = 1$$

Dinno and Merchant claimed that this is a safe design method because results of tests that they conducted gave higher strengths than predicted. However, the beams they used were significantly smaller than those used in practice (d = 5/8 in.) and the flange and web width-thickness ratios were also very small. In addition, an invalid assumption was made in directly adopting Hodge's work in the derivation of [2.16] as shown in Appendix A. Augusti (1966) formally demonstrated that this method is an upper bound solution based on the yield stress as the limiting criterion.

Farwell and Galambos (1969) presented a simple analytical method for beams under torsion based on elasto-plastic behaviour. They also conducted a testing program for I-shaped beams under torsion alone and achieved good agreement with their predictions.

Kollbrunner, Hajdin, and Ćorić (1978) and Kollbrunner, Hajdin, and Obradović (1979) described the behaviour of a cantilever and a fixed ended beam, respectively, subjected to combined bending and torsion and proposed the interaction equation

$$\frac{(M-M_{pw})^2}{M_{pf}^2} + \frac{B}{B_p} = 1 \qquad [2.17]$$

to predict full plastification of the section. They claimed that when eccentricities are large, high strains at the flange tips prevent the attainment of full plasticity and the limit load was modified to that corresponding to a maximum allowable strain leading to a predicted ultimate load in the elasto-plastic region.

It was assumed that the ratio M/B remains constant during loading through the elastic and inelastic regions. Thus, for a given eccentricity, the limiting bending moment, and therefore the limit load, can be calculated. The method requires the solution of a cubic and a quadratic equation but predicted strengths appear to agree well with the authors' test results.

Razzaq and Galambos (1979) presented a series of involved differential equations for predicting the strength of beams under biaxial bending with or without torsion. The special case of uniaxial bending about the major principal axis with torsion is of interest in this discussion. Separate equations were derived for beams first loaded by an

eccentric vertical load and then in uniform flexure, and for beams first loaded in uniform flexure and then by an eccentric load, consistent with the procedures used in the testing program. An elasto-plastic strain-hardening (tri-linear) stress-strain curve was assumed. The procedure is suitable for predicting behaviour in both the elastic and inelastic regions. Good agreement was obtained between test and predicted strengths, although the method is limited to the two types of loadings investigated.

2.5 Summary

Although the subject of combined bending and torsion on I-shaped steel beams has been addressed by many different authors, there does not appear to be a simple limit states design method available that is suitable for commonly encountered torsion conditions. There is a multitude of approximate elastic design methods available that usually require a large number of charts or graphs, and fail to consider the interaction of the bending and torsion mechanisms. Simpler methods, such as the flexural analogy, can lead to overly conservative designs.

Boulton presented a limit states design method based on the entire cross-section reaching the yield stress and includes the helix effect. This results in a complex design procedure. Dinno and Merchant presented a simple limit states design method that is based on an invalid assumption. Kollbrunner et al. demonstrated a limit states design method

where a maximum strain is imposed as the limit state. This method requires the solution of fairly complex equations. Razzaq and Galambos presented a method that is suitable only for certain loading conditions and requires graphs to aid in the solution of the governing equations. All sets of researchers claimed good agreement between predicted strengths and their own test results.

3. EXPERIMENTAL PROGRAM

3.1 General

Because of the lack of published experimental data, a limited experimental program was undertaken for comparison with the theory developed herein. Four tests were conducted on I-shaped cantilever beams approximately 1 metre long as shown in Figs. 3.1 and 3.2. The beams were loaded by an essentially vertical load, with initial eccentricities of 0, 30, 100, and 220 mm. Tension tests were performed on 13 coupons to determine material properties.

A W150X18 beam was selected for two reasons. With a length of 1 metre, both the sand heap and warping torsional resistances for this cross-section are significant and the respective contributions may therefore be determined with reasonable certainty. In addition, the loads required to fail the relatively small beam are easily achieved in the laboratory.

3.2 Test Set-up and Procedure

The experiments were conducted in the I. F. Morrison Structural Laboratory at the University of Alberta. Specimens were loaded in the Materials Testing System (MTS) testing facility which has a tensile capacity of 4450 kN. A 610 mm long I-shaped spacer with braced flanges was bolted vertically to a supporting column as seen in Figs. 3.1 and 3.2 so that the column could be bolted through holes in the

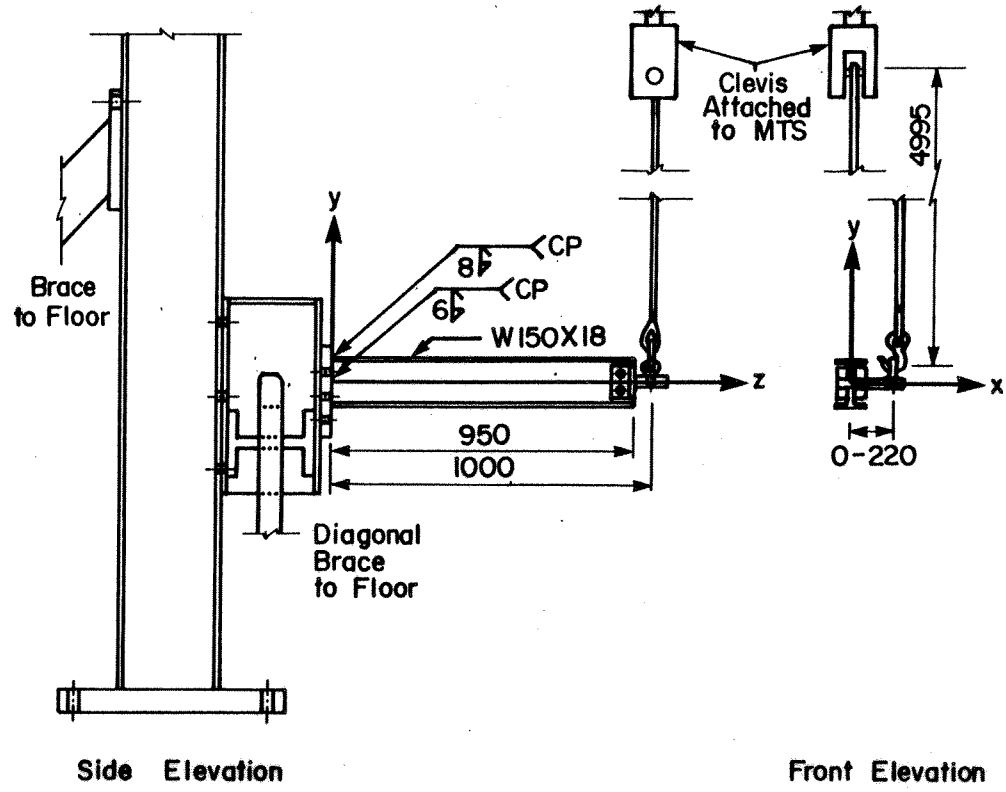

Figure 3.1 Schematic diagram of test set-up

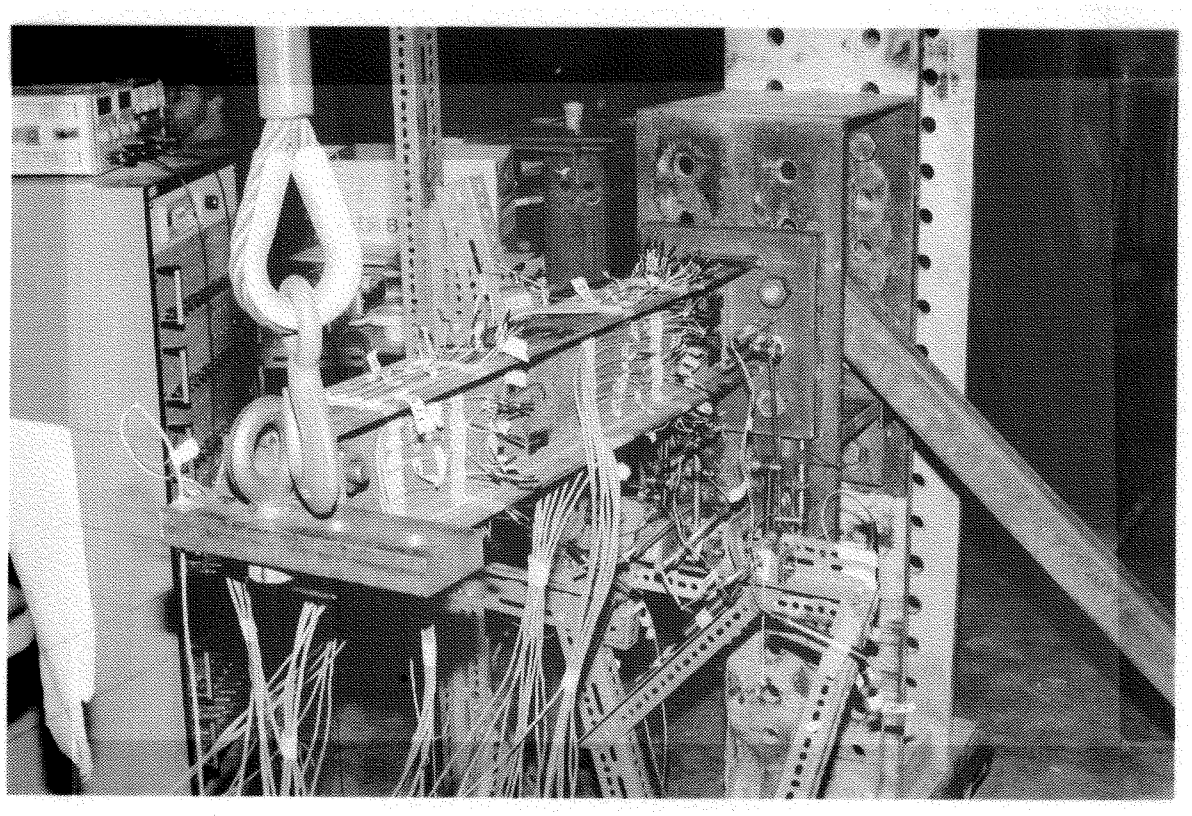

Figure 3.2 Test beam 2

strong floor and so that the MTS testing head was directly above the free end of the test specimen. Lateral bracing was also provided at the support.

One end of each cantilever test beam was welded with full penetration welds to a thick end plate which, in turn, was bolted to the steel supporting column to provide a fixed end condition. At the free end, one of two brackets, shown in Fig. 3.3., was bolted to the web to allow the beams to be loaded eccentrically. The brackets were designed to transfer load to the web with a minimum of local distortion and without interfering with the warping of the flanges. With two similar brackets, there were seven possible eccentricities to choose from. For each test, an eccentricity was chosen on the basis of the previous test results to give a broad spectrum of behaviour. All bolted connections were designed to be slip-resistant at the ultimate load.

The load was applied using a 7/8 in. fibre core wire rope approximately 5 metres long, with a steel thimble at the top and a steel thimble and hook at the bottom. The wire rope was supported by a 2 in. pin and clevis assembly. The hook was fitted into an eye bolt in the loading bracket. With this arrangement, deflections and rotations in any direction were accommodated with the load remaining virtually vertical throughout. Any deviation of the load from vertical can be calculated. The cable was load-tested to establish its load-deformation characteristics. The

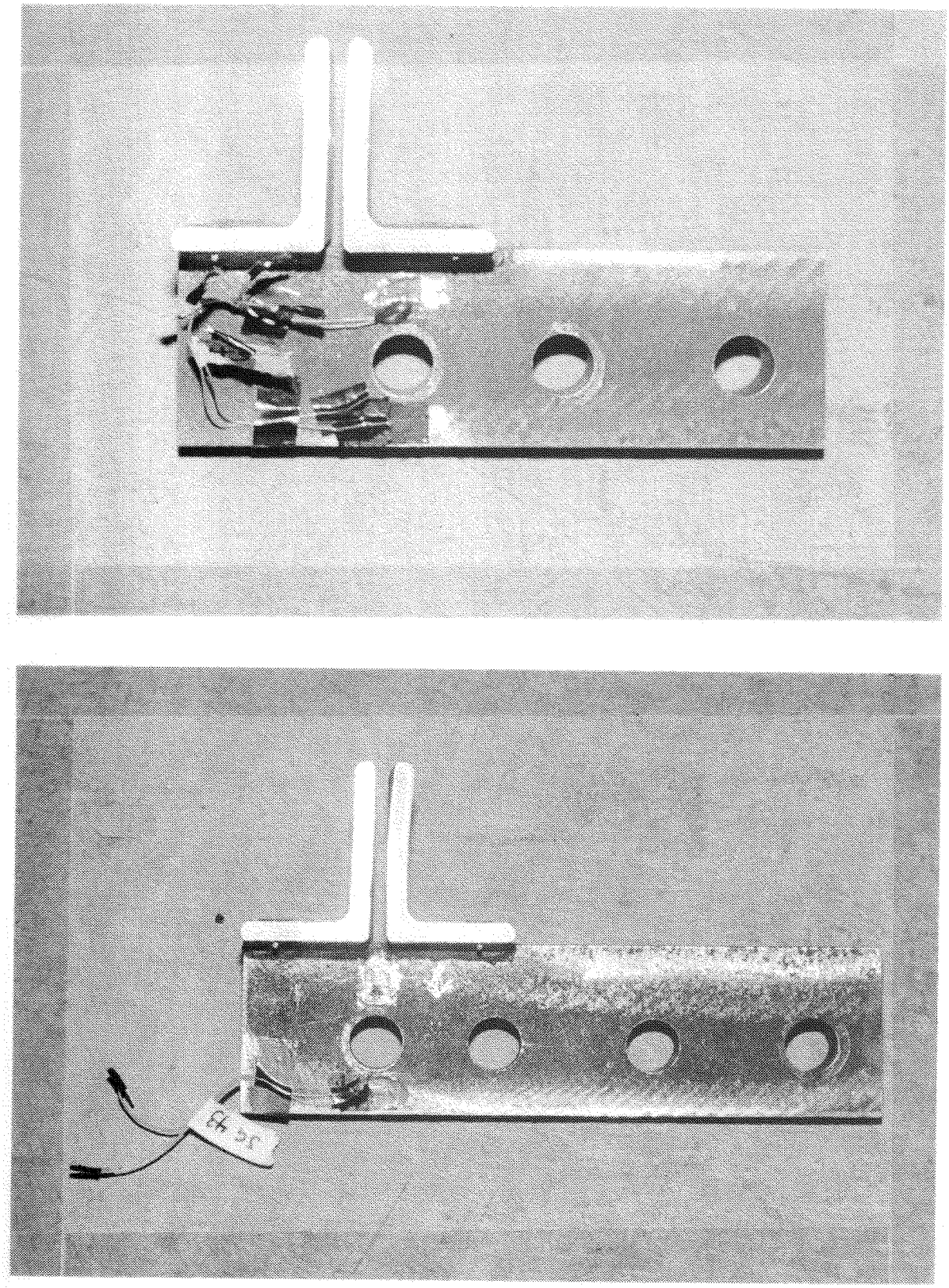

Figure 3.3 Loading brackets

fitting with the lowest strength in the cable assembly was the Crosby 320A alloy eye hook with a specified safe working load of 40 kN. It had been proof tested to 80 kN before delivery.

Prior to each test, the specimen was carefully positioned so that the beam was level and the web vertical. The distance between the end plate and the point of application of the load, as well as the distance from the load to the end of the beam were measured for use in post-test calculations. The instrumentation was attached and the specimens were subjected to a small load to check for instrumentation malfunctions and subsequently unloaded. All instrumentation was then reset to zero.

The MTS testing machine was used to apply loads hydraulically in the stroke control mode so that behaviour in the inelastic range could be studied with greater precision. The beams were loaded incrementally until the applied load was 3 to 10% below its maximum value.

3.3 Instrumentation and Measurement

During the tests, longitudinal strains on both flanges and the web were recorded using Micro-Measurements high elongation electrical resistance strain gauges with a resistance of 120.0 ± 0.15% ohms, a gauge length of 7 mm, and a gauge factor of 2.055 ± 0.5% at 24 degrees Celsius. Showa strain rosettes were used to observe strains at 0, 45, and 90 degrees from the longitudinal axis. These rosettes

have gauges with a resistance of 120.0 ± 0.5% ohms, a gauge length of 2 mm, and a gauge factor of 2.06 ± 1% at room temperature. The locations of the gauges and rosettes were identical for all beams as shown in Fig. 3.4. The strain gauges were capable of measuring strains in excess of 20%. The rosettes ceased to function at approximately 2.5% strain. In addition, Showa strain gauges with a resistance of 120.0 ± 0.5% ohms, a gauge length of 5 mm and a gauge factor of 2.11 ± 1% were applied to the loading bracket and the end plate to ensure that these strains remained elastic throughout each test. These gauges were also used in the ancillary tests.

Deflections were measured at two locations using linear variable displacement transformers (LVDTs). All LVDTs were calibrated before the first test. At the fixed end, four Hewlett Packard 24DCDT-100 LVDTs with a linear operating range of 5 mm and two 7DCDT-500 LVDTs with a linear operating range of 25 mm were used to monitor the end plate translations and rotations to determine whether a truly fixed condition had been achieved. These instruments have a linearity error of less than 0.5% over the rated linear range. At the free end, six Intertechnology PT-101 position/displacement transducers capable of measuring spacial displacements were used. These LVDTs continuously measure displacements in any direction by means of a thin spring-loaded cable attached to the beam. The position transducers have ranges that vary from 250 mm to 635 mm and

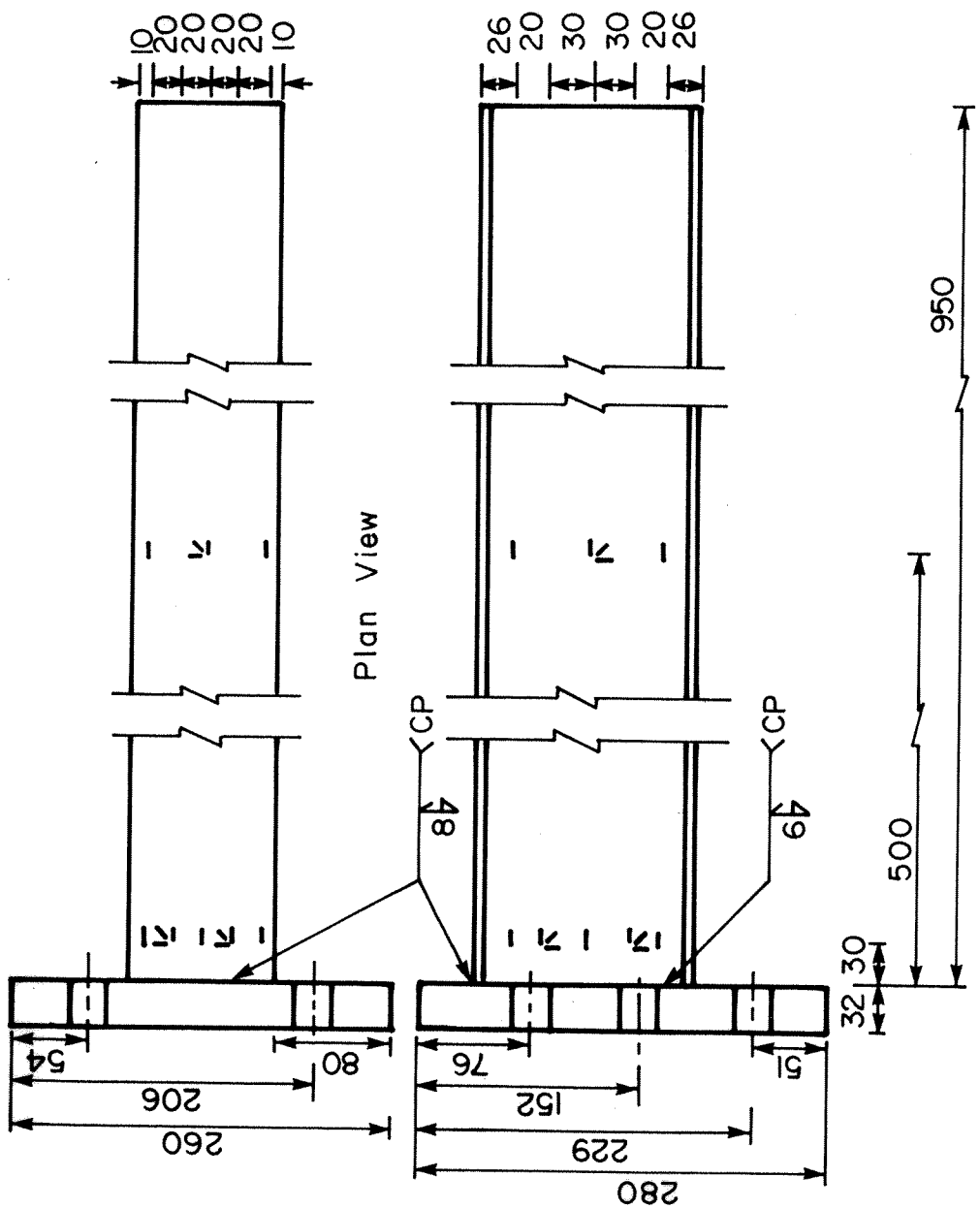

Figure 3.4 Strain gauge and rosette locations

linearity errors from 0.1% to 0.15% full scale.

Six position transducers are the minimum required to establish uniquely the location in space of the plane of the cross-section at the free end. Alternately stated, there are six degrees of freedom (three displacements and three rotations) and therefore six measurements are sufficient to quantify them. Three transducer cables (preferably arranged orthogonally) attached to one point on the plane are sufficient to determine the location of that point as the beam deflects and rotates. The solution of 3 simultaneous equations, based on the Pythagorean theorem, give the displacements u, v, and w. Two transducers are sufficient to determine the location of a second point, as its distance from the first remains unchanged throughout the test. Similarly, one transducer is sufficient to determine the location of a third point on the plane. The three points uniquely define the orientation of the plane in space, and deflections and rotations in any direction can be calculated. The three points used were on the loading bracket as shown in Fig. 3.5. For accurate deflection measurements at the free end, the bracket, to which the LVDT cables were attached, must remain fixed in location with respect to the beam web. This was checked during each test and found to be true.

Power was supplied to the strain gauges with two Anatek 7V power supplies set to supply all gauges with approximately 6.0 volts. An Anatek 25V power supply provided

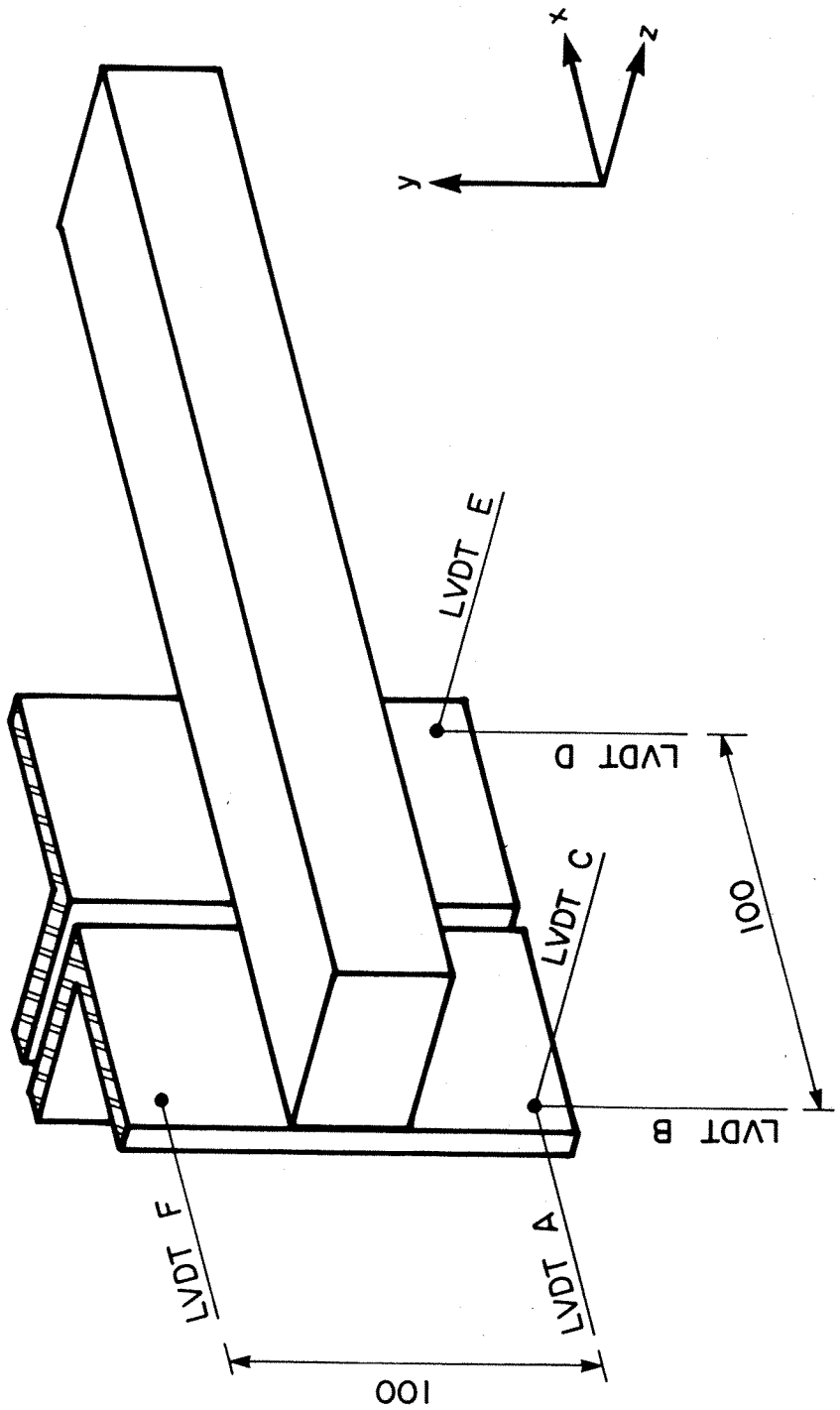

Figure 3.5 Loading bracket and LVDTs

the LVDTs with approximately 10 volts.

Loads were monitored using a 110 kN load cell attached to the MTS testing machine above the clevis. This was the smallest load cell available for the MTS and therefore provided the most precise loading information. The load cell was powered by a 10 volt power supply within the MTS system.

Strains and deflections were measured for each load increment. All electronic data were recorded using a Data General Eclipse S/120 computer data acquisition system by means of a remote terminal. This system allows a large number of measurements to be made simultaneously. The strain gauge, LVDT, load cell, and MTS stroke output were each assigned a channel on the Eclipse system. In addition, power supplies for the strain gauges, LVDTs, and load cell were assigned channels to monitor voltage fluctuations that could affect the data output. No appreciable fluctuations occurred in any of the tests. A total of 65 data acquisition channels were used.

Prior to each test, procedures were undertaken to ensure that data obtained were as accurate as possible. Strain gauges were calibrated in banks of 10, less than 12 hours before each test. The gauges were then re-balanced immediately prior to the test. Voltage from each power supply was set to the desired value and instrumentation was meticulously inspected. When the test was to begin, all instrumentation was initialized to readings of zero using the testing software of the Eclipse.

As a check, duplicate measurements of important quantities were made by hand approximately 10 times during each test. Vertical and lateral deflections were measured using a standard tape measure. Fig. 3.6 shows the apparatus, consisting of a large protractor and plumb line, that was used to measure free end rotations.

3.4 Test Results

The four tests were similar, with the eccentricity of the load being the only variable. All specimens were cut from the same beam. The dimensions of the specimens are given in Table 3.1.

Two problems were encountered in test 1. First, the loading bracket slipped against the beam web until the bolts came into bearing. This caused the loading bracket to rotate a small amount which had to be taken into account in subsequent calculations. Second, deflections of the supporting column were larger than anticipated.

To remedy the slippage problem, small metal shims were placed between the legs of the angles facing the web and the beam flanges to prevent any rotation. This arrangement was successful in preventing bracket rotations for tests 2, 3, and 4 without interfering with the warping of the flanges at the free end. Column deflections were very substantially reduced for tests 2, 3, and 4 by bracing the supporting column as shown in Fig. 3.7.

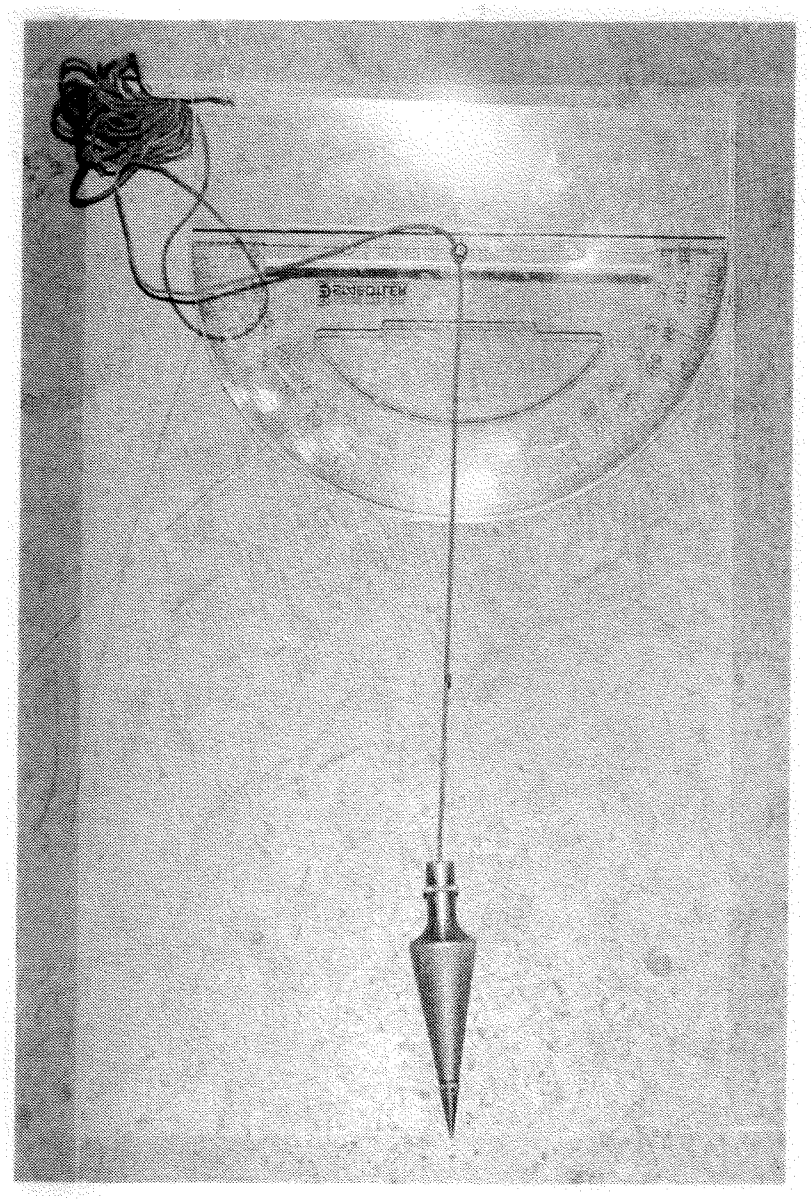

Figure 3.6 Protractor and plumb line

Table 3.1 Test beam dimensions

BEAM		d (mm)	b (mm)	t (mm)	w (mm)
1	$\bar{x}$	154.36	99.46	6.67	6.07
	s	-	0.0599	0.131	0.0742
	V	-	0.0602%	1.97%	1.22%
2	$\bar{x}$	154.34	99.46	6.68	6.01
	s	-	0.0726	0.139	0.1302
	V	-	0.0730%	2.08%	2.17%
3	$\bar{x}$	154.37	99.41	6.69	5.89
	s	-	0.0959	0.121	0.1178
	V	-	0.0965%	1.80%	2.00%
4	$\bar{x}$	154.63	99.46	6.65	5.90
	s	-	0.0917	0.137	0.1076
	V	-	0.0922%	2.05%	1.82%

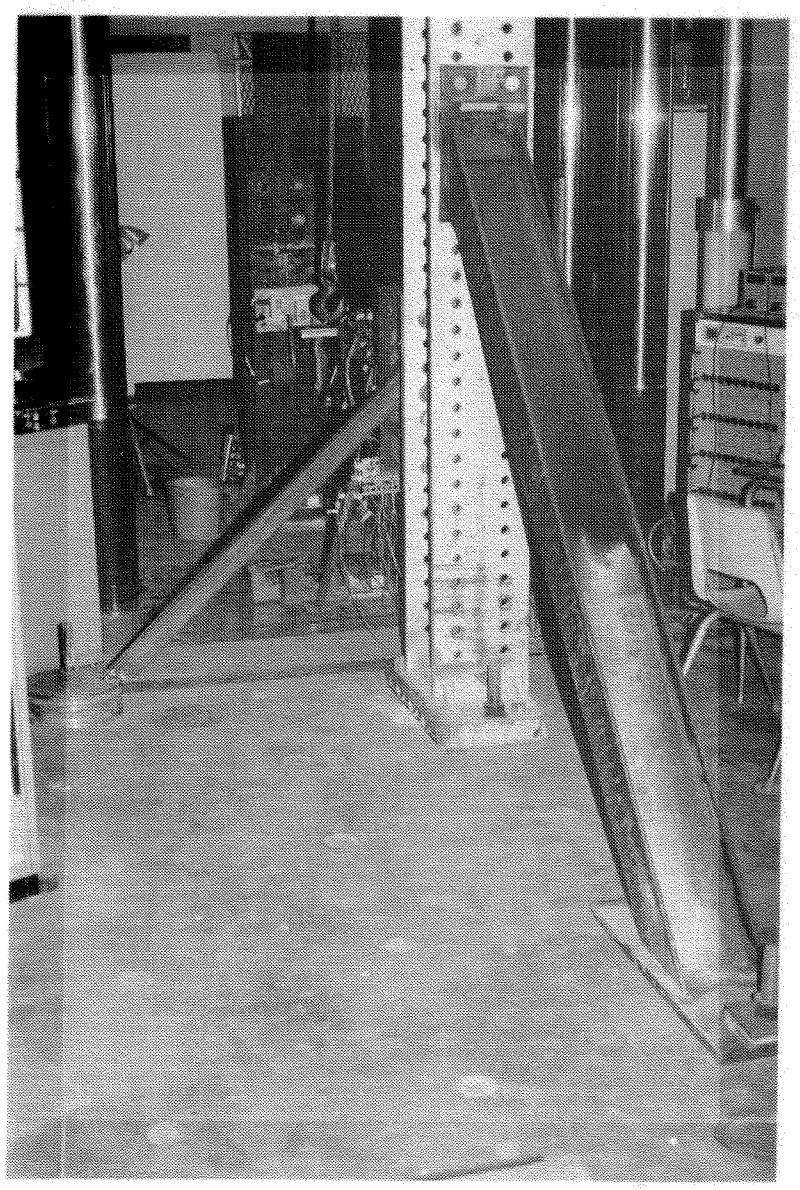

Figure 3.7 Braced supporting column

In Figs. 3.8, 3.9, 3.10, and 3.11 are plotted moment-torque, torque-rotation, load-lateral displacement, and moment-vertical displacement curves for the four tests. The torque is the torsional moment about the z axis, the moment is the moment about the major (x) axis at the fixed end, and the load is the vertical component of the applied load. The displacements are those of the free end relative to the fixed end.

Fig. 3.8 shows that for beam 1, loaded concentrically, torque is not developed significantly until the moment exceeds the fully plastic value shown by point A. Therefore, the origin of the torque-rotation curve for this beam in Fig. 3.9 corresponds to an applied moment of about 47 kN*m. Fig. 3.11 shows that the beam first deflects elastically, then inelastically and finally reaches a maximum moment of 58 kN*m, considerably in excess of the fully plastic moment based on the measured cross-sectional properties and yield strength. The flexural strains at the fixed end must therefore exceed the strain hardening strain substantially. Fig. 3.10 shows that the lateral deflections increased rapidly once the fully plastic moment was exceeded (point A). These lateral deflections created a torque at the fixed end which decreased to essentially zero at the free end. For beam 1, the moment-torque curve (Fig. 3.8) and load-lateral deflection curve (Fig. 3.10) are very similar because apart from the change in the lever arm resulting from the deflection of the beam, the moment is proportional to the

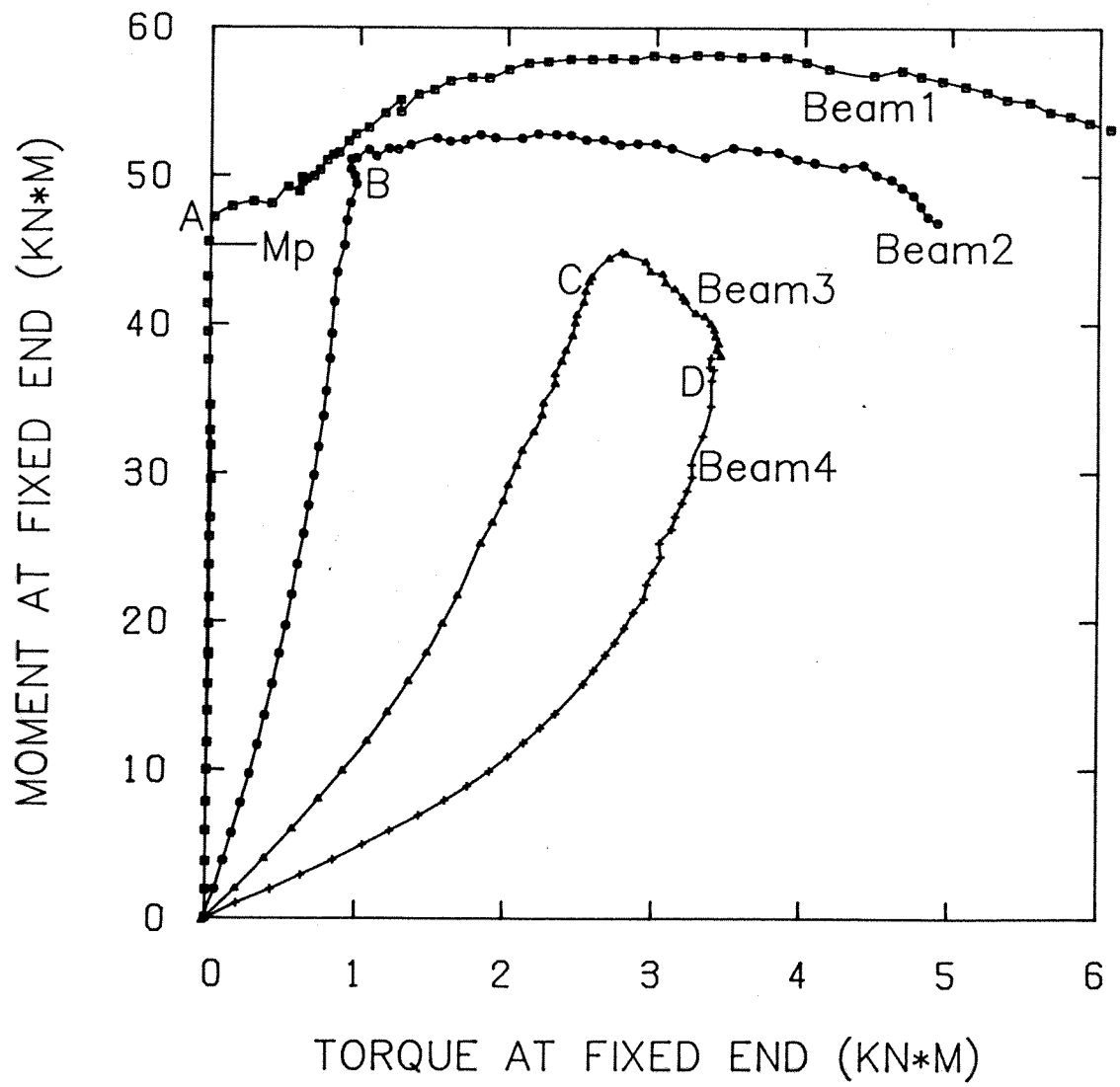

Figure 3.8 Moment versus torque test curves

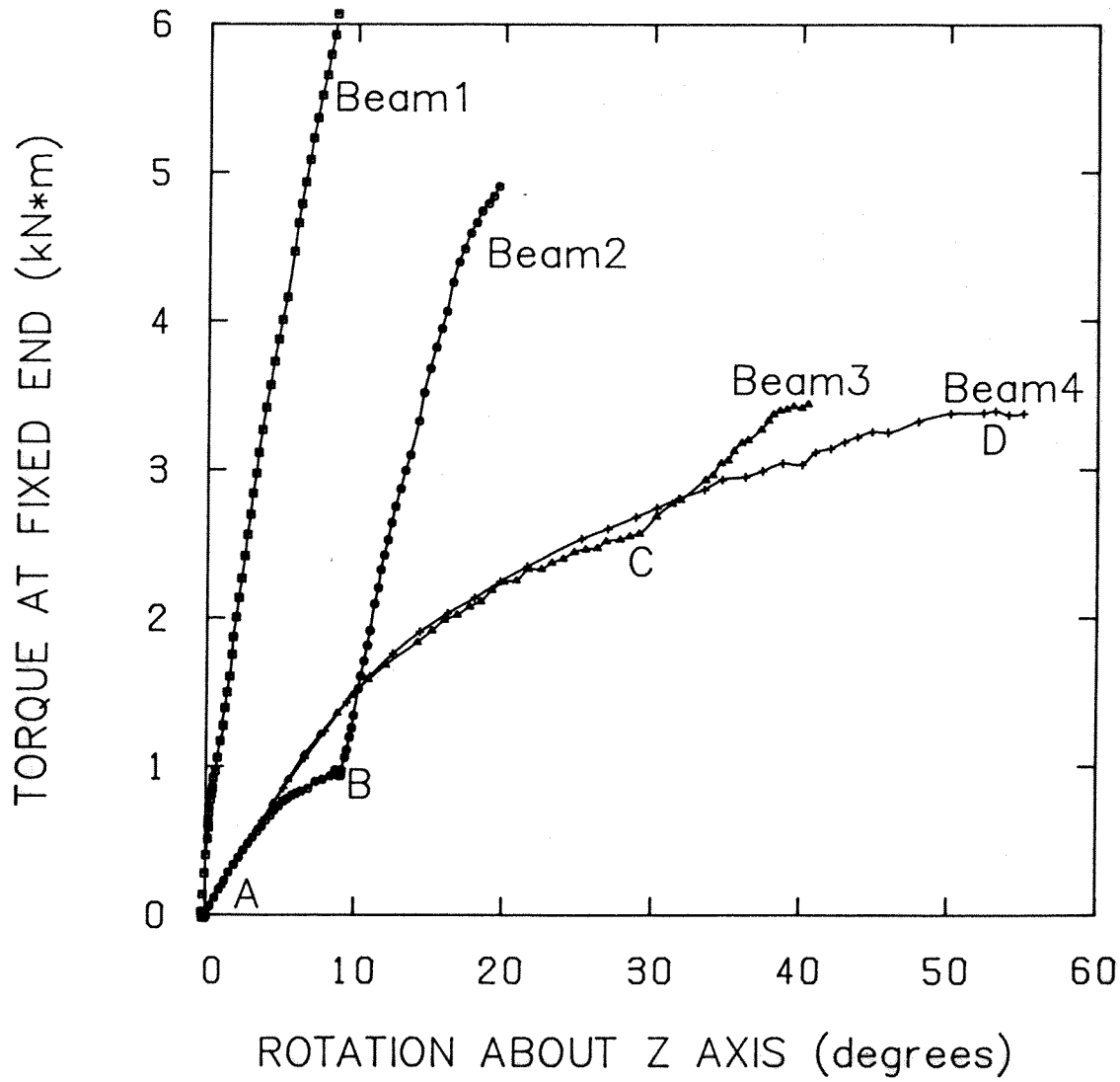

Figure 3.9 Torque versus rotation test curves

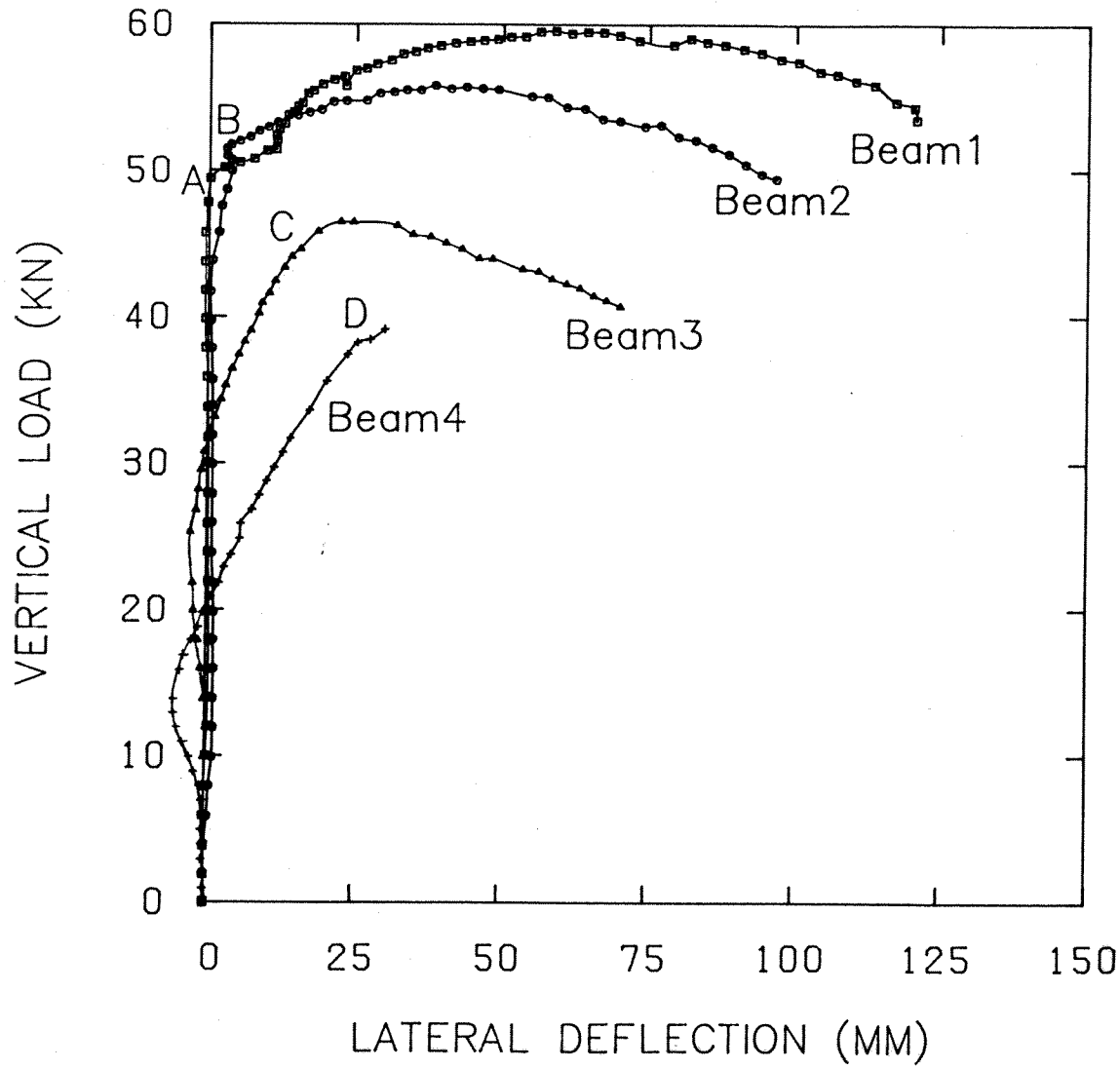

Figure 3.10 Load versus lateral displacement test curves

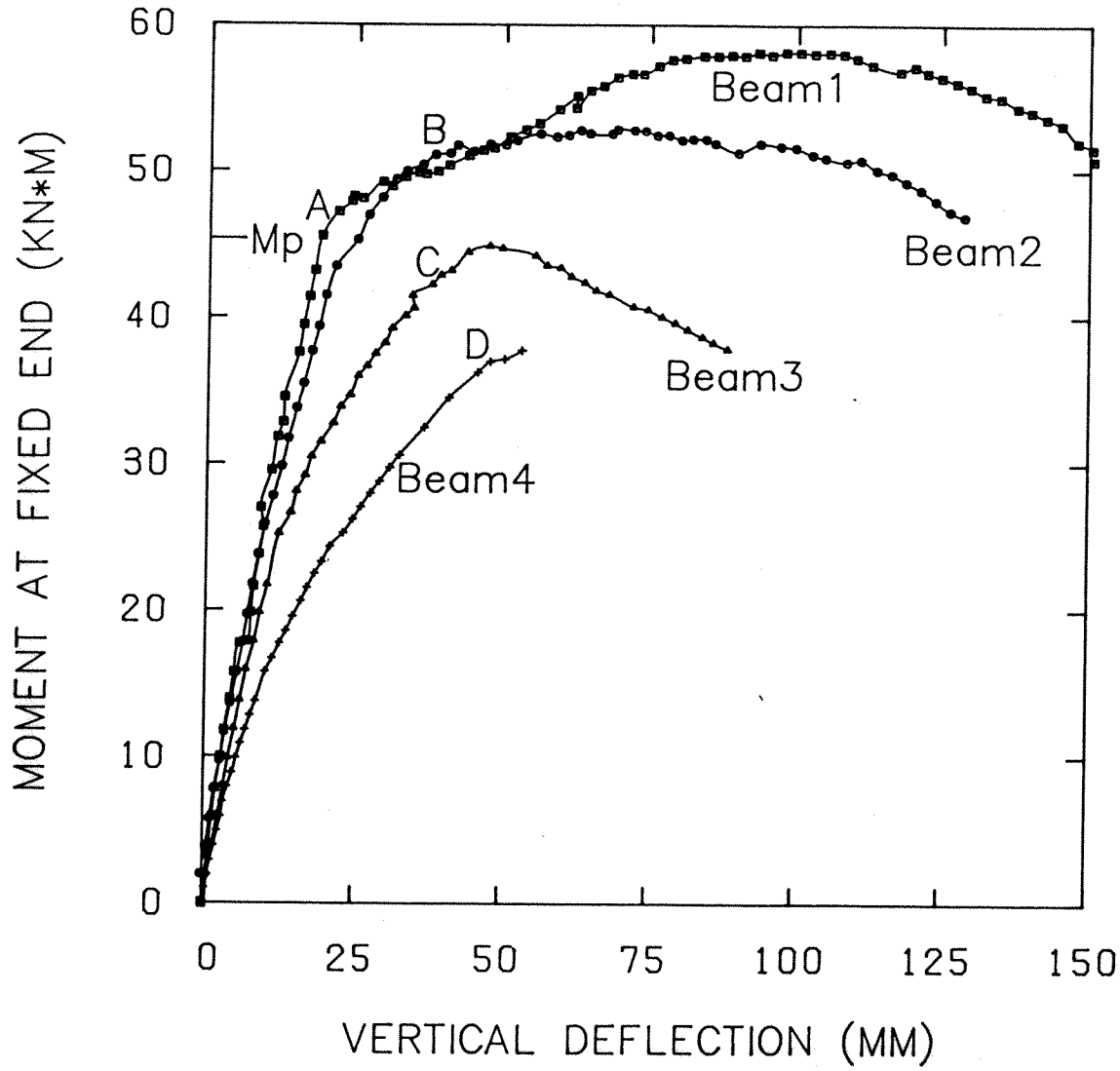

Figure 3.11 Moment versus vertical displacement test curves

vertical load and the torque arises only because the beam has deflected sideways. This lateral deflection takes place when the stiffness of the beam has been reduced because of straining beyond the yield point.

Consider the four curves for beam 2. The initial slope of the moment-torque curve (Fig. 3.8) corresponds to the initial eccentricity of 30 mm. With increasing moment, the torque increases less rapidly because the eccentricity of the load decreases due to the rotation. At an applied moment of about 51 kN*m (point B), the torque starts to increase very rapidly corresponding to the increase in lateral displacement at point B on Fig. 3.10. As shown by Fig. 3.11, this corresponds, as it did for beam 1, to moments about the strong axis in excess of the fully plastic moment and therefore to the condition that the beam stiffness was substantially reduced due to straining beyond yield, and indeed beyond the strain hardening strain. The change in behaviour of the moment-torque curve (Fig. 3.8) at point B is reflected by the change in the torque-rotation curve (Fig. 3.9) also at point B. The increased torque carried beyond point B results only from the lateral deflection of the beam.

Beam 3 had an initial eccentricity of 100 mm as the initial slope of the moment-torque curve (Fig. 3.8) indicates. The steepening moment-torque curve shows that the eccentricity decreased due to rotation about the z axis. At point C on the moment-torque curve, the torque begins to

increase more rapidly and the moment subsequently decreases. The corresponding point on the torque-rotation curve (Fig. 3.9), also indicated as point C, shows a change in the torque-rotation behaviour at this point. Although not as fine a demarcation, beyond point C in Fig. 3.10 the lateral deflections increase rapidly.

The moment-torque curve for beam 4 displays an initial behaviour similar to that for beams 2 and 3. The initial slope corresponds to the initial eccentricity of 220 mm, and the curve steepens as the rotation decreases the eccentricity. The very steep moment-torque curve at point D corresponds to an angle of twist of 53 degrees as shown in Fig. 3.9.

Examination of the post-test deflected shapes of each beam revealed that the most severe stressing occurred successively farther from the fixed end as the initial eccentricity increased. Local buckling began in the compression flanges 70 mm from the end plate in beam 1 and 520 mm from the plate in beam 4. Because the fixed end is the most heavily loaded section of the beam, this indicates that the effect of rotation about the longitudinal axis had an increasing effect as the initial eccentricity increased. Beam 4, for example, did not fail where the bending moment about the x axis was a maximum because the cross-section had undergone large rotations at other locations and the vertical load caused bending about the weak axis as well.

As would be expected, flanges warped in opposite directions as the load was applied, up to the load where significant lateral deflections were incurred. As the load increased further, the top flange reversed curvature at the point where the local buckle occurred. Once the local buckle began to form, the majority of the distortion took place at this cross-section.

Throughout the tests, load, MTS stroke, strains, and free and fixed end deflections were measured. These data were then reduced using four computer programs shown in Appendix B. The program *DEFL* uses the load, MTS stroke and the six measured deflections from the free end of the beam to calculate deflections and rotations about the three coordinate axes. It also calculates any lateral or axial loads, and moments at the fixed end about all three axes, taking into account any deflections that have occurred. Output from the program *FEDEFL* is used to take "fixed" end movements into account. *FEDEFL* uses fixed end LVDT readings to calculate deflections and rotations at the end plate and those that result at the free end due to rigid body movement. *GAUGE* uses the high elongation strain gauge readings to determine the corresponding stresses based on the mean stress-strain curve observed in the tension tests described subsequently. *ROSETTE* uses strain readings from the 0-45-90 degree rosettes to calculate the corresponding stresses as well as principal normal stresses, maximum shear stresses, and the angle to the principal plane from the

plane of the cross-section.

3.5 Ancillary Tests

A 300 mm length of beam from the same heat as the test specimens was sawn into 13 longitudinal coupons that were tested in uniaxial tension to determine the stress-strain characteristics of the steel. Four coupons were cut from each flange and five from the web, utilizing the entire cross-section with the exception of a small portion at each web-flange junction as shown in Fig. 3.12. The coupons were machined to 12.5 ± 0.2 mm wide at the reduced section and were the full thickness of the flange or web. Cross-sectional dimensions were measured with a digital micrometer.

Strain gauges were mounted on each side of each coupon and were wired to form a Wheatstone bridge. By using a half bridge, the effects of any bending that the coupons may have been subjected to during the test were eliminated and the sensitivity of the strain readings was doubled as compared with the use of a single gauge. Initially, strain gauge readings were made using a Budd Strain Indicator. A gauge length of 100 mm was used for manual measurements when strains became large enough that the gauges ceased to function or became unbonded. All coupons were tested in a 880 kN capacity Baldwin universal testing machine in accordance with ASTM Designation E8M-85 (ASTM, 1986).

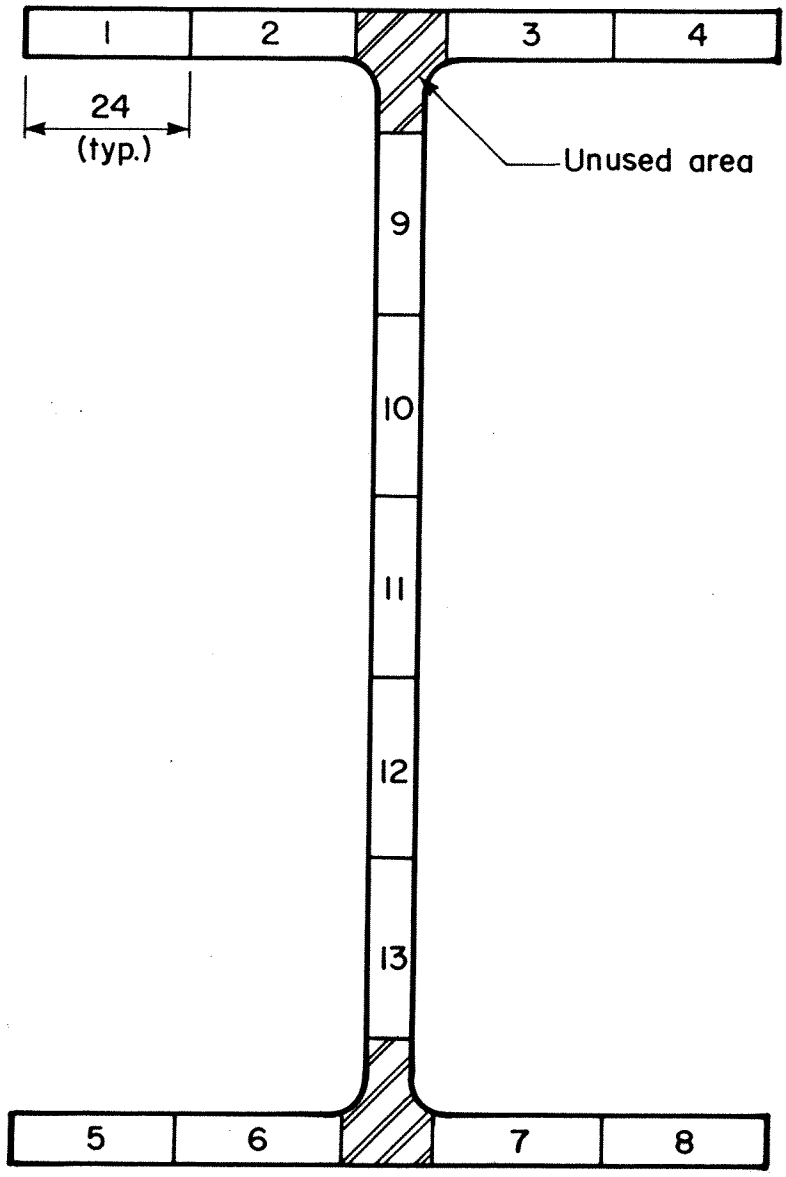

Figure 3.12 Location of tensile coupons on cross-section

Figs. 3.13 and 3.14 show typical stress-strain curves for coupons taken from the flange and the web, respectively. A summary of the data obtained from these tests is given in Table 3.2 including mean values and coefficients of variation.

3.6 Strain Distributions Under Combined Flexure and Torsion

From the strain readings obtained using the electrical resistance strain gauges positioned 30 mm from the fixed end, the strain distribution across the cross-section can be obtained. Such strain distributions for beams 3 and 4 are shown in Figs. 3.15a and 3.16a for the loads corresponding to points C and D of Figs. 3.8, 3.9, 3.10 and 3.11. Beams 3 and 4 have been selected because at the end of the first phase of torsional behaviour (points C and D, respectively), both beams are subjected to substantial bending moments and torques. Points C and D have been chosen for reasons discussed in Section 5.1.3.1.

The non-linear strain variations across the flanges and through the depth of the web indicate that the flanges and web warp. It is also noted that there are three locations where the strain is zero, one in each flange and one in the web. The limited strain readings also show that the strain gradient at at least two of the flange tips out of four is steep.

Based on the stress-strain curves obtained from the ancillary tests, these strain distributions give the normal

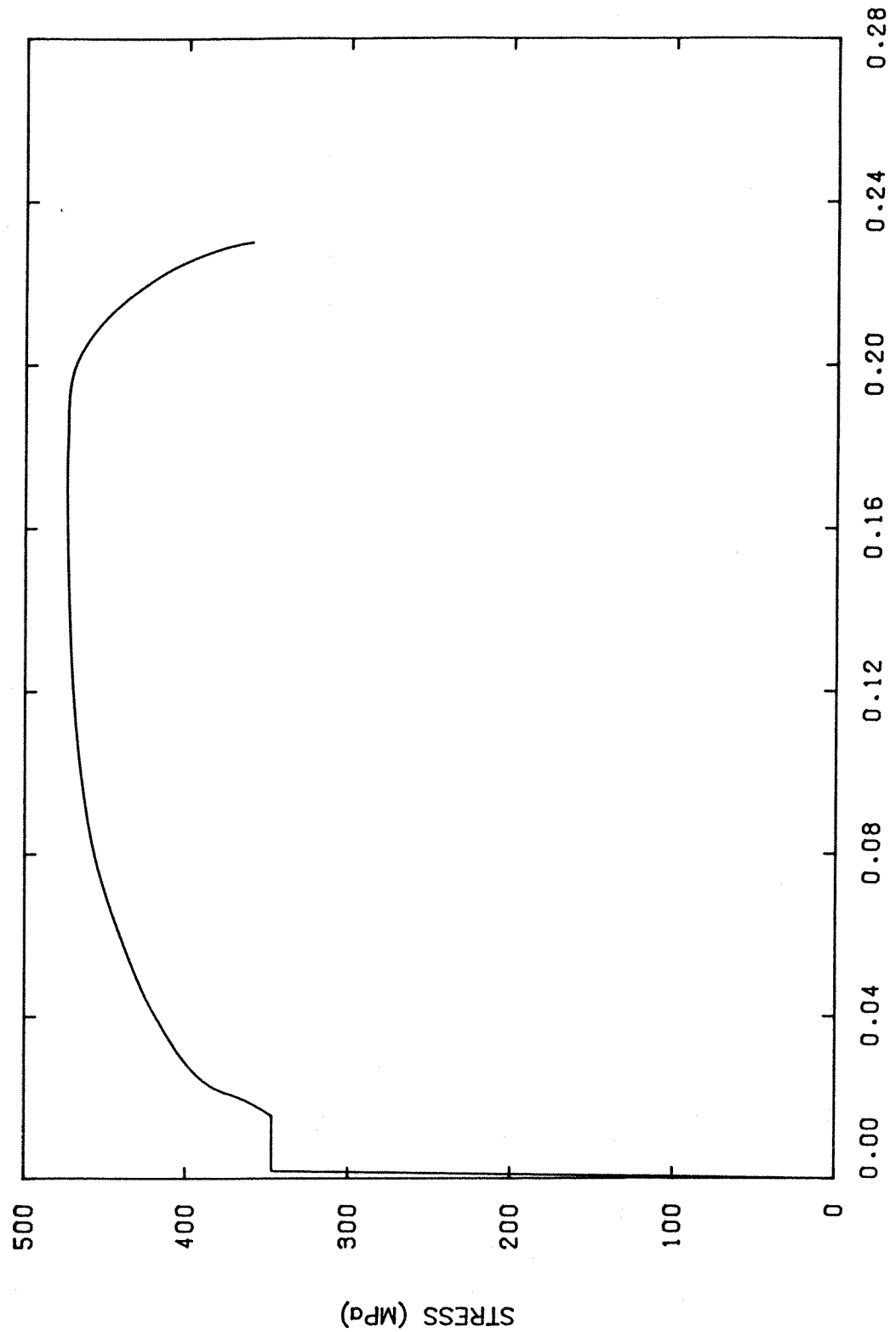

Figure 3.13 Typical stress-strain curve (flange coupon)

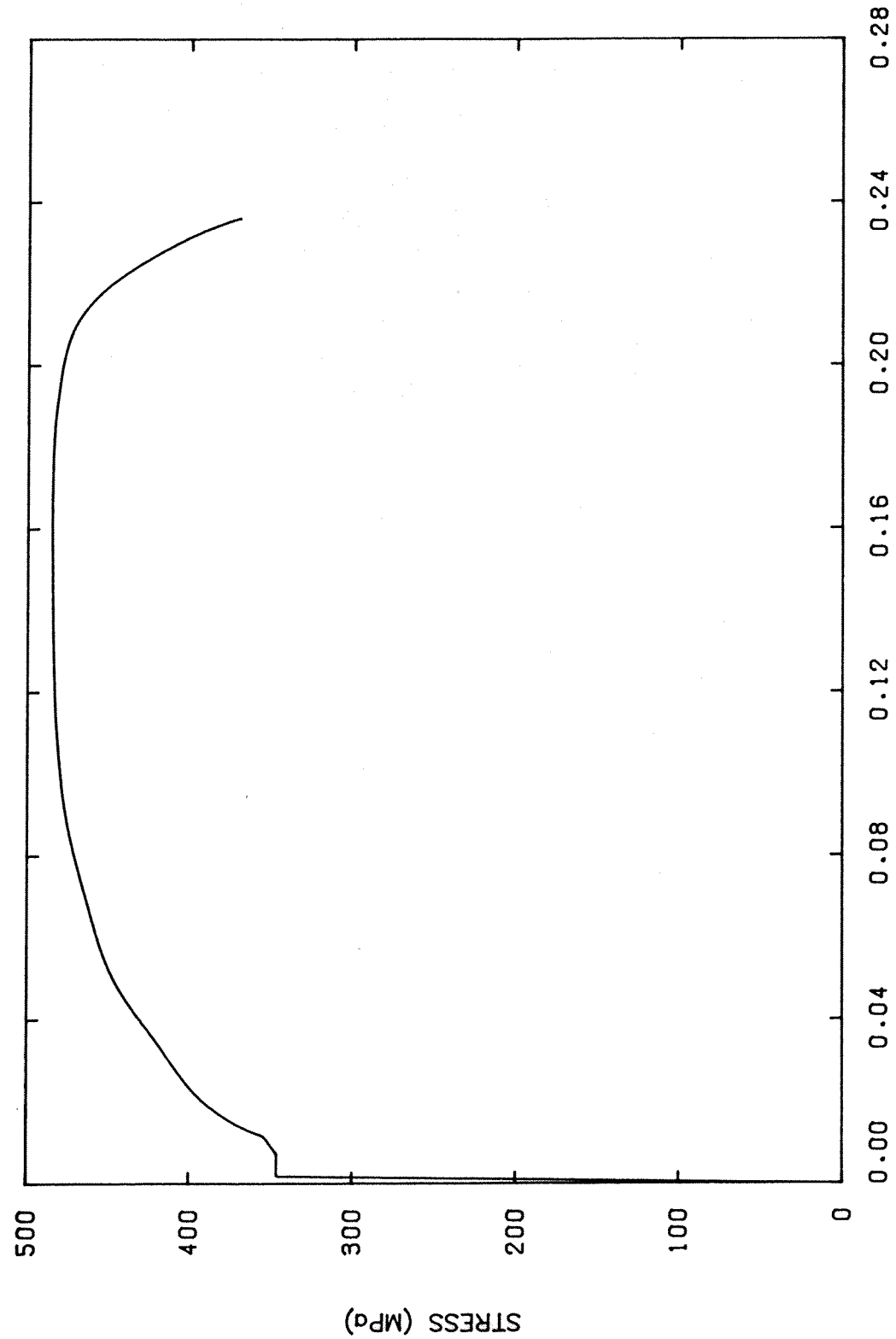

Figure 3.14 Typical stress-strain curve (web coupon)

Table 3.2 Tensile coupon test results

Test No.	σ_y (MPa)	σ_{yu} (MPa)	σ_{ys} (MPa)	σ_u (MPa)	ϵ_y	ϵ_{st}	ϵ_f	E (MPa)	E_{st} (MPa)
1	345	-	-	470	0.00190	-	0.210	198,996	-
2	331	-	314	472	0.00190	0.0138	0.290	200,858	5770
3	333	344	310	472	0.00180	0.0152	0.264	204,584	5880
4	343	352	320	466	0.00190	0.0160	0.246	199,065	8650
5	349	364	330	472	0.00190	0.0110	0.190	203,176	4080
6	330	-	313	467	0.00185	0.0160	0.275	201,746	9600
7	332	338	313	466	0.00170	0.0164	0.278	201,963	6670
8	347	352	329	474	0.00190	0.0154	0.230	204,627	4550
9	346	351	328	484	0.00185	-	-	203,990	6090
10	336	354	318	462	0.00185	0.0168	0.257	204,091	5138
11	342	358	325	469	0.00180	-	0.250	205,581	-
12	333	354	317	464	0.00180	0.0184	0.248	207,749	2930
13	348	352	330	485	0.00185	0.0104	0.236	202,922	4880
$\bar{x}$	340	352	321	471	0.00185	0.0149	0.248	203,027	5840
V(%)	2.12	2.01	2.32	1.47	3.21	17.0	11.5	1.23	33.1

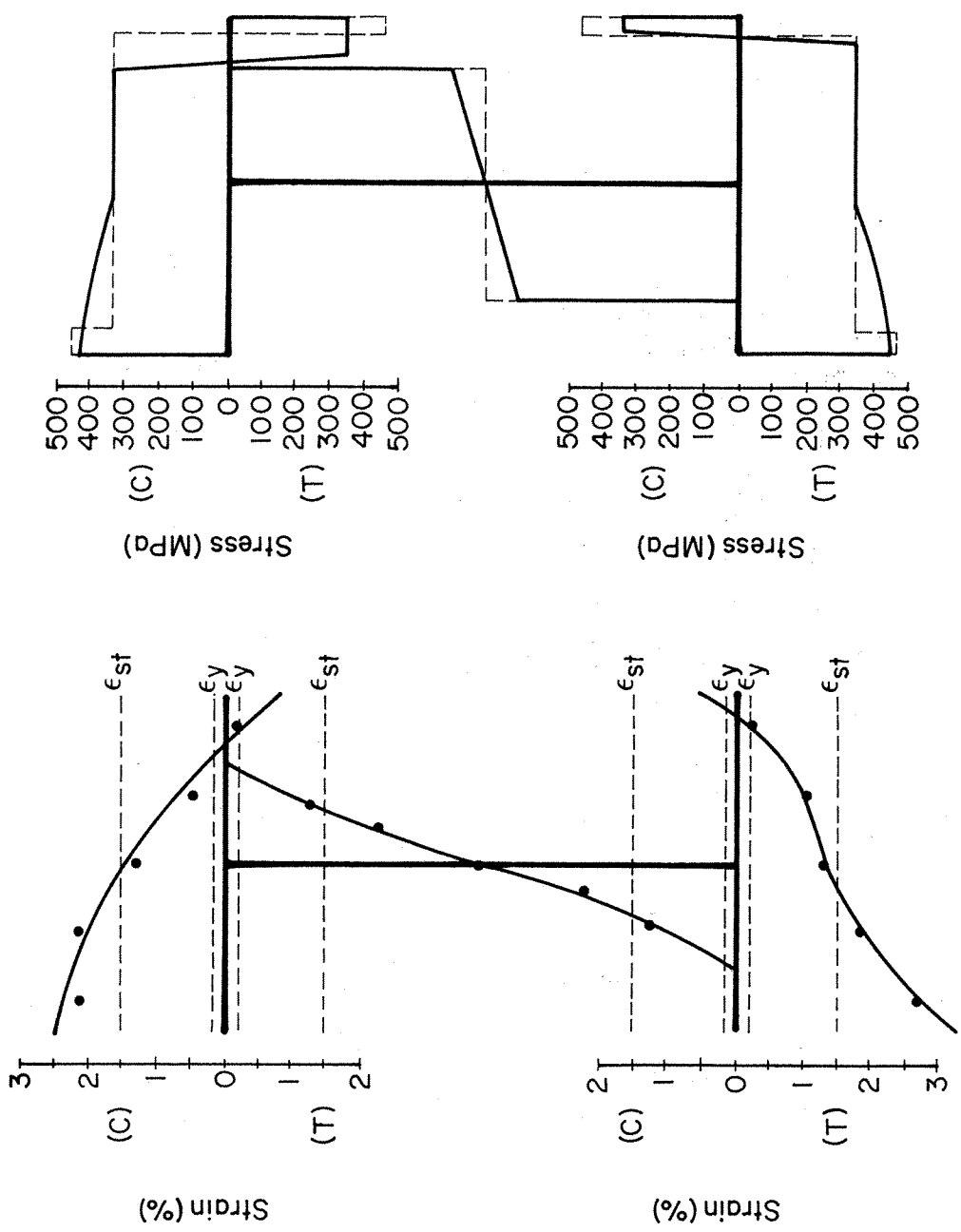

(a) Strain distribution (b) Stress distribution

Figure 3.15 Strain and stress distributions on cross-section - beam 3

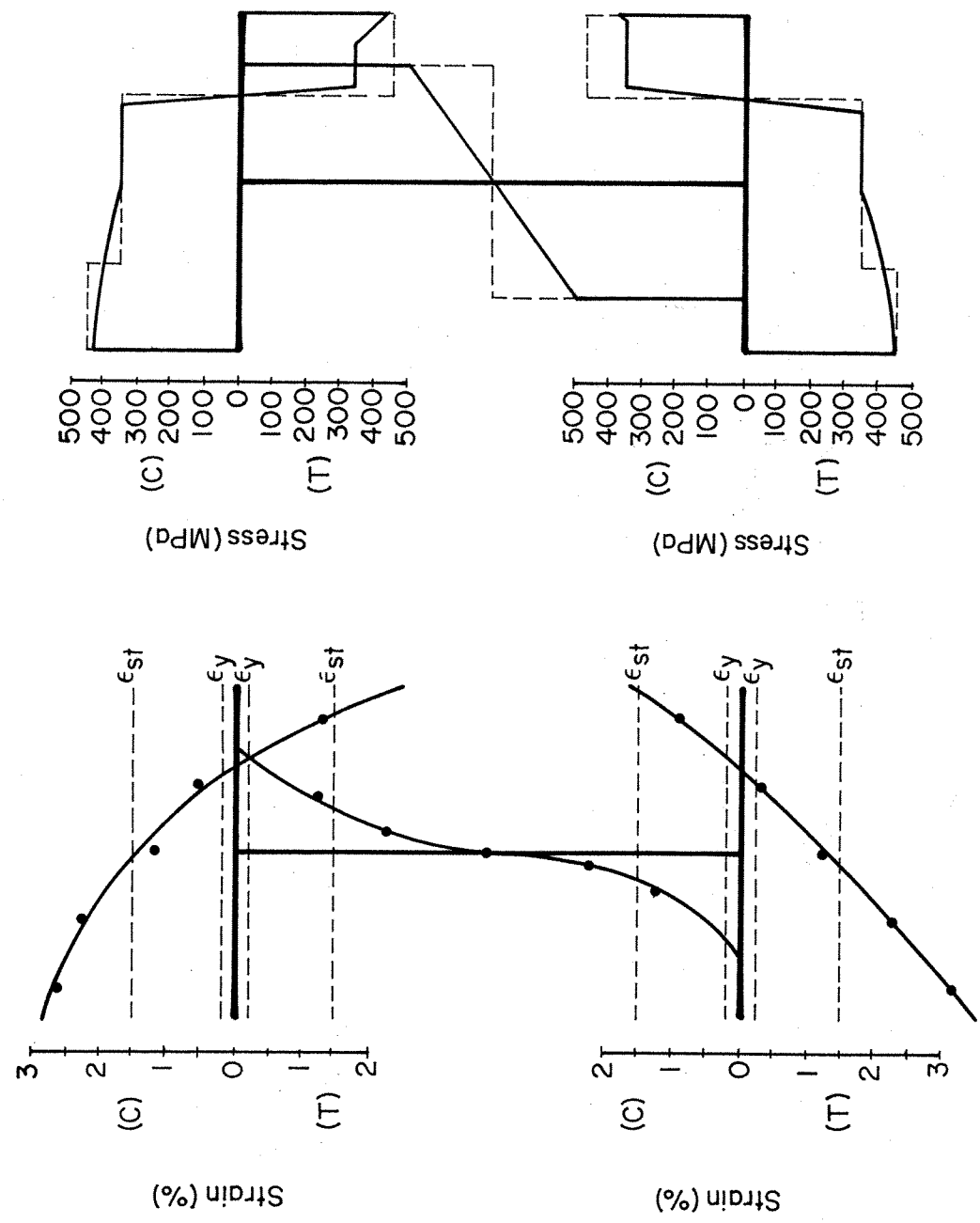

Figure 3.16 Strain and stress distributions on cross-section - beam 4

stress distributions over the cross-section shown in Figs. 3.15b and 3.16b. At the load steps corresponding to the end of the first phase of torsional behaviour, point C for beam 3 and point D for beam 4, the stress distributions show that only a small portion of the web and each flange is behaving elastically. As well, a significant portion of each flange carries stresses approaching the ultimate tensile strength. Idealized stress distributions approximating those consistent with the strain measurements, and as further discussed in Section 4.3, are shown by dashed lines in Figs. 3.15b and 3.16b.

4. ANALYSES

4.1 Introduction

A method of developing a sound limit states design procedure, is to use a lower bound approach which requires that (Lay, 1982):

1. Internal and external forces must be in equilibrium.
2. Assumed internal forces may not exceed the relevant force capacity.
3. Materials must exhibit ductile behaviour.

Interaction equations are often used for the design of members subject to more than one type of load. For combined bending and torsion, the bending moment, the pure torsion, and the warping torsion must be considered. In the fully plastic condition, these are the plastic bending moment, M_p, the sand heap torque, T_{sh}, and the plastic warping torque, T_{wp}. The first two are properties of the cross-section but the plastic warping torque is a function of the cross-section, end conditions, type of load, position of load, and length of beam. It is not uniquely defined for a given cross-section.

Serviceability limit states must also be met and one method of ensuring that deflections remain relatively small is to limit stresses to the yield value at service loads. As well, deflections may be limited in accordance with the anticipated use of the structure or by deformations that can be tolerated by materials supported by the beam.

4.2 Torsion Quantities

4.2.1 Torsional End Conditions

The torsional resistance of a member depends on the torsional end conditions which may be fixed, pinned, free, or some intermediate condition.

A torsionally fixed condition exists when the end of a beam is built into a completely rigid support. In this case, the section does not twist and the flanges do not warp, that is, the angle of twist, ϕ, and the rate of change of the angle of twist, ϕ', are both zero.

A torsionally pinned condition exists when the beam is supported by the web alone. In this case, the section does not twist but the flanges are free to warp and no flange moments develop. The angle of twist, ϕ, is zero as the section remains vertical and the second derivative, ϕ'', is zero as no flange moments exist.

A torsionally free condition occurs when the beam is not restrained in any way and the beam may twist and warp freely. Hence, no flange moments develop and ϕ'' is zero.

Real end conditions can be approximated by the idealized conditions.

4.2.2 Sand Heap Torque

The sand heap torque (Nadai, 1931) corresponds to the condition where the cross-section is fully yielded in shear. Sand is assumed to be piled on the cross-section and the

angle of repose of the sand corresponds to the shearing yield stress. Twice the volume of the sand is the total torque carried by the cross-section. If an I-shaped beam is considered to be made up of three rectangles, the sand heap torque, assuming the von Mises-Hencky yield criterion to be valid, is

$$[4.1] \qquad T_{sh} = \frac{1}{6\sqrt{3}}[4t^3+6(b-t)t^2+3(d-2t)w^2+w^3]\sigma_y$$

If the yield stress is replaced by the ultimate stress, σ_u, in [4.1], the result is the ultimate sand heap torque, T_{shu}, based on the von Mises-Hencky criterion extended to the ultimate condition. The quantity T_{sh}/σ_y or T_{shu}/σ_u is a property of the cross-section called the sand heap modulus, Z_{sh}, and could be tabulated in steel handbooks.

Equation [4.1] neglects the contribution of the fillets to the torque carrying capacity of the cross-section which is generally considered to be negligible. However, the volume of sand in the heap varies as the thickness squared, and for a W150X18, the fillets contribute an additional 16.5% to the sand heap torque.

4.2.3 Plastic Warping Torque

The plastic warping torque, T_{wp}, is the torque that causes full plastification of the flanges due to tensile or compressive normal stresses. These stresses (Fig. 2.12) give rise to internal plastic flange moments (for rectangular

flanges) of

$$M_{fp} = \frac{b^2 t \sigma_y}{4} \qquad [4.2]$$

Full plastification occurs only at the most highly stressed cross-section, and the corresponding flange shear distribution, V_f, depends on the end and loading conditions. A torsionally pinned beam with a concentrated torque at midspan has the torque, flange shear, and flange moment diagrams shown in Fig. 4.1. The flange shear is

$$V_f = \frac{2M_{fp}}{L} \qquad [4.3]$$

The warping plastic torque, obtained by multiplying the flange shear by the distance between flange centroids, and combining [4.2] and [4.3], is

$$T_{wp} = \frac{1}{2}[b^2 t(d-t)/L]\sigma_y \qquad [4.4]$$

The plastic warping torque for other end and loading conditions can be developed similarly and in general is given by

$$T_{wp} = [Kb^2 t(d-t)/L]\sigma_y \qquad [4.5]$$

Values of the warping factor, K, for different end and loading conditions are given in Table 4.1. If the yield

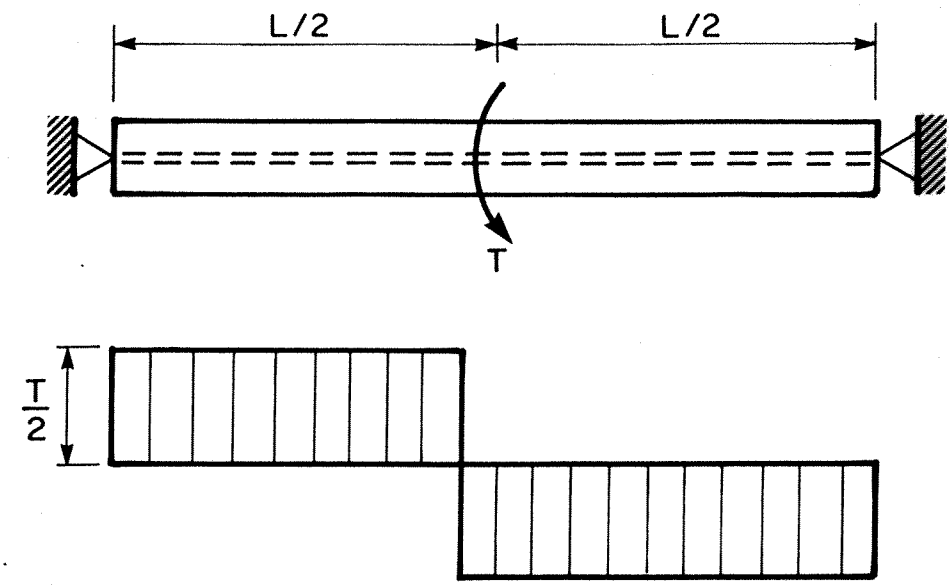

(a) Torque

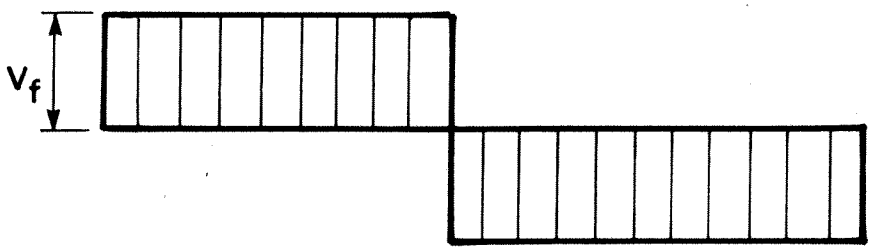

(b) Flange shear

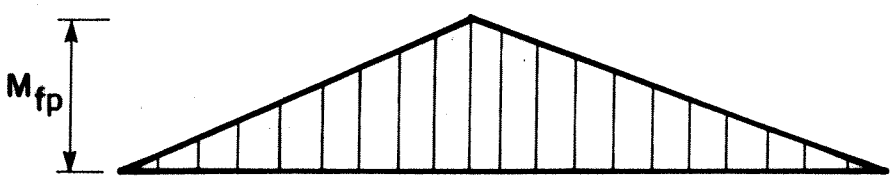

(c) Flange moment

Figure 4.1 Flange shear and moment diagrams for a pin-ended beam

Table 4.1 Values of warping factor K

LOAD CONDITION	TORSIONAL END CONDITIONS			
	Pinned-Pinned	Fixed-Fixed	Fixed-Free	Fixed-Pinned
Uniformly Distributed Torque	1	3/2	1/2	5/4
Concentrated Torque at Midspan	1/2	1	-	11/12
Concentrated Torque at Free End	-	-	1/4	-
Concentrated Torque at X	* $\frac{1}{4(X/L)}$	* $\frac{2(X/L)+1}{4(X/L)}$	** $\frac{1}{4(X/L)}$	** $(X/L) < 0.586$ $\frac{2+2(X/L)-(X/L)^2}{4(X/L)(2-(X/L))}$ $0.586 < (X/L) < 0.653$ $\frac{2+2(X/L)-(X/L)^2}{4(X/L)^2(3-(X/L))}$ $(X/L) > 0.653$ $\frac{1}{4(1-(X/L))}$

Notes: * X measured from closer end
** X measured from fixed end

stress is replaced with the ultimate stress, σ_u, in [4.5] the result is the ultimate warping torque, T_{wu}. The quantity T_{wp}/σ_y or T_{wu}/σ_u, the plastic warping modulus, Z_w, is not a property of the cross-section.

4.3 Bending-Torsion Interaction Model

4.3.1 Ultimate Limit States

4.3.1.1 Class 1 Beams

The proposed idealized fully plastic stress distribution on the cross-section of a class 1 beam subjected to both flexure and warping torsion is shown in Fig. 4.2. This distribution is a reasonable approximation to the distribution determined from the strain measurements near the fixed end as shown in Figs. 3.15b and 3.16b. The web and central portion of the flanges resist the bending moment, and stresses in the flange tips form a couple, M_f, that resists torque. The warping torsional normal stresses are assumed to reach the ultimate strength of the material, while the flexural normal stresses are considered to reach the yield strength only, as discussed subsequently in Section 4.3.1.2.

The flanges are bent in simple flexure in the lateral direction due to warping. Therefore, the plastic flange moments (due to warping) and bending moments on the remainder of the section, are a maximum at the same

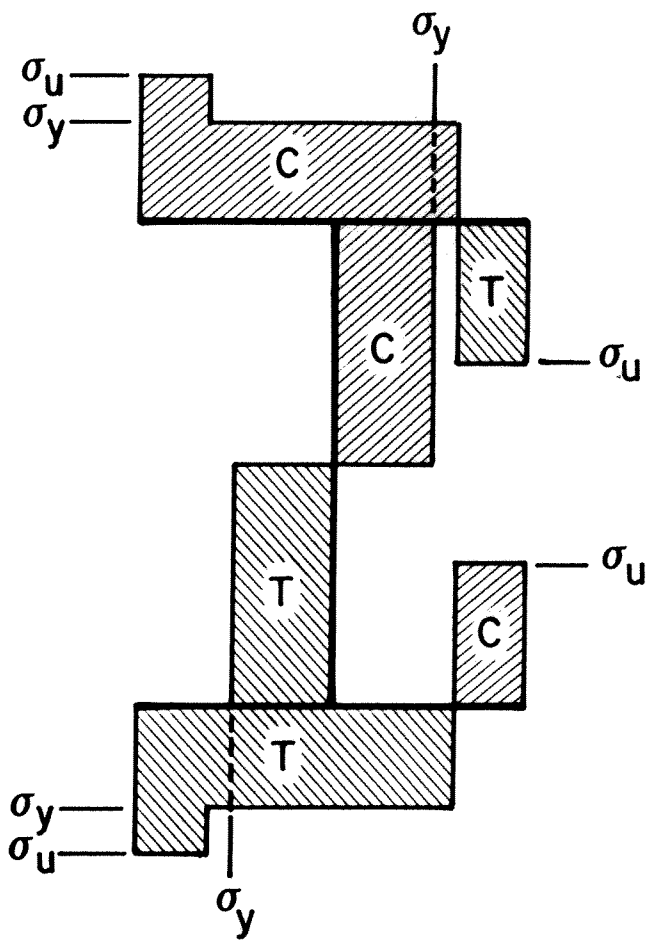

Figure 4.2 Normal stress distribution for interaction model

location on the beam, when the flexural and torsional end conditions are the same. An example of this is a simply supported beam subjected to an eccentric vertical load at midspan as shown in Fig. 4.3. The vertical shear force, and flange shear force diagrams are the same shape, as are the bending moment and warping or flange moment diagrams. This analysis is also valid when flexural and torsional end conditions are not the same, provided only that the maximum bending moment and the maximum flange moment due to torque occur at the same cross-section. This is the case, for example (perhaps somewhat unusual), when a beam is flexurally pinned and torsionally fixed with a concentrated eccentric load at midspan, as shown in Fig. 4.4.

In addition to normal stresses, the cross-section is assumed to be able to carry the full sand heap torque based on the ultimate stress, T_{shu}, whether or not the section of maximum torque and maximum moment are coincident. It is recognized that this may violate commonly accepted failure criteria, as discussed subsequently in Section 4.3.1.3. Flexural shear stresses are normally relatively small and are neglected.

Failure is considered to occur when the load-carrying capacity of one section of a beam is exceeded, regardless of the degree of redundancy, i.e., no allowance is made for moment redistribution. Because of the assumption that warping normal stresses reach the

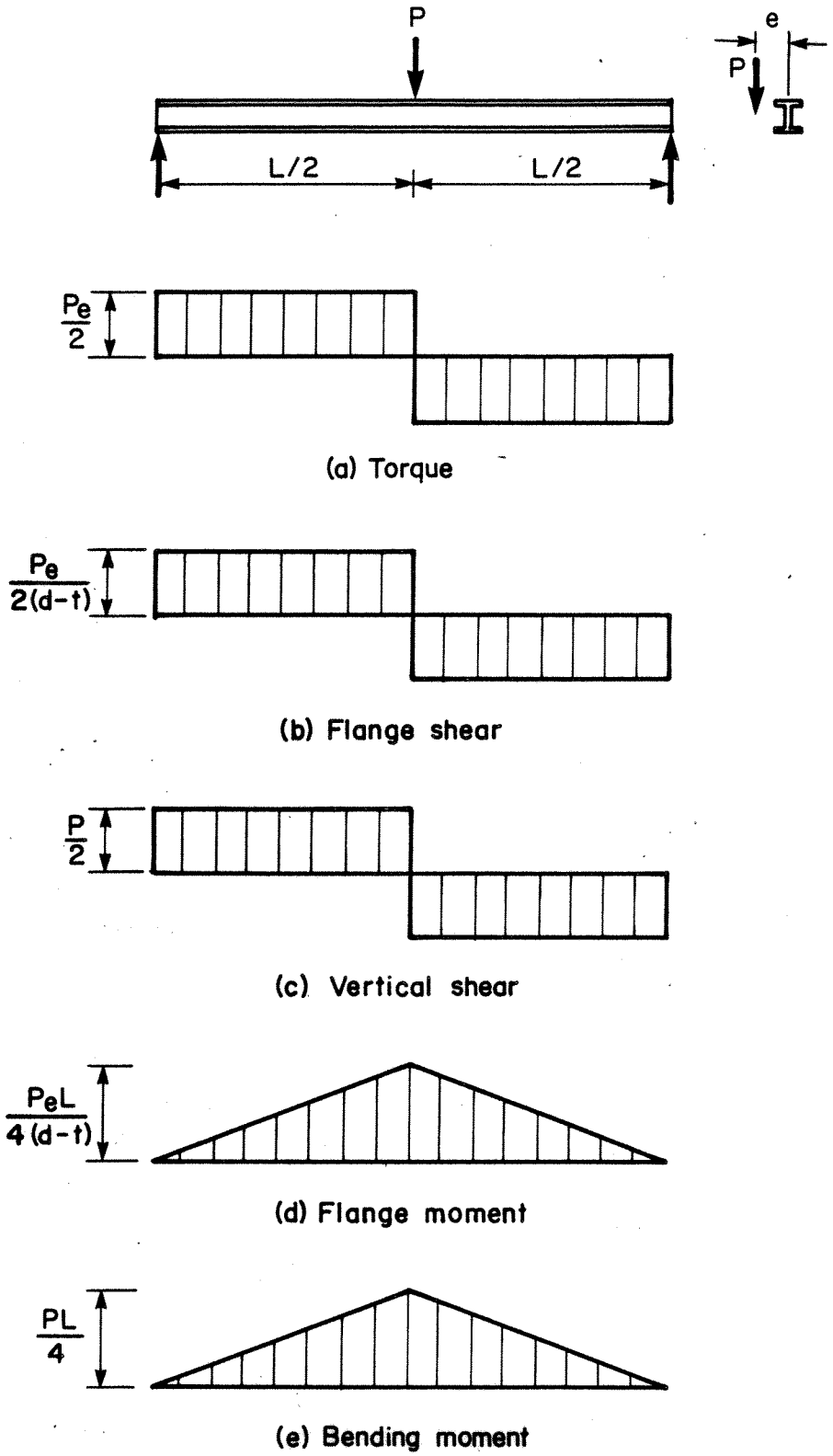

Figure 4.3 Torque, shear, and moment diagrams for a simply supported beam

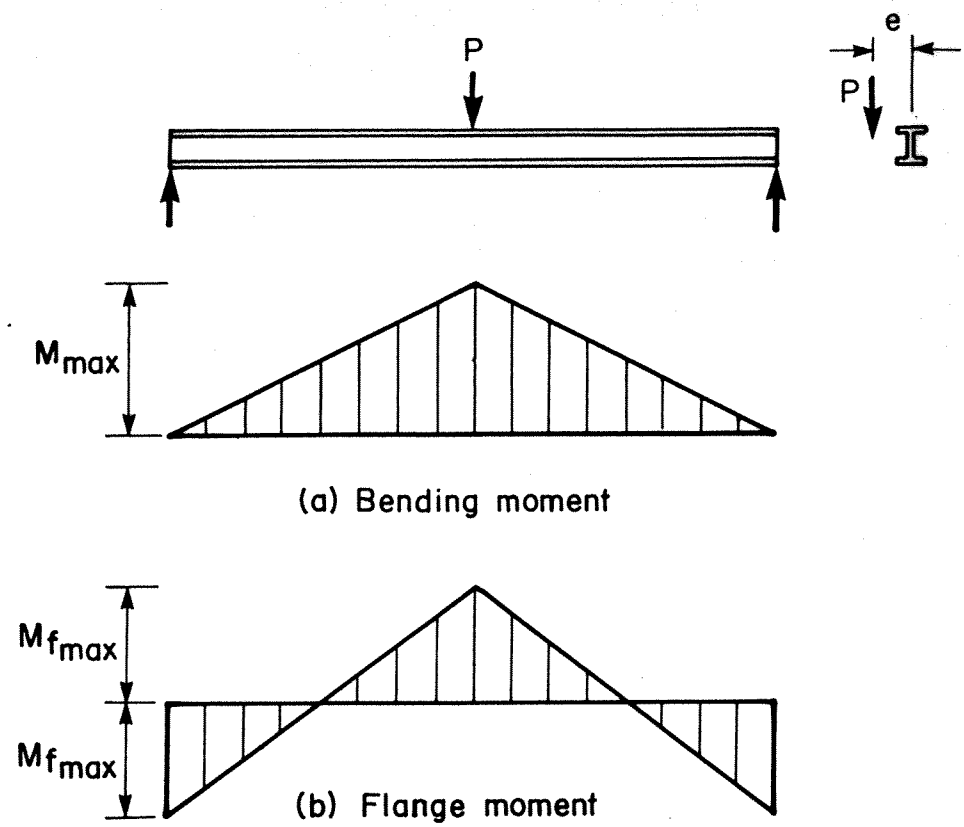

Figure 4.4 Moment diagrams for a flexurally pinned, torsionally fixed beam

ultimate stress, as described in Section 4.3.1.2, the model is restricted to class 1 sections only. Fig. 4.5 shows the non-dimensionalized moment-torque interaction diagram for class 1 beams. The interaction diagram is constructed as follows.

The maximum bending moment is the fully plastic moment, M_p, based on the yield stress of the material as given in the Canadian standard CAN3-S16.1-M84 (CSA, 1984) and as corroborated by extensive tests (Yura et al., 1978), that is,

$$M_{max} = M_p = Z\sigma_y \qquad [4.6]$$

This moment can be carried provided no warping torsion is needed to be developed and thus the interaction diagram extends horizontally at $M/M_p = 1.0$ from point A to the point representing the ultimate sand heap torque, point B. The sand heap torque is considered to coexist with the fully plastic moment.

The maximum torque is the ultimate torque, T_u, that is,

$$T_{max} = T_u = T_{shu} + T_{wu} = Z_{sh}\sigma_u + Z_w\sigma_u \qquad [4.7]$$

where T_{shu} and T_{wu} are calculated using [4.1] and [4.5] respectively, based on the ultimate stress. It is considered that this torque can be carried even when the

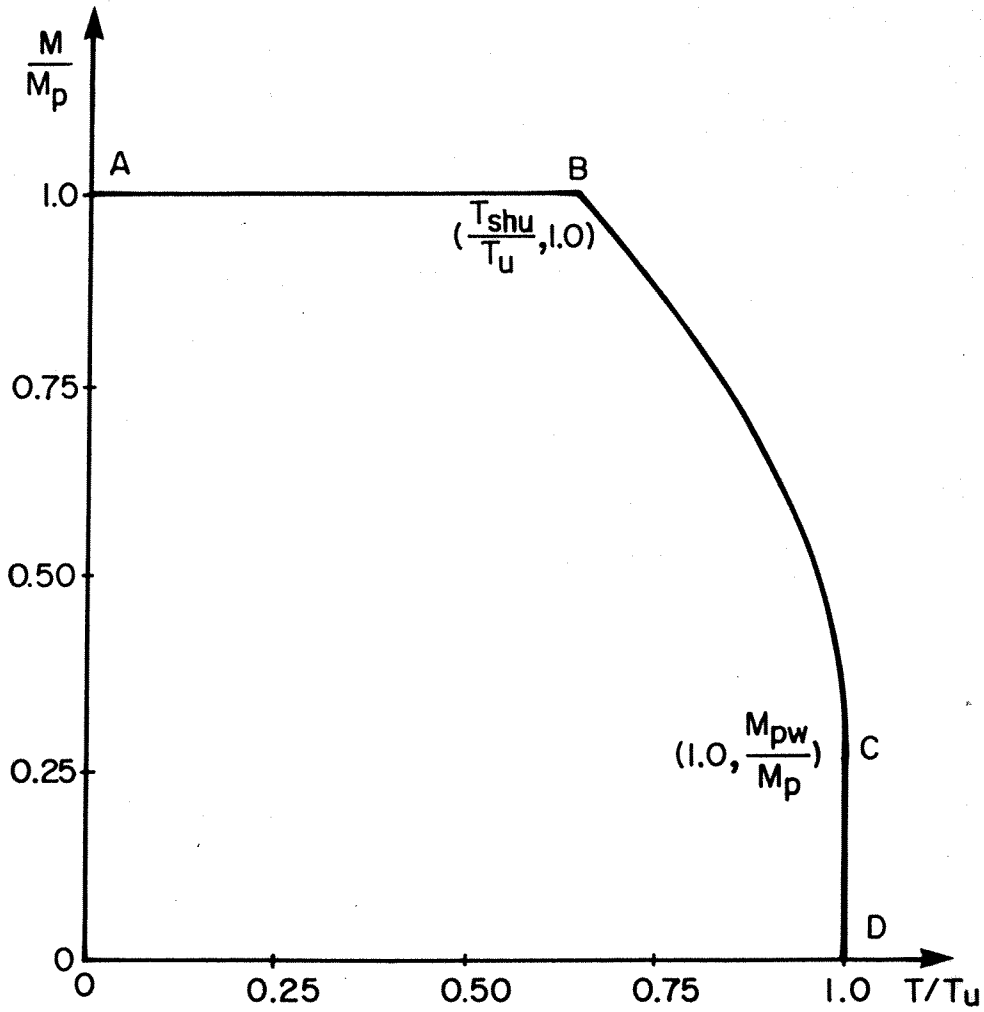

Figure 4.5 Moment-torque interaction diagram for class 1 beams

web is fully yielded due to flexural moments as represented by point C. Thus, at $T/T_u = 1.0$ the diagram extends vertically from point D to point C.

When the flanges are carrying both bending normal stresses and warping normal stresses, the interaction curve is a parabola extending from its vertex at C to B. The length of each flange tip that carries warping stresses is

$$[4.8] \qquad b_w = \frac{b}{2} - \frac{M_{bf}}{2t(d-t)\sigma_y}$$

where M_{bf} is the portion of the bending moment carried by the flanges. The flange shear and the warping flange moment are related by

$$[4.9] \qquad V_f = \frac{4KM_f}{L} = \frac{4K}{L}[b_w t(b-b_w)\sigma_u]$$

Substituting [4.8] into [4.9] and noting that the warping torque is a couple consisting of the flange shears gives

$$[4.10a] \quad T_w = (d-t)\frac{4K}{L}\left[\frac{b}{2} - \frac{M_{bf}}{2t(d-t)\sigma_y}\right]t\left[\frac{b}{2} + \frac{M_{bf}}{2t(d-t)\sigma_y}\right]\sigma_u$$

$$[4.10b] \quad T_w = \frac{4Kt(d-t)\sigma_u}{L}\left[\frac{b^2}{4} - \frac{M_{bf}^2}{4t^2(d-t)^2\sigma_y^2}\right]$$

$$[4.10c] \quad T_w = -M_{bf}^2\left[\frac{K\sigma_u}{t(d-t)L\sigma_y^2}\right] + \frac{Kb^2t(d-t)\sigma_u}{L}$$

The last term of [4.10c] is the ultimate warping torque, T_{wu}. Thus, [4.10c] can be rewritten as

$$\frac{M_{bf}^2}{M_{pf}^2} + \frac{T_w}{T_{wu}} = 1, \qquad [4.11]$$

the equation of a parabola (with vertex at C when the contribution of the web to bending resistance and sand heap torque to torsion resistance are added). This is similar to [2.17], derived by Kollbrunner et al. (1978), but with warping stresses at the ultimate value.

The computer program *MTINT*, given in Appendix C, calculates the moment-torque interaction curves for available W-shapes, or I-shaped sections consisting of three rectangular plates, for different end and loading conditions as expressed by the warping factor, K.

4.3.1.2 Normal Stresses at Failure

In Fig. 4.2, normal stresses are assumed to reach the ultimate tensile strength for the portion of the cross-section that resists warping torsion, while the flexural stresses are assumed to reach the yield stress only. These assumptions are in reasonable agreement with the test results, as discussed previously. Furthermore, the assumption that the flexural stresses reach the yield stress is consistent with the results of Dawe and Kulak (1981), who showed that in simple flexure, local buckling limits the ultimate moment that is achieved to

a value consistent with reaching the yield stress, even for many class 1 beams. Yura et al. (1978) found a test/predicted moment ratio of 1.10 with a coefficient of variation of 0.11 for compact beams based on the plastic moment capacity. Under torsion alone, however, only half of each flange is in compression and the strain gradient is from a maximum at the flange tip to zero at the web. This less severe strain condition allows stresses to exceed the yield value for class 1 beams and is the basis for the assumption that the stresses approach the ultimate stress before local buckling occurs. The presence of torsional shear stresses tends to cause early straining beyond the strain hardening strain and thus the development of stresses exceeding the yield value.

4.3.1.3 Violation of Lower Bound Theorem

One of the criteria of the lower bound theorem is that the assumed internal forces do not exceed the relevant force capacity. The assumption that ultimate shear stresses can co-exist with ultimate normal stresses on an element of the cross-section apparently violates this criterion. There are, however, mitigating circumstances. For that portion of the flange in compression, the maximum stress could exceed the maximum tensile stress as there is no tendency for the section to neck; the material simply expands perpendicular to the compressive force. For that portion in tension, the

shearing stresses do not tend to reduce the cross-sectional area and therefore do not exacerbate the situation in the plane of the cross-section. The combined bending and torsion tests showed that necking occurred perpendicular to the longitudinal axis and was very localized. The cross-sectional area on the principal plane remained virtually constant. Therefore, in this plane the tensile stress could exceed the maximum "engineering" ultimate strength without exceeding the true ultimate strength.

In resisting torsional loads, both the ultimate sand heap resistance, T_{shu}, and the ultimate warping resistance, T_{wu}, have been considered to be fully active. In elastic theory, the two torsional components vary along the length of the beam depending on the degree of warping restraint. Specifically, no St. Venant torque exists at a point of full warping restraint. It is postulated, however, that in the inelastic region, plastification of the flanges allows sufficient flange rotation for sand heap stresses to be developed. Kinks in the flanges of the test specimens in opposite directions at the fixed end confirm that upon plastification, the expected flange rotations did occur. Also, the large torques observed during the experimental program seem to corroborate this theory.

4.3.1.4 Helix Effect

Boulton (1962) observed that torques higher than the theoretical fully plastic torque could be carried and ascribed this to the helix effect as described in Section 2.4. The rotations required to obtain significant benefit from the helix effect are, however, so large that this phenomenon is of academic interest only. In a torsion test on a fixed ended beam, Boulton showed that an increase in torsional strength of 6.6% occurred when the beam was twisted at a rate of 0.9 degrees/inch. Assuming uniform twist over the length of the beam, this corresponds to an angle of twist of 35.4 degrees for the cantilever beams tested during this research. Considering the difference in end conditions, for these tests the increase in strength would be expected to be even less than 6.6% and is therefore neglected.

4.3.1.5 Lateral Torsional Buckling

In order for the assumed stress distributions to be achieved, lateral instability of the member as a whole must not occur. Thus, when the length of the beam is such that the flexural moment capacity is limited by lateral torsional buckling, the interaction curve for bending and torsion should also be limited by that value.

Tests of Razzaq and Galambos (1979) on class 1 beams subjected to bending and torsion where the

flexural capacity was limited by lateral torsional buckling showed that strain hardening played no role in the behaviour of the beams. Therefore, under these circumstances it is proposed that the maximum torque be limited to the plastic torque, T_p, based on the yield stress rather than the ultimate torque, T_u. As a further simplification, the parabolic portion of the interaction curve is replaced by a straight line.

4.3.1.6 Extension to Class 2 and 3 Sections

Class 2 cross-sections are those which reach the full plastic moment before local buckling occurs, but are not capable of undergoing large plastic hinge rotations. Because the interaction diagram limits the bending moment to the plastic value, the requirement remains the same for bending. For class 2 cross-sections, local buckling may, however, occur before the large strains at the flange tips associated with ultimate torsional stresses are reached. Therefore, it is proposed that torsional warping and shear stresses be limited to yield values. This would result in an interaction curve of the same shape as that shown in Fig. 4.5, except that the maximum torque corresponds to

$$[4.12] \qquad T_p = T_{sh} + T_{wp} = Z_{sh}\sigma_y + Z_w\sigma_y$$

where T_{sh} and T_{wp} are calculated from [4.1] and [4.5], respectively. For sections prone to lateral torsional

buckling, the maximum allowable bending moment is limited accordingly, as for class 1 beams. At present, there are no experimental data available to substantiate this approach.

Class 3 cross-sections are those which can reach the yield moment, M_y, before local buckling occurs. In the elastic range, stresses will vary linearly across the flanges and web. Therefore, the plastic stress distribution discussed in Section 4.3.1.1 is invalid.

It is therefore proposed that the limiting moment be the yield moment, M_y, and the limiting torque be the yield torque, T_y, where

[4.13] $$M_y = S\sigma_y$$

and T_y is calculated using an elastic analysis such as that proposed by Heins and Seaburg (1963) with a maximum warping normal stress on the beam equal to the yield stress. Because the torque is carried partially by St. Venant torque and partially by warping torque, this implies the presence of some torsional shear stresses as well. The value of the St. Venant torque present, T_{sv}, is calculated using the curves presented by Heins and Seaburg.

Fig. 4.6 shows the proposed interaction diagram for class 3 beams. It is assumed that the St. Venant torque can be carried without any reduction in moment capacity

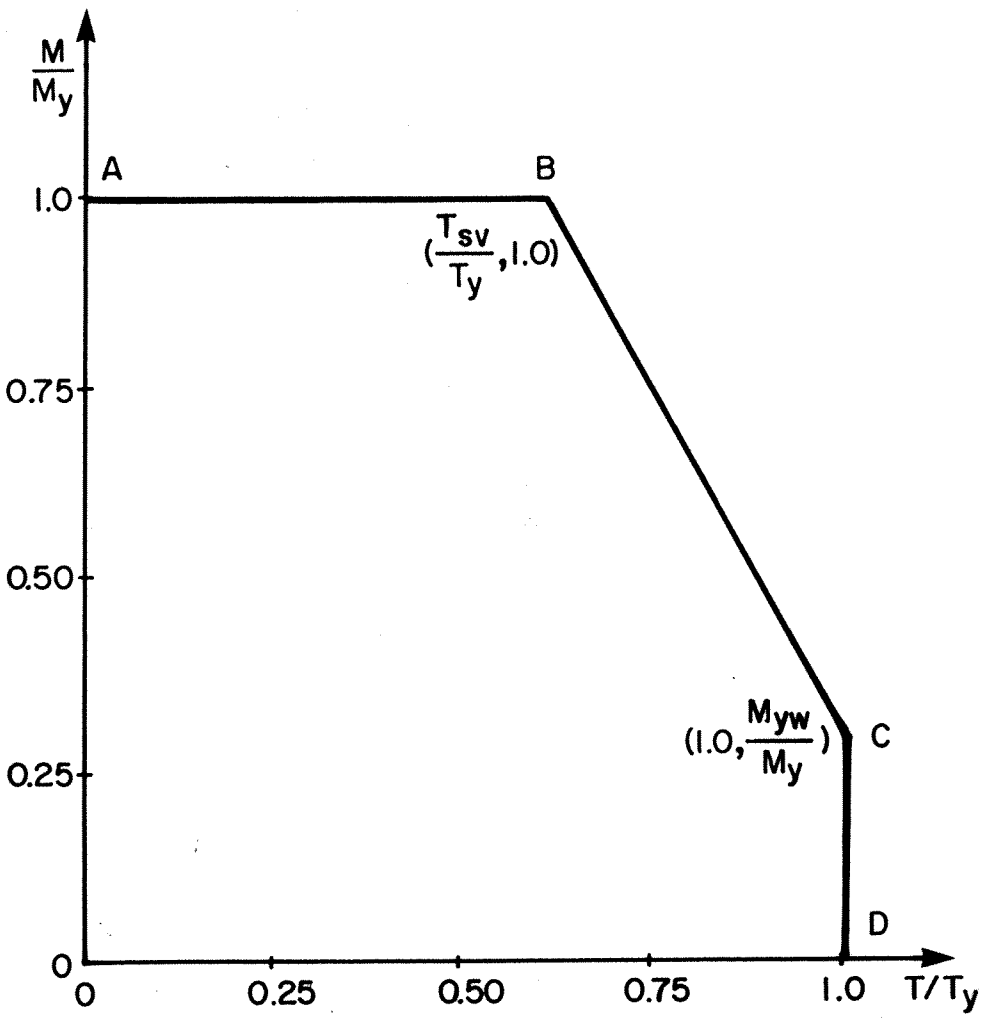

Figure 4.6 Moment-torque interaction diagram for class 3 beams

and the web can carry some moment without any reduction in torsional strength. Points B and C are simply joined with a straight line because the parabolic curve of Fig. 4.5, based on fully plastic conditions, is no longer valid. The maximum bending moment for beams prone to lateral torsional buckling would be reduced as for class 1 and 2 beams. The detrimental interaction of the bending and torsion mechanisms, as described in Section 2.3, is neglected.

Although the elastic analysis for class 3 beams is significantly more time consuming than the inelastic analysis for class 1 and 2 beams and requires the use of graphs, it is interesting to note that only 3 out of 190 W-shape sections listed in the CISC Handbook (CISC, 1984) are class 3.

4.3.2 Serviceability Limit States

A simple approach to ensure that deflections are not excessively large under service loads is to require that the beam does not yield under these loads. Deflections will be essentially elastic. In general, shear stresses are low under service loads and only normal stresses need be checked. It is therefore proposed that one serviceability limit state be based on first yield of the cross-section due to normal stresses with the analysis carried out on the undeformed shape.

Torsional normal stresses and flexural normal stresses will always be additive at at least one point on the cross-section. Adding the effects of bending about the strong axis and torsion, without exceeding the yield stress, results in the linear equation

$$[4.14] \qquad \frac{M}{M_y} + \frac{T}{T_{wy}} = 1$$

where T_{wy} is determined from an elastic analysis such as that prescribed by Heins and Seaburg (1963). The limiting values are the yield moment, M_y (when T equals zero), and the yield warping torque, T_{wy} (when M equals zero). A straight line from M_y on the vertical axis to T_{wy} on the horizontal axis of the moment-torque interaction diagram is the serviceability limit for unfactored loads.

It is recognized that this method neglects the effects of residual stresses and the interaction effects between bending and torsion. Because yielding would take place only at one point on one cross-section along the beam and therefore would be constrained by the surrounding material, it is expected that in most cases this omission would not result in large deflections.

In some cases, however, even elastic deflections may be excessive and therefore another serviceability criterion to be met is that the distortion of the member be limited to certain acceptable values. As for beams in flexure, a deflection limit may be imposed. Of greater significance,

however, is the angle of rotation that the beam undergoes. Excessive rotations may cause cracking of brittle building elements, cause mismatch of building components, and prevent the beam from fulfilling its intended function.

5. DISCUSSION OF TEST RESULTS

5.1 This Research

5.1.1 General

The orientation of the loading cable (see Fig. 3.1) varied slightly from the vertical as the test beams deflected and twisted with the result that loads and moments were applied in three orthogonal directions. Although the tests continued until the load began to decrease, the torque at the fixed end was still increasing due to increasing lateral deflections for beams 1, 2, and 3.

5.1.2 Load Path Dependence

The data indicate that the magnitude of the bending moment at a given torque depends on whether the moment or the torque was applied first. For the four beams, at a torque of 3.3 kN*m, the bending moments were 58.0, 51.3, 40.5, and 32.5 kN*m respectively, as seen in Fig. 5.1. Therefore, the strength of the beam depends on the load path. A bending moment, applied first, can be maintained for a large increase in torque. As more torque is applied concomitantly with the moment, the maximum moment attained decreases.

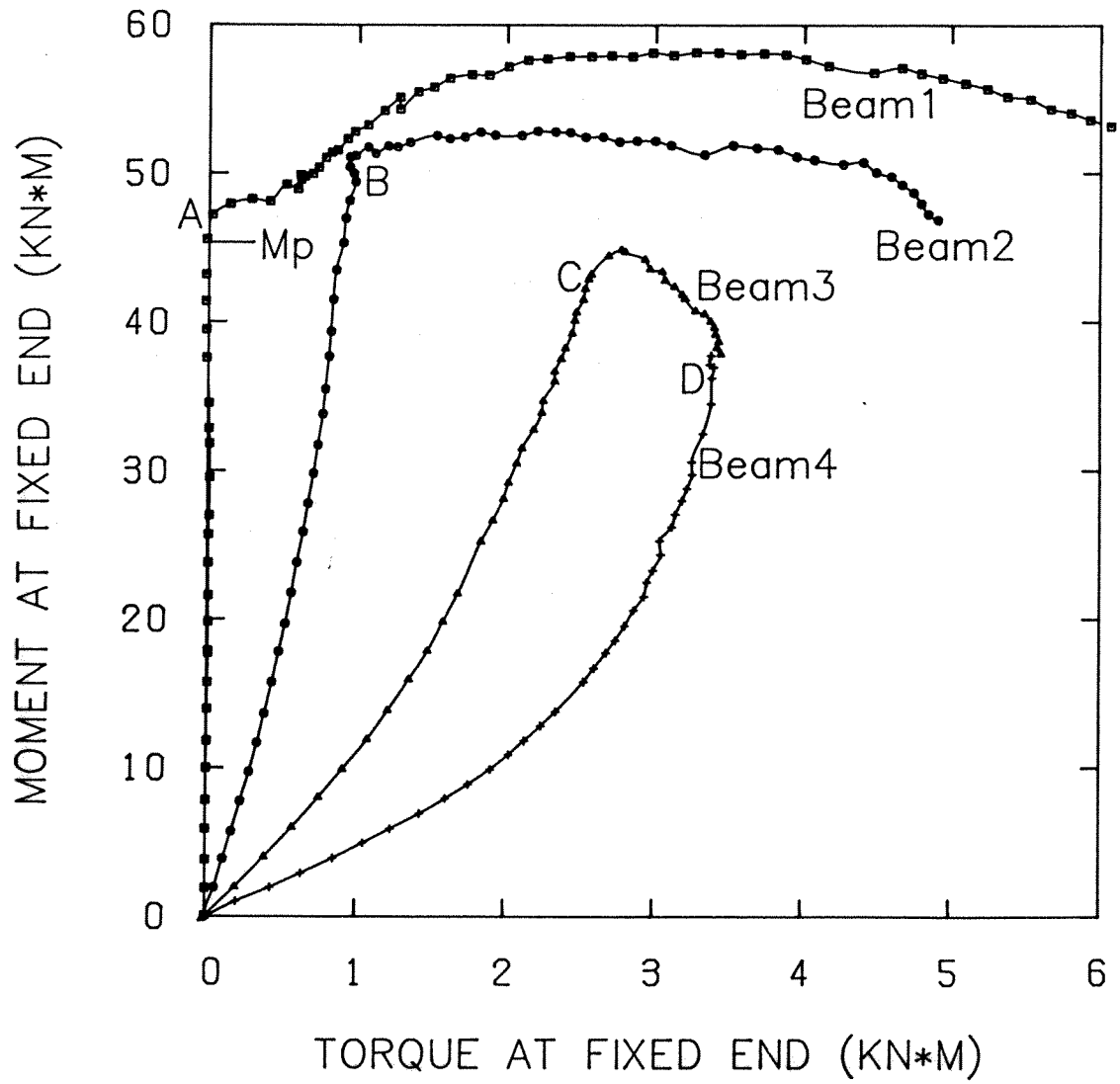

Figure 5.1 Moment versus torque test curves

5.1.3 Second Order Effects

5.1.3.1 Torsional Behaviour

Beams loaded with smaller eccentricities would be expected to fail at higher moments and lower torques. Beam 1, however, carried the highest moment and the highest torque. Fig. 5.2 shows that the torque-rotation behaviour has two distinct components, as best seen for beams 2 and 3. At certain torques, designated by points B and C respectively, the curves suddenly steepen. For beam 1, the curve is always steep; the first component does not exist and point A designating the change in behaviour lies at the origin. For beam 4, the curve never steepens; the second component does not exist and point D designating the change in behaviour lies at the apex of the curve. The first component is related to the torque due to the load being applied eccentrically, that is, the torque on the undeformed member. The second component arises when the beam deforms significantly and is chiefly due to the lateral deflection of the beam.

Beam 1 exhibits only the second type of behaviour (point A lies at the origin). The beam was loaded concentrically and the torque developed only because of the lateral displacement of the free end relative to the fixed end. Beam 4 exhibits only the first behavioural component (point D lies at the apex). As the lateral deflections increased, compensating rotations took place resulting in no overall increase in torque due to

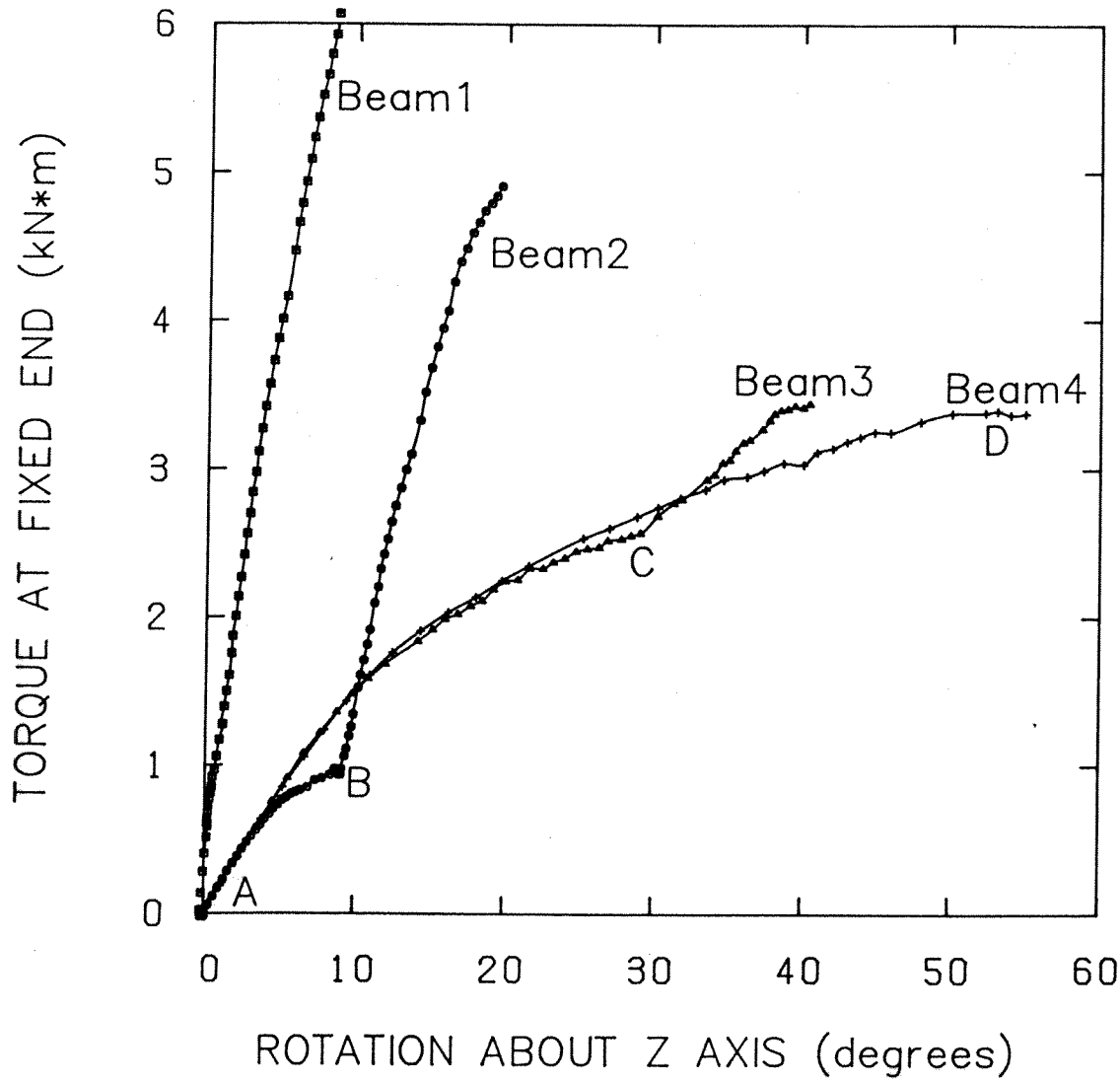

Figure 5.2 Torque versus rotation test curves

deformations. Beams 2 and 3 exhibit both types of behaviour.

The high torques developed because of the second order effects which are considered non-utilizable for two reasons. First, they occur as a result of large lateral deflections and would not exist if these deflections had been restricted. Second, the deflected shape must be known beforehand for this torque to be considered. Therefore, the maximum torque of the first component of the torque-rotation curves and the corresponding moment are considered to represent the ultimate limit state for the beams subjected to combined flexure and torsion.

Fig. 5.3 shows the torque-rotation curves truncated at the points A,B,C, and D of Fig. 5.2, with the second order effects omitted. Beam 4 carries the largest torque and beam 1 carries none. Having eliminated the torques developed as a consequence of the large lateral deflections, the effect of load path dependence no longer exists.

5.1.3.2 Absolute Maximum Moments and Torques

Although it is proposed that the additional moments and torques that resulted from deformation of the beams not be used for ultimate limit states design, the question remains how the beams could sustain such high moments and torques simultaneously.

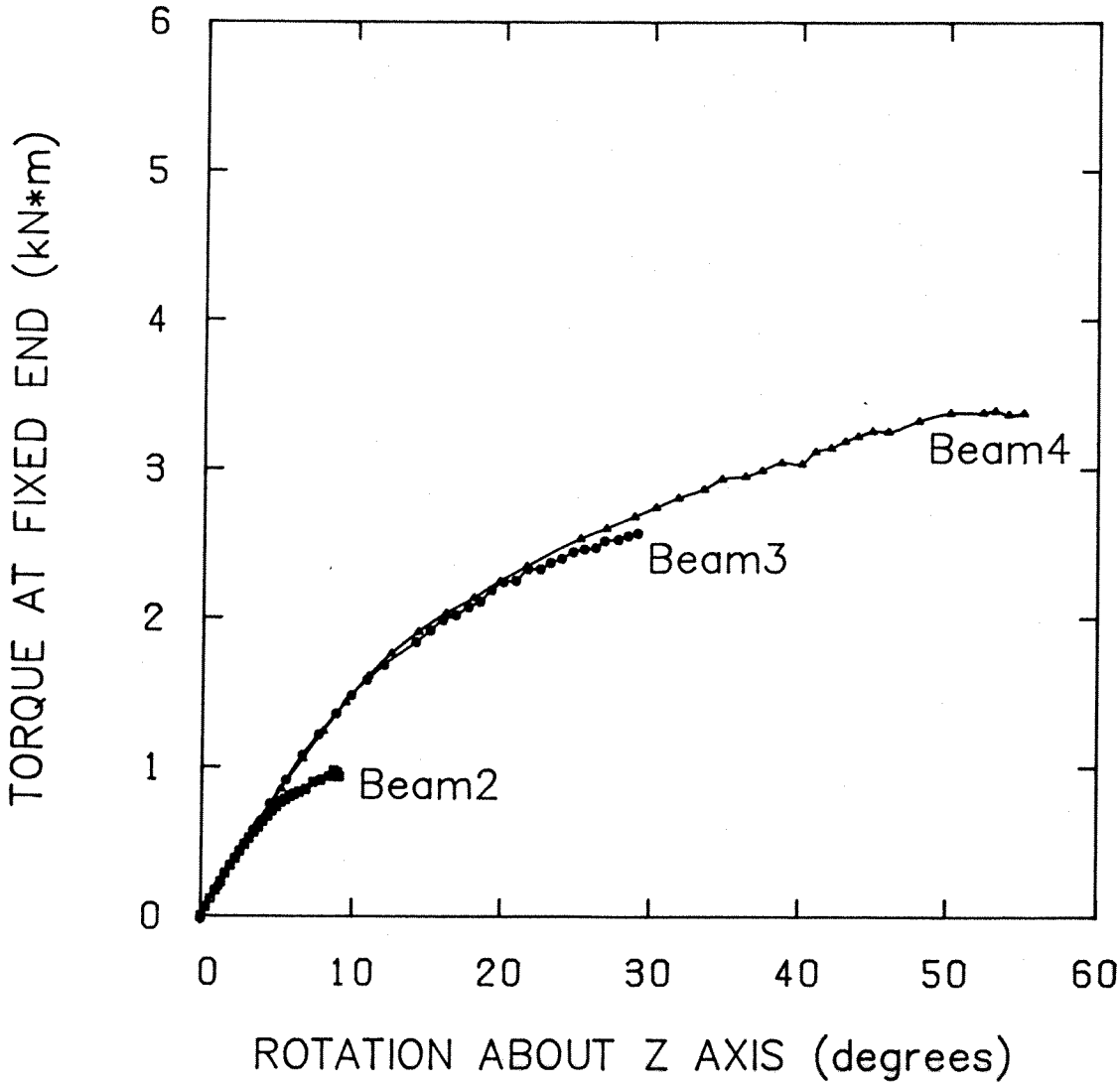

Figure 5.3 Truncated torque versus rotation test curves

For beam 1, after a bending moment corresponding to complete yielding of the cross-section was obtained, the torque increased to a value greater than the sum of the fully plastic St. Venant (sand heap) torque and the full warping torque based on the undeformed shape. The maximum moment carried was 91% of the ultimate moment while the beam sustained the full sand heap and warping torque, all based on the ultimate tensile strength of the material. The strains were significantly greater than the yield strain and approached the ultimate strain.

An examination of the beam after failure showed that the beam was kinked laterally at about 285 mm from the fixed end, as shown in Fig. 5.4, with the specimen remaining virtually undeformed from this point to the free end. Because the beam was loaded concentrically, the warping torque developed only within 285 mm of the fixed end. Large transverse shears, and therefore a large warping torque, at this location correspond to relatively small warping normal stresses at the fixed end. This is analogous to a short beam having high shears and small moments. By examining the deflected shape of the beam, the moments and torques were calculated for the final load step at both the fixed end and at a point 100 mm away along the beam. The torque was assumed to be zero from the lateral kink to the free end. Fig. 5.5 shows the torque distribution along the

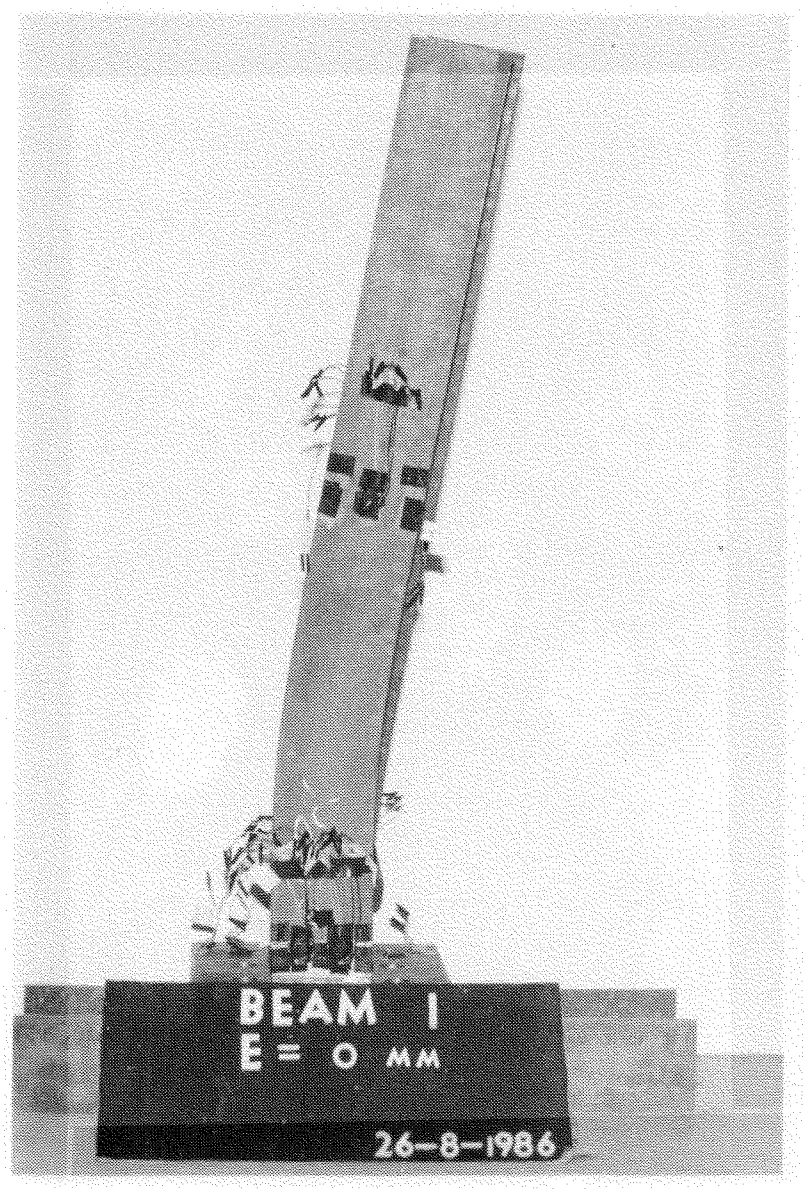

Figure 5.4 Final deformed shape of beam 1

length of the beam calculated on this basis. The contribution of the warping torque is taken as the difference between the total torque and the ultimate sand heap torque of 2.18 kN*m. The warping torque corresponds to a flange moment at the fixed end of approximately 1.62 kN*m. The inclination of the loading cable from the vertical causes a moment about the y axis of 0.41 kN*m and, for the top flange, these moments are additive and total 2.03 kN*m. Assuming that ultimate stresses can exist (as confirmed by strain measurements), the flange moment that can be carried simultaneously with the applied strong axis moment of 50.9 kN*m is 3.61 kN*m. Thus, the bending moments about the x and y axes and the warping moment can be carried simultaneously. Furthermore, at three of the four flange tips one of the torque, moment about the strong axis, and moment about the weak axis causes normal stresses of the opposite sign to the other two. At these locations, there is therefore a counteracting effect. Where the three cause compression, the ultimate (engineering) tensile strength does not in fact connote failure. The cross-section expands in compression and does not neck. Compression failure of steel beams is related to local buckling. Because of the high strain gradients both across the cross-section and along the beam, consistent with the observed local deformations, local buckling was delayed. It is also postulated that ultimate shear

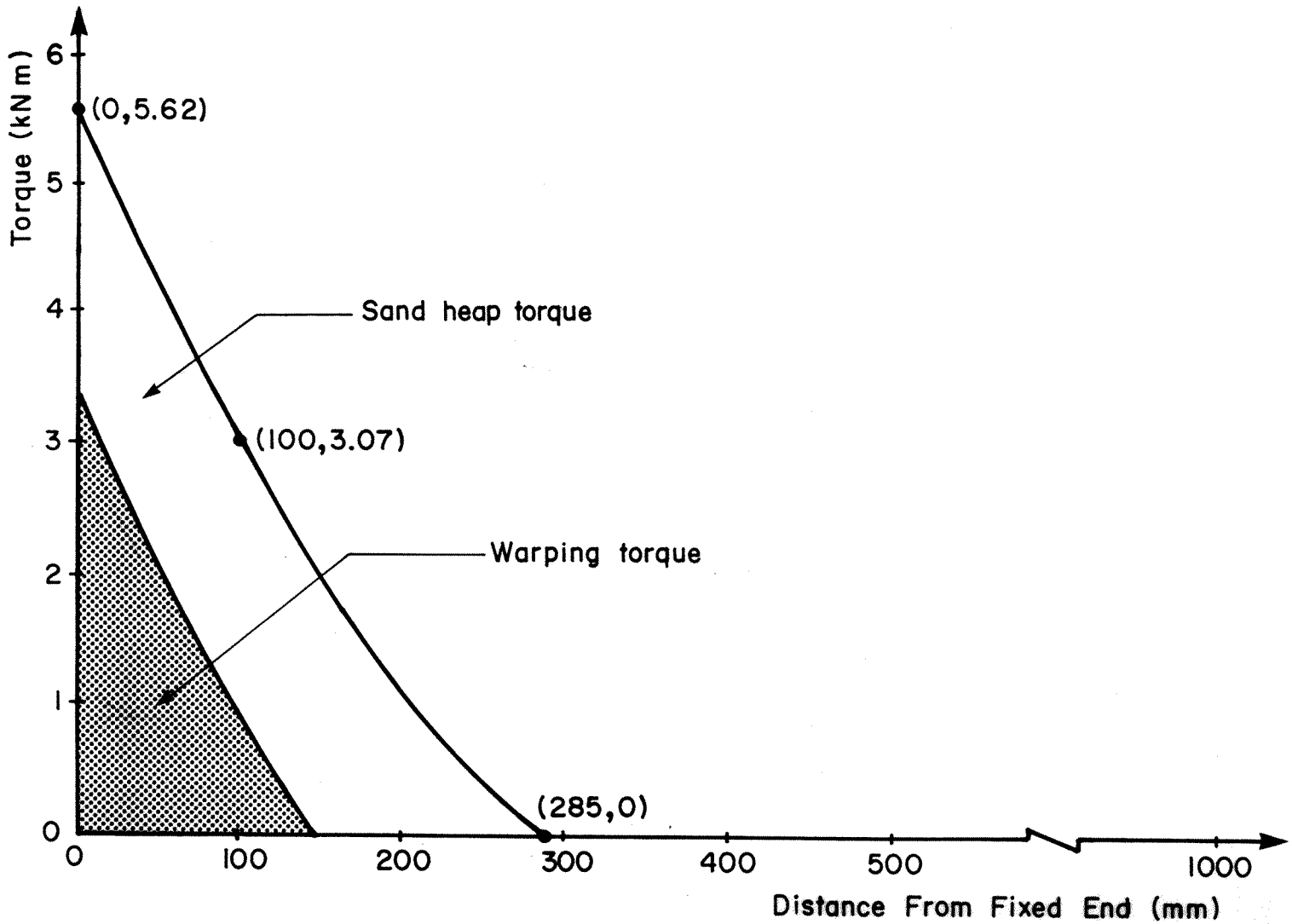

Figure 5.5 Final torque distribution on beam 1

stresses can coexist with ultimate tensile stresses in apparent violation of the von Mises-Hencky criterion extended to the ultimate condition. A possible explanation is that the shearing stresses do not cause necking and that they are accommodated between the engineering ultimate strength and the true ultimate strength.

Beam 3, loaded with an initial eccentricity of 100 mm, ultimately sustained a torque, based on the initial undeformed geometry, greater than the ultimate sand heap and warping torque combined as well as a bending moment equal to 83% of the fully plastic moment. An analysis similar to that for beam 1, with calculations made at 0, 200, and 275 mm from the fixed end gave the torque distribution shown in Fig. 5.6. Assuming the ultimate sand heap torque is present, the flange moment at the fixed end due to warping torque is approximately 2.82 kN*m which adds to the moment about the y axis of 0.29 kN*m in the top flange for a total of 3.11 kN*m. Based on ultimate stresses, the cross-section can resist a flange moment of 6.10 kN*m when the coexisting moment about the strong axis is 37.9 kN*m. Therefore, the applied loads are resisted.

5.1.4 Comparison of Test Results with Predicted Capacity

The interaction diagram for the test beams, as discussed in Section 4.3.1.1, is shown in Fig. 5.7 in

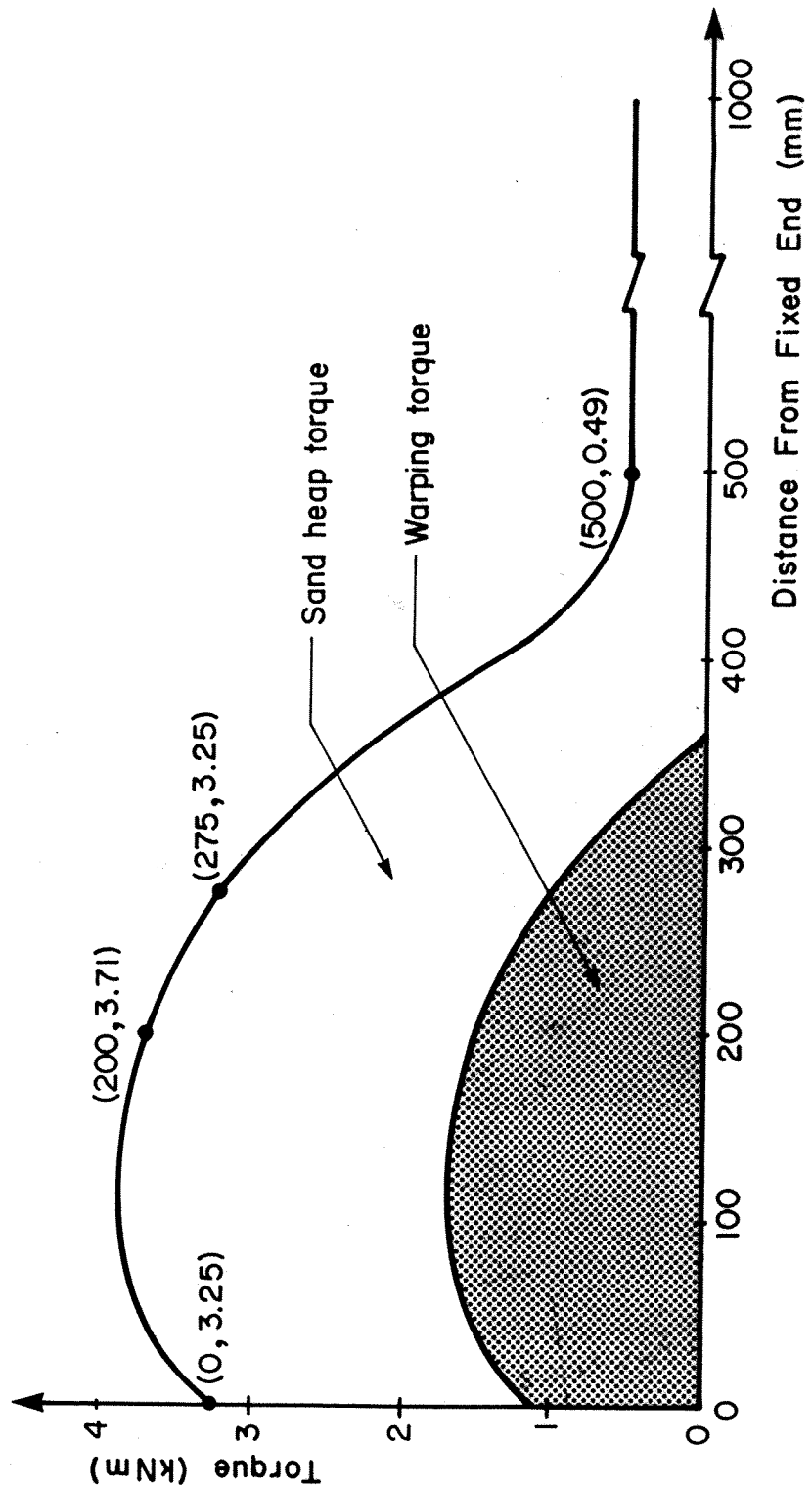

Figure 5.6 Final torque distribution on beam 3

non-dimensionalized form. Also plotted in the figure are the four test results for which the second order effects have been eliminated, as discussed in Section 5.1.3.1. All of the test points fall outside the proposed interaction diagram. The average test/predicted ratio for the four tests, as given in Table 5.1, is 1.086. The test results are in good agreement with the proposed interaction diagram for class 1 beams. The use of ultimate normal and shear stresses to calculate torsional resistance appears to be justified.

Table 5.2 gives the deflections and rotations of the free end of the four beams at the serviceability limit corresponding to theoretical first yield, as described in Section 4.3.2. Of all these values, only the vertical deflection for the concentrically loaded beam of 1/65 of the span appears somewhat high. In a practical design situation, one may choose to impose a lower limit.

5.1.5 Restraint of Weld

At the fixed end of the beam, a full penetration groove weld connected the specimen to a thick end plate. The rigidity of the weldment restrains the adjacent flanges due to the Poisson effect and a uniaxial plane strain condition develops allowing greater stresses to be achieved than in a tensile coupon test. The effects of this restraint are assumed to dissipate rapidly along the length of the beam and have not been considered in this analysis.

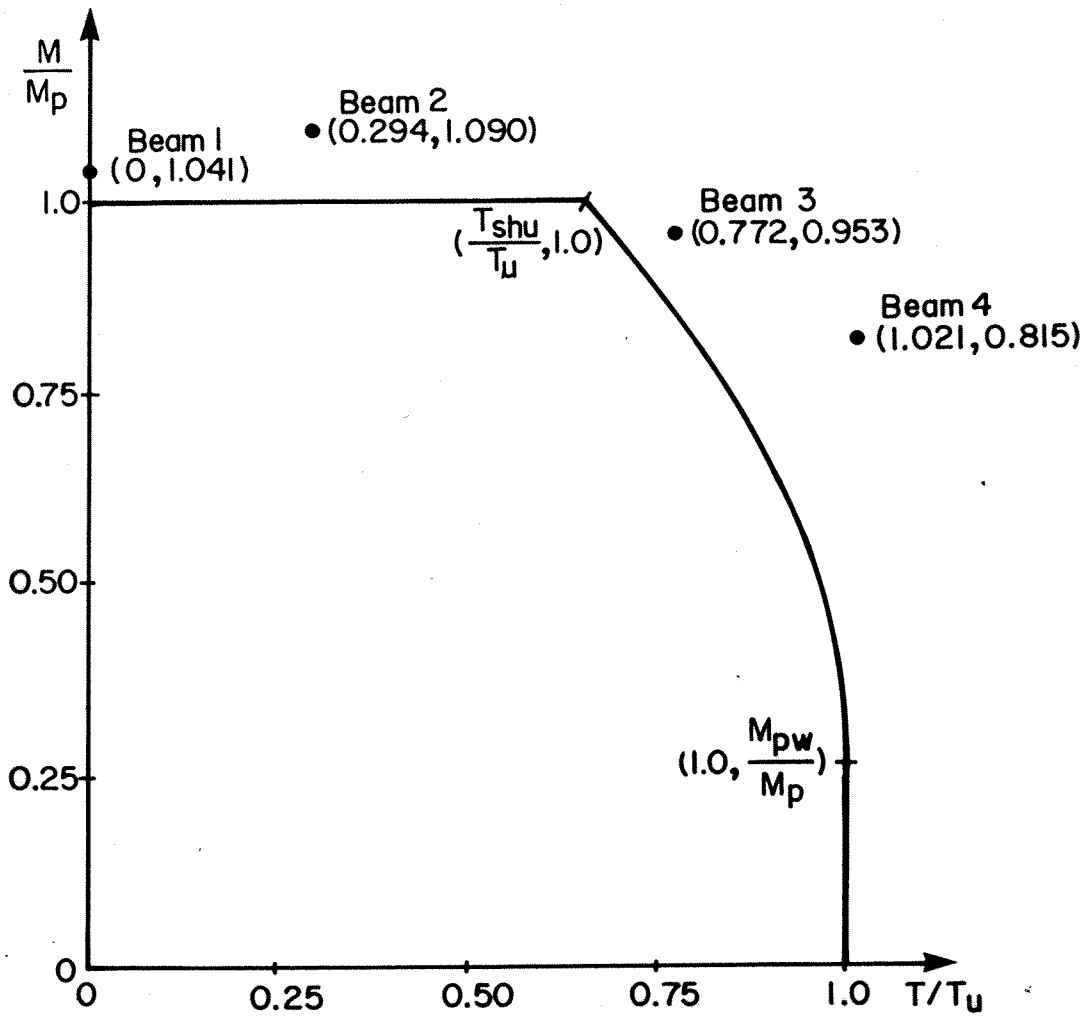

Figure 5.7 Moment-torque interaction diagram and test results

Table 5.1 Test to predicted ratios

BEAM	Test/Predicted
1	1.041
2	1.090
3	1.051
4	1.160
Mean	1.086

Table 5.2 Deflections of test beams at serviceability limit

BEAM	DEFLECTIONS (mm)		DEFLECTIONS/SPAN		ROTATIONS (radians)
	vertical	lateral	vertical	lateral	
1	15.4	0.4	1/65	1/2500	0.002
2	6.3	1.3	1/160	1/770	0.051
3	3.3	0.1	1/303	1/10000	0.079
4	1.9	0.3	1/526	1/3300	0.093

5.1.6 Horizontal Loads

As the tests progressed, deflections of the free end caused the load applied by the cable to deviate slightly from vertical. In spite of this, the axial loads, lateral loads, and lateral moments did not exceed 0.31 kN, 0.64 kN, and 0.64 kN*m respectively at the end of the first phase of the torque-rotation curves. These were considered to be negligible.

5.2 Other Test Results

5.2.1 Introduction

The four sets of test data presented represent the experimental work on I-shaped steel beams under bending and torsion where inelastic behaviour is of primary concern. All tests performed were on class 1 beams. Comparisons with the proposed interaction diagram are difficult because sometimes the work is incomplete; the ultimate limit state has not been defined explicitly or material behaviour beyond strain hardening has not been reported.

5.2.2 Dinno and Merchant (1965)

Dinno and Merchant tested six 21 inch long small, stocky I-shaped specimens machined from solid mild steel bars to the cross-section shown in Fig. 5.8. The b/t and h/w ratios are 2.5 and 4.0 respectively. Two inches were left solid at each end to provide full warping restraint. Various

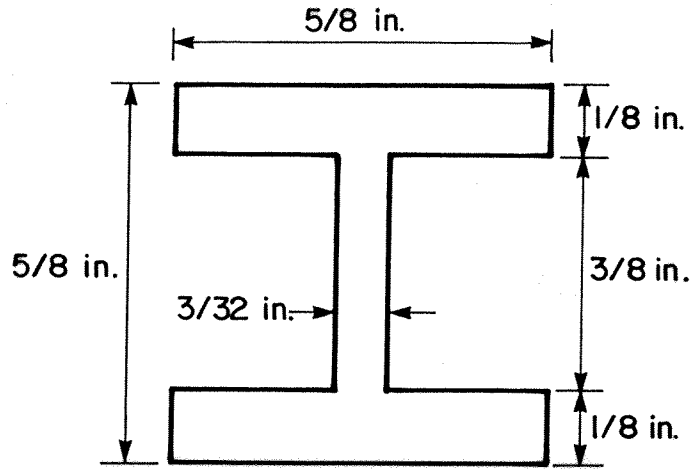

Figure 5.8 Cross-section of test beams

(Dinno and Merchant, 1965)

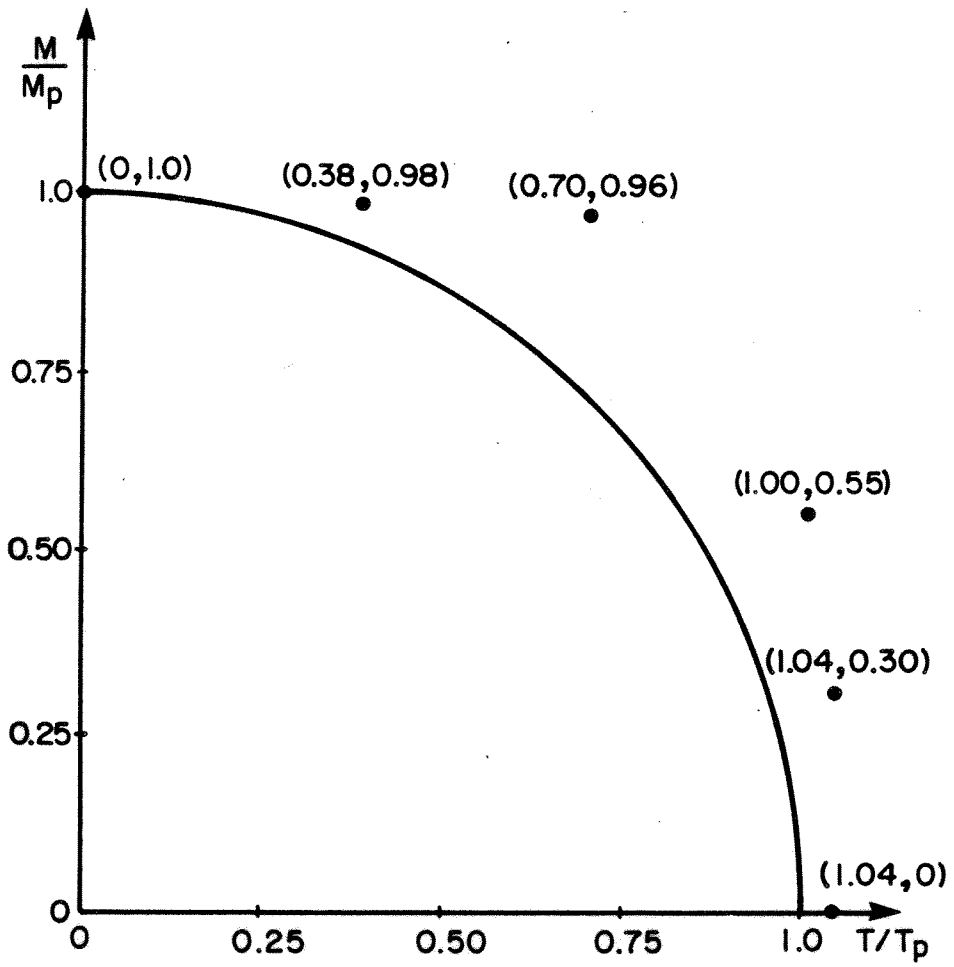

Figure 5.9 Dinno and Merchant's (1965) design curve

and test results

ratios of moment to torque were applied. The torque was constant and the bending moment varied along the beam, although the precise method of loading was not reported. The results of their tests are presented in Fig. 5.9 along with the circular curve they propose as a design limitation. The limiting torque, T_p, is based on the yield stress for both the sand heap and warping contributions.

Comparison of the test results with the proposed interaction diagram is not directly possible as they did not report the ultimate tensile strength of the material, nor have they defined what was considered to be the failure criterion. In addition, the diminutive size of the test specimens make any comparison to beams used in practice highly suspect.

5.2.3 Kollbrunner, Hajdin, and Ćorić (1978)

Kollbrunner, Hajdin, and Ćorić tested an I-shaped eccentrically loaded cantilever beam with a length of 1300 mm. This class 1 section had flanges that were 6.4 x 80 mm and a web that was 6.4 x 120 mm. The limiting load was arbitrarily defined as that when the maximum strain was five times the yield strain. Using this criterion, the test point is plotted on the interaction diagram in Fig. 5.10 and falls well inside the curve. In Fig. 5.11, the torque-rotation curve for this test shows, however, that the test was terminated before the full strength had been reached.

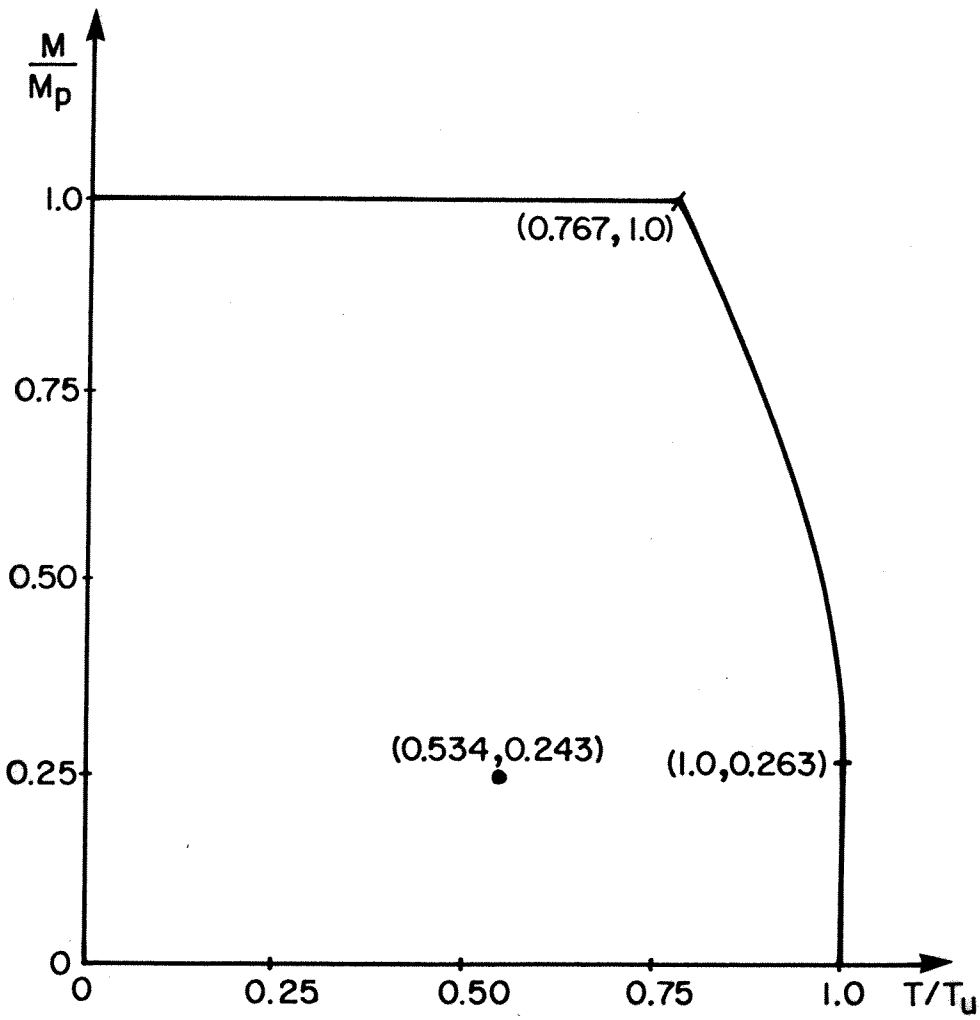

Figure 5.10 Kollbrunner's et al. (1978) test result

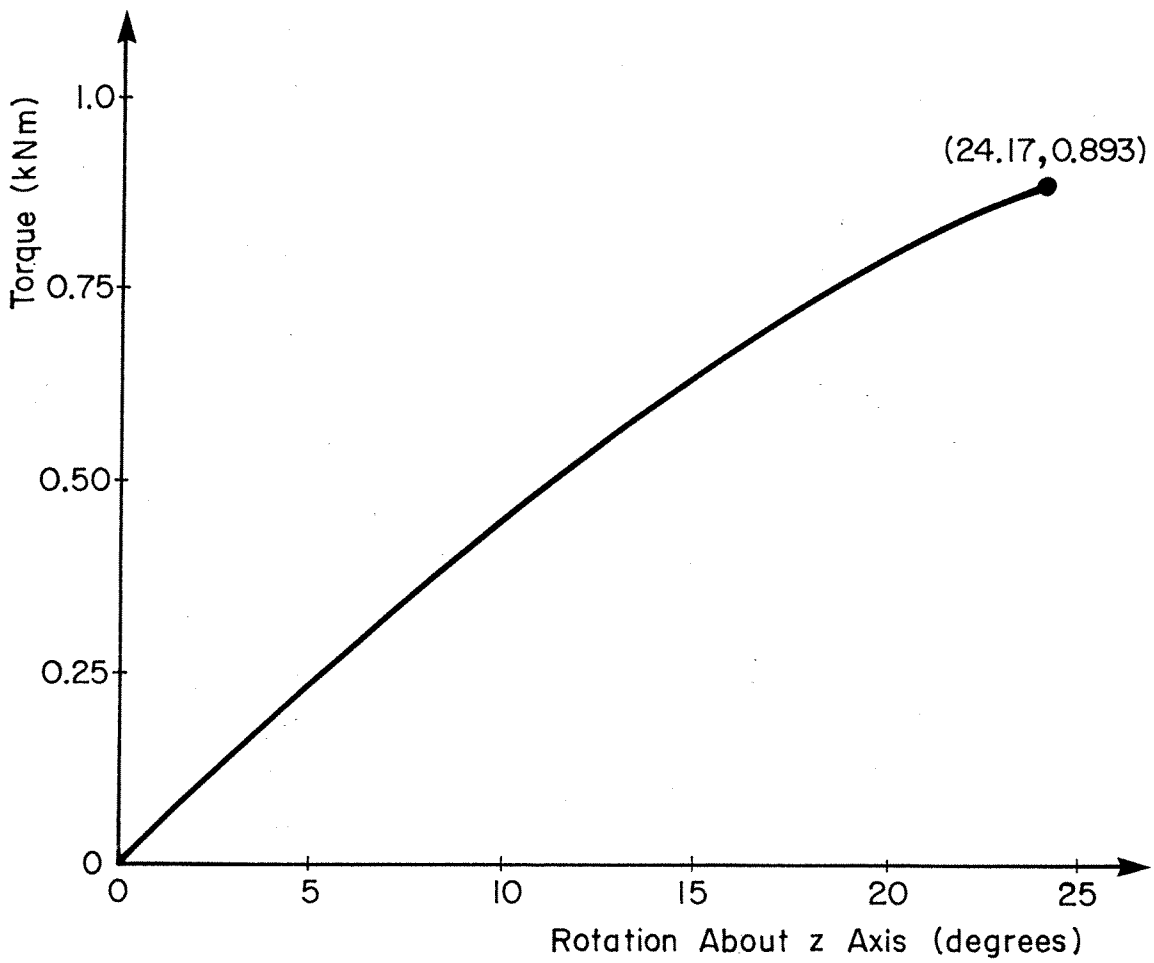

Figure 5.11 Torque versus rotation curve

(Kollbrunner et al., 1978)

5.2.4 Kollbrunner, Hajdin, and Obradović (1979)

Kollbrunner, Hajdin, and Obradović tested five fixed ended 1600 mm long I-shaped beams, comprised of three steel plates, under bending and torsion. The flanges were 5.7 x 60 mm and the web 8.4 x 94 mm. This is a class 1 section. The beams were loaded by means of a vertical load, with an eccentricity of 200 mm, applied at one quarter point.

The ultimate strength of the material, and the criterion for selecting the maximum load are not given. Also, for the ultimate load achieved, the flexural moment can be carried by the web alone without exceeding the yield stress. Comparisons with the interaction diagram are therefore meaningless.

5.2.5 Razzaq and Galambos (1979)

Razzaq and Galambos tested two class 1 M150X6.5 beams under uniaxial bending and torsion and two under uniaxial bending alone. The ends were flexurally pinned and torsionally fixed, with springs providing restraint about the vertical axis. The beams subjected to both bending and torsion were first loaded by an eccentric vertical load at midspan and subsequently with uniform end moments to collapse.

The length of the beams was such that they would be expected to fail by lateral torsional buckling. The interaction diagram of Fig. 5.12 has been constructed on this basis, as discussed in Section 4.3.1.5, and assuming

the ends are flexurally pinned and torsionally fixed. The test results plotted in Fig. 5.12 give test/predicted ratios of 0.93 and 1.01 for the beams subjected to combined bending and torsion and 1.04 and 1.31 for the beams subjected to bending only.

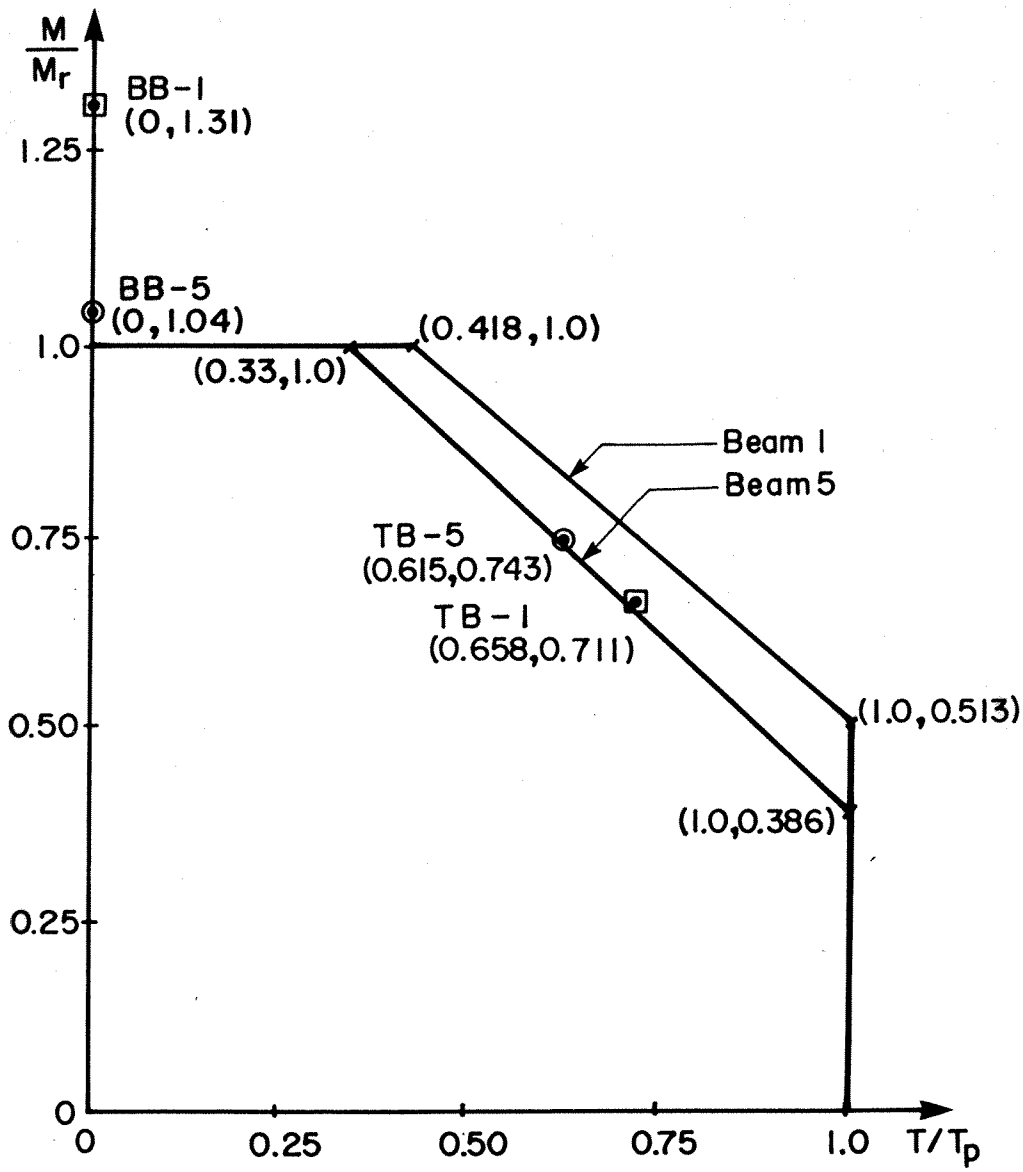

Figure 5.12 Razzaq and Galambos' (1979) test results

6. DESIGN METHODOLOGY

6.1 General

In limit states design, the designer checks the adequacy of his structure against two classes of limit states, the ultimate limit states and the serviceability limit states.

6.2 Ultimate Limit States

Based on the ultimate strength moment-torque interaction diagram developed in Section 4.3.1, an ultimate limit states design procedure can be developed. The general procedure is first presented and then design checks are given which may reduce the amount of work considerably. The steps, in general, for class 1 and 2 sections are:

1. Compute the factored moment, M_f, and torque, T_f, on the beam.
2. Select a beam with $M_p > M_f$.
3. Construct the moment-torque interaction diagram in Fig. 6.1 (for class 1 sections) as follows:
   a. Establish point E with $M/M_p = 1.0$ and extend the line from E horizontally toward H.
   b. For class 1 sections, determine the ultimate torque, $T_u = T_{shu} + T_{wu}$. The point F, $T/T_u = 1.0$, is thus found and the point H has an abscissa T_{shu}/T_u. For class 2 sections, pending experimental confirmation, it is suggested that

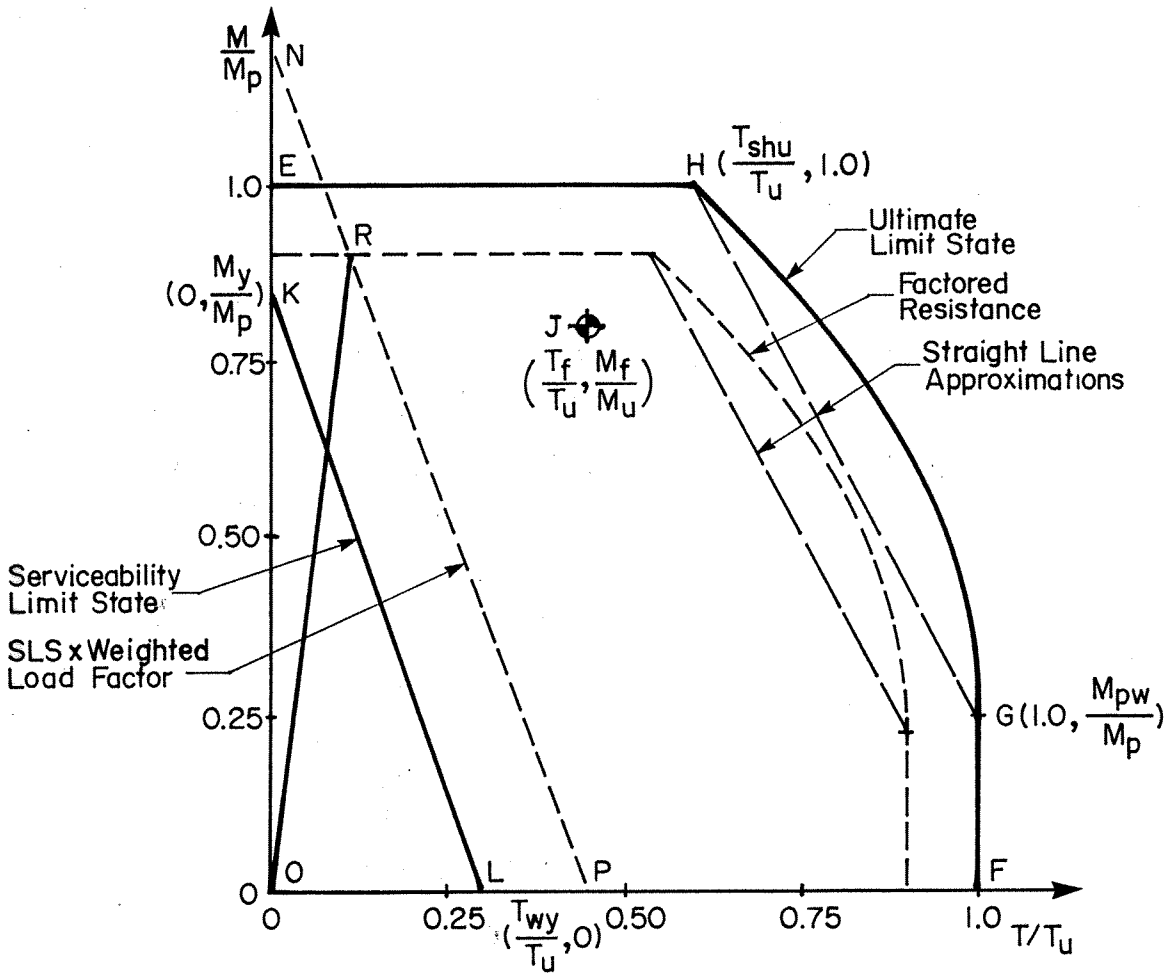

Figure 6.1 Moment-torque interaction diagram for design

the calculated torques be based on the yield strength of the material.

c. The point G, directly above F, has an ordinate equal to the fully plastic moment of the web divided by M_p.

d. A parabola with vertex at G is drawn from G to H. Conservatively, a straight line could be used between these two points.

e. The factored resistance curve has coordinates of ϕ times the curve EHGF.

4. Provided point J, representing the applied factored moment and torque, lies within the factored resistance curve, the beam is satisfactory.

For class 3 sections, the interaction diagram would be constructed in a similar manner except that:

1. the maximum bending moment is M_y.
2. the maximum torque is determined as the sum of the St. Venant torque and the warping torque based on an elastic analysis with the yield stress as the limiting warping normal stress.
3. the moment corresponding to point G is the yield moment of the web.
4. as the parabolic curve from G to H depends on full plastification, it is replaced by a straight line.

For class 1 and 2 beams, where the flexural capacity is limited by lateral torsional buckling, it is proposed that the interaction diagram be based on a maximum moment

corresponding to the lateral torsional buckling moment resistance and a maximum torque equal to the plastic torque based on the yield value, as discussed in Section 4.3.1.5. The diagram is completed with a straight line from G to H. For class 3 sections, the diagram would be constructed similarly but with the torque limited to the yield torque.

In certain special circumstances, the analysis can be greatly simplified.

Case 1. The factored torque is less than the St. Venant torsional resistance.

Under these circumstances, the full moment resistance (M_p, M_y or M_r, based on lateral torsional buckling, as appropriate) can be sustained because the design point is to the left of point H of Fig. 6.1.

Case 2. The factored moment is less than the moment capacity of the web.

This represents the condition when the beam is loaded chiefly in torsion and the bending moment is small. The beam can carry the full torsion depending on its class.

The analysis is further simplified if cross-sectional properties such as M_{pw}/M_p and Z_{sh} are tabulated.

Because an interaction diagram is needed for each selection of beam cross-section, it is desirable to minimize the number of iterations in the design process by careful

beam selection. For example, if the factored torque is large, a beam with a moment capacity significantly greater than M_f would probably be required. Also, certain cross-sectional characteristics are more significant than others in resistance of different types of loads. The flange area and the distance between flange centroids are important for moment resistance, the flange and web areas (especially the thicknesses) are important for St. Venant torsional resistance, and the flange width and the distance between flange centroids are important for warping torsional resistance.

6.3 Serviceability Limit States

The serviceability limit state based on first yield at a point on the cross-section (Equation [4.14]), when plotted on Fig. 6.1 drawn for class 1 sections, is a straight line joining the point K $(0,M_y/M_p)$ to the point L $(T_{wy}/T_u,0)$. For class 2 and 3 sections, the serviceability limit state interaction line would mark off a relatively greater portion of the ultimate limit state diagram.

The line N-P has coordinates increased over those of the line K-L by the weighted load factor (1.25 to 1.50). Any straight line from the origin represents a given initial eccentricity of the applied load. The point R represents the case when the ultimate limit state and the serviceability limit state are satisfied simultaneously. Above the line O-R the ultimate limit state controls and below the line the

serviceability limit state controls. Note that point J meets strength requirements but not serviceability requirements.

The second serviceability limit state related to the distortion of the member depends on the particular characteristics of the member and the contiguous building elements. Having met the first serviceability limit state of first yield, the rotations and deflections of the beam can be calculated elastically. The designer then decides whether or not these are acceptable.

6.4 Summary

Examination of Fig. 6.1 suggests that the serviceability controls for beams subject to substantial torsional moments. Therefore, prior to drawing the entire interaction diagram, the warping yield torque should be determined to define point L, the yield moment to define point K, and the St. Venant torque to define point H. If line N-P intersects the factored resistance curve on the flat portion (point R), it is not necessary to construct the remainder of the interaction diagram.

The slope of the line O-R represents a specific moment-torque ratio. If the moment-torque ratio is larger, strength governs when using the first serviceability criterion; if it is smaller, serviceability governs. Stricter serviceability limits may be imposed.

7. SUMMARY AND CONCLUSIONS

7.1 Summary and Conclusions

1. Limited experimental and analytical work has been conducted to determine the behaviour beyond yield and the ultimate strength of I-shaped beams subject to flexure and torsion.
2. Four tests on class 1 cantilever beams with loading eccentricities of 0, 30, 100, and 220 mm were conducted to investigate the strength behaviour to the ultimate condition.
3. The tests revealed that the torsional behaviour has two distinct phases. The second phase, dominated by second order geometric effects, is considered non-utilizable.
4. From an assumed stress distribution on the cross-section, with bending normal stresses at the yield value and warping normal stresses and sand heap shear stresses at ultimate, an ultimate strength interaction diagram has been developed for class 1 beams. A computer program is presented for calculating these diagrams for any I-shaped beam.
5. The apparent violation of the von Mises-Hencky failure condition at the ultimate strength is justified by the fact that the true ultimate stress can be significantly greater than the engineering ultimate stress under certain conditions.

6. The design method proposes that if the applied torque can be carried by the St. Venant torsional resistance alone, the beam may be designed exclusively for flexure. When flexural moments can be resisted by the web, the full torsional resistance is utilized.
7. The interaction diagram is in good agreement with the test results. The mean test/predicted ratio for the four beams based on first phase torsional behaviour is 1.086.
8. Ultimate strength interaction diagrams are proposed by extrapolation for classes of sections other than those tested and for beams whose flexural capacity is limited by lateral torsional buckling. These proposals should be confirmed by further tests.
9. Two serviceability limit states criteria are proposed. The first criterion is that yielding at any point on the cross-section should not occur under the action of the specified loads. The second criterion is that distortion of the member must not exceed a value consistent with the satisfactory performance of the member and the contiguous building elements.
10. Together with the serviceability limit states criteria, the ultimate strength interaction diagrams provide a comprehensive design approach.

7.2 Areas for Future Research

Due to the lack of published experimental data on combined bending and torsion at the ultimate limit state, the fact that the ultimate limit state criterion is often not defined and the limited nature of the tests conducted during this research, a need exists for a comprehensive experimental investigation. The design procedure developed appears to be applicable for a wide variety of conditions but should be corroborated by further tests. Factors that should be investigated include

1. end conditions
2. beam continuity
3. loading conditions, above or below the shear centre
4. length of beam
5. class of cross-section
6. lateral torsional buckling
7. ratio of St. Venant to warping torsional resistance
8. grade of steel

In addition to providing information on the ultimate strength of beams under bending and torsion, these tests would provide statistical data for determining a resistance factor and allow codification of the design procedure.

This research has dealt primarily with ultimate strength criteria, and further work on serviceability limits would be useful.

REFERENCES

American Institute of Steel Construction (AISC). 1978. "Specification for the Design, Fabrication and Erection of Structural Steel for Buildings". American Institute of Steel Construction, Chicago, Illinois, 103 pp.

American Society for Testing and Material (ASTM). 1986. "Standard Methods for Tension Testing of Metallic Materials (Metric), Designation E8M-85". Annual Book of ASTM Standards, Vol. 3.01. ASTM, Philadelphia, Pennsylvania, pp. 146-169.

Augusti, G. 1966. "Full Plastic Torque of I-beams". International Journal of Mechanical Sciences, Vol. 8, pp. 641-649.

Boulton, N.S. 1962. "Plastic Twisting and Bending of an I-beam in Which the Warp is Restricted". International Journal of Mechanical Sciences, Vol. 4, pp. 491-502.

British Standards Institution (BSI). 1985. "Structural Use of Steelwork in Building, Standard BS 5950: Part 1". British Standards Institution, London, England, 111 pp.

Canadian Institute of Steel Construction (CISC). 1984. "Handbook of Steel Construction". Canadian Institute of Steel Construction, Willowdale, Ontario.

Canadian Standards Association (CSA). 1984. "Steel Structures for Buildings - Limit States Design, Standard CAN3-S16.1-M84". Canadian Standards Association, Rexdale, Ontario, 103 pp.

Chu, K. and Johnson, R.B. 1974. "Torsion in Beams With Open Sections". Journal of the Structural Division, ASCE, Vol. 100, ST7, pp. 1397-1419.

Darwish, I.A. and Johnston, B.G. 1965. "Torsion of Structural Shapes". ASCE Proceedings, Vol. 91, pp. 203-227.

Dawe, J.L. and Kulak, G.L. 1984. "Local Buckling of W Shape Columns and Beams". Journal of the Structural Division, ASCE, Vol. 110, ST6, pp. 1292-1304.

Dinno, K.S. and Gill, S.S. 1964. "The Plastic Torsion of I-sections with Warping Restraint". International Journal of Mechanical Sciences, Vol. 6, pp. 27-43.

Dinno, K.S. and Merchant, W. 1965. "A Procedure for Calculating the Plastic Collapse of I-sections Under Bending and Torsion". The Structural Engineer, Vol. 43, No. 7, pp. 219-221.

Farwell, C.R. and Galambos, T.V. 1969. "Nonuniform Torsion of Steel Beams in Inelastic Range". ASCE Proceedings, Vol. 95, ST 12, pp. 2813-2829.

Galambos, T.V. 1968. "Structural Members and Frames". Prentice-Hall, Englewood Cliffs, New Jersey, 373 pp.

Goldberg, J.E. 1953. "Torsion of I-Type and H-Type Beams". ASCE Transactions, Vol. 118, pp. 771-793.

Hamilton, S.B. 1952. "The Historical Development of Structural Theory". Proceedings of the Institute of Civil Engineering, No. 32 (May 6), pp. 374-402.

Heins, C.P. 1975. "Bending and Torsional Design in Structural Members". Lexignton Books, Lexington, Mass., 367 pp.

Heins, C.P. and Seaburg, P.A. 1963. "Torsion Analysis of Rolled Steel Sections". Bethlehem Steel Corporation, Bethlehem, Pennsylvania, 78 pp.

Hodge, P.G. 1959. "Plastic Analysis of Structures". McGraw-Hill Book Co., New York, 364 pp.

IMSL. 1980. Subroutine ZSCNT, IMSL, Houston, Texas.

Johnston, B.G. 1982. "Design of W-shapes for Combined Bending and Torsion". Engineering Journal of the AISC, Vol. 19, 2nd quarter, pp. 65-85.

Johnston, B.G., Lin, F., and Galambos, T.V. 1980. "Basic Steel Design". Prentice-Hall, Englewood Cliffs, New Jersey, 352 pp.

Kollbrunner, C.F., Hajdin, N., and Ćorić 1978. "Elastic - Plastic Thin-walled I-section Beam Subjected to Bending and Warping Torsion". Institut fur Bauwissenschaftliche Forschung Publikations, No. 43 (Dec), pp. 1-51.

Kollbrunner, C.F., Hajdin, N., and Obradović 1979. "Elastic - Plastic Fixed Ended Beam of I-section Subjected to Bending and Warping Torsion". Institut fur Bauwissenschaftliche Forschung Publikations, No. 46 (May), pp. 1-40.

Kubo, C.G., Johnston, B.G., and Eney, W.J. 1956. "Non-Uniform Torsion of Plate Girders". ASCE Transactions, Vol. 121, pp. 759-785.

Lay, M.G. 1982. "Structural Steel Fundamentals". Australian Road Research Board, Victoria, Australia, 241 pp.

Lin, P.H. 1977. "Simplified Design for Torsional Loading of Rolled Steel Members". Engineering Journal of the AISC, 3rd quarter, pp. 98-107.

Lyse, I., and Johnston, B.G. 1936. "Structural Beams in Torsion". ASCE Proceedings, Vol. 62, No. 2, pp. 236-237.

McGuire, W. 1968. "Steel Structures". Prentice-Hall, Englewood Cliffs, New Jersey, 1112 pp.

Nadai, A. 1931. "Plasticity". McGraw-Hill Book Co., New York, 349 pp.

Pastor, T.P., and DeWolf, J.T. 1979 "Beams with Torsional and Flexural Loads". Journal of the Structural Division, ASCE, Vol. 105, No. ST3, pp. 527-538.

Razzaq, Z., and Galambos, T.V. 1979. "Biaxial Bending Tests With or Without Torsion". Journal of the Structural Division, ASCE, Vol. 105, No. ST11, pp. 2163-2185.

Salmon, C.G., and Johnson, J.E. 1980. "Steel Structures". 2nd edition, Harper and Row, Publishers, New York, 946 pp.

Seely, F.B., and Putnam, W.J. 1936. Discussion of "Structural Beams in Torsion". by I. Lyse and B.G. Johnston, ASCE Transactions, Vol. 101, pp. 907-912.

Sourochnikoff, B. 1951. "Strength of I-beams in Combined Bending and Torsion". ASCE Transactions, Vol. 116, pp. 1319-1342.

Timoshenko, S.P. 1983. "History of Strength of Materials". Dover Publications, New York, 452 pp.

Timoshenko, S.P., and Gere, J.M. 1961. "Theory of Elastic Stability". 2nd edition, McGraw-Hill, New York, 541 pp.

Trahair, N.S. 1977. "The Behaviour and Design of Steel Structures". John Wiley and Sons, New York, 320 pp.

Ugural, A.C., and Fenster, S.K. 1979. "Advanced Strength and Applied Elasticity". Elsevier North Holland Publishing Co., New York, 433 pp.

Vlasov, V.Z. 1961. "Thin-walled Elastic Beams". Israel Program for Scientific Translations Ltd., Jerusalem, 493 pp.

Walker, A.C. (ed.) 1975. "Design and Analysis of Cold-Formed Sections". International Textbook Co. Ltd., London, 174 pp.

Westergaard, H.M. 1964. "Theory of Elasticity and Plasticity". Dover Publications, New York, 176 pp.

Yura, J.A., Galambos, T.V., and Ravindra, M.K. 1978. "The Bending Resistance of Steel Beams". Journal of the Structural Division, ASCE, Vol. 104, No. ST9, pp. 1355-1370.

APPENDIX A - ERROR IN DINNO AND MERCHANT'S (1965) WORK

In the derivation of [2.16], Dinno and Merchant (1965) have directly adopted the work of Hodge (1959) to obtain what they claim to be a safe design curve. Although the derivation by Hodge is perfectly sound, an erroneous extrapolation has been made in concluding that [2.16] is a lower bound solution for I-shaped beams. Both Hodge, and Dinno and Merchant use the yield stress as the limiting criterion.

At any point on the cross-section, the shear stress, τ, is given by

[A.1] $$\tau^2 = (\tau_{zx}^2+\tau_{zy}^2) < (\sigma_y/a)^2$$

where $a = \sqrt{3}$ for the von Mises-Hencky yield criterion. Equation [A.1] states that the shear stress must be less than the shear yield stress. When warping stresses are negligible, the corresponding dimensionless torque is

[A.2] $$\frac{T}{T_p} = \frac{\tau}{(\sigma_y/a)}$$

Superimposed on the cross-section are normal flexural stresses. Because of the presence of shear stresses, the moment may not reach its full plastic value. Therefore,

[A.3] $$\sigma < \sigma_y$$

The corresponding dimensionless moment is

[A.4] $$\frac{M}{M_p} = \frac{\sigma}{\sigma_y}$$

Hodge then uses the von Mises-Hencky yield ellipse

[A.5] $$\sigma^2 + a^2\tau^2 = \sigma_y^2$$

to combine [A.2] and [A.4] to obtain

[A.6] $$\left[\frac{M}{M_p}\right]^2 + \left[\frac{T}{T_p}\right]^2 = 1$$

This approach is valid for beams with solid or closed cross-sections where normal stresses due to torsional warping are negligible, that is, only St. Venant torsion is included. Dinno and Merchant, however, adopt [A.6] for I-shaped beams by including the warping torque in the equation for T_p as given by [2.15]. Since [A.6] was based on the fact that the moment contributes normal stresses and the torque contributes shear stresses, the extension to use for beams with appreciable warping normal stresses is invalid.

APPENDIX B - DATA REDUCTION COMPUTER PROGRAMS

B.1 Program *DEFL*

```
CCCCCCCCCCCCCCCCCCC
CCCCCCCCCCCCCCCCCCC
CC
CC   Program   "DEFL"
CC
CC   NOTE: This program requires the use of IMSL subroutine
CC           ZSCNT (IMSL, 1980) for the solution of simultaneous
CC           equations.
CC
CC   Function:   to calculate loads, moments, torque, deflections
CC           and rotations from position/displacement transducer
CC           readings.
CC
CCCCCCCCCCCCCCCCCCC
CCCCCCCCCCCCCCCCCCC
CC
        INTEGER N,ITMAX,IER
        REAL WK(68),X(3),PAR(20),FNORM,LOAD,MX,MXNOM,MY,LB,LC
        EXTERNAL FCN1,FCN2,FCN3,FCN4
CCC
C   N=NO. OF EQUNS;NSIG=DIGITS OF ACCURACY;ITMAX=MAX. NO. ITERATIONS
CCC
        N=3
        NSIG=5
        ITMAX=150
        M=0
CCC
C   E=ECCENTRICITY IN MM; LB=LENGTH OF BEAM (PLATE TO LOAD PT) IN M
CCC
        READ(5,5)E,LB
5       FORMAT(F5.1,F7.1)
        WRITE(6,7)E
7       FORMAT(16('#')/,'#  E  =',F6.1,'  MM  #',/16('#')//)
CCC
C   L=POINT ON X-SEC THAT PROGRAM IS CALCULATING COORDS OF
CCC
10      L=1
CCC
C   LSN=LOAD SET NO.;NLC=NO. LOG. CHANNELS;NSR=NO. SETS READINGS
CCC
        READ(5,12)LSN,NLC,NSR
12      FORMAT(3I8)
        IF(M.GT.0)GO TO 13
CCC
C   THIS IS EXECUTED FIRST CYCLE ONLY SO THAT NSR IS NOT LOST
CCC
        NR=NSR
        M=M+1
CCC
C   PAR(N)=LVDT READING IN MM;LOAD IN KN;STROKE IN MM
CCC
13      READ(5,15)LOAD,PAR(11),PAR(12),PAR(13),PAR(14),PAR(15)
       *,PAR(16),STROKE
15      FORMAT(5E15.6,/3E15.6)
        WRITE(6,18)LOAD,LSN
18      FORMAT('  MTS  LOAD=',F7.3,'  KN',/1X,19('*'),/1X,
       *'(LSN=',I2,')'/)
28      IF(L.NE.1)GO TO 30
```

```
CCC
C   INITIAL ESTIMATE OF SOLUTION THEN
C   SOLVE FOR COORDS OF PT 1 IF L=1 (AND STORE)
CCC
         X(1)=PAR(11)
         X(2)=PAR(12)
         X(3)=PAR(13)
         CALL ZSCNT(FCN1,NSIG,N,ITMAX,PAR,X,FNORM,WK,IER)
         PAR(1)=X(1)
         PAR(2)=X(2)
         PAR(3)=X(3)
         GO TO 100
30       IF(L.NE.2)GO TO 40
CCC
C   SOLVE FOR COORDS OF PT 2 IF L=2 (AND STORE)
CCC
         X(1)=PAR(1)+100.
         X(2)=PAR(14)
         X(3)=PAR(15)
         CALL ZSCNT(FCN2,NSIG,N,ITMAX,PAR,X,FNORM,WK,IER)
         PAR(4)=X(1)
         PAR(5)=X(2)
         PAR(6)=X(3)
         GO TO 100
CCC
C   SOLVE FOR COORDS OF PT 3 IF L=3
CCC
40       X(1)=PAR(16)
         X(2)=PAR(2)+100.
         X(3)=PAR(3)-5.
         CALL ZSCNT(FCN3,NSIG,N,ITMAX,PAR,X,FNORM,WK,IER)
CCC
C   O/P COORDINATES OF POINT L (ORIGIN AT POINT 1)
C   FNORM=F(1)**2+...+F(N)**2 AT CALCULATED COORDINATES
C   IER=ERROR PARAMETER (=0 IF NO ERROR)
CCC
100      WRITE(6,110)L,X(1),L,X(2),L,X(3),FNORM,IER
110      FORMAT('X',I1,'=',F6.1,2X,'Y',I1,'=',F6.1,2X,
        *'Z',I1,'=',F6.1,2X,'FNORM=',F12.4,2X
        *,'IER=',I3)
CCC
C   NOTE THAT IF FNORM=100 OR LESS, SHOULD HAVE GOOD RESULTS.
CCC
         IF(L.NE.3)GO TO 150
CCC
C   CALCULATE DEFLECTIONS & ROTATIONS
C   NOTE: USING A COORD SYSTEM WITH ORIGIN AT PT1
C   THEREFORE, TRANSLATE U,V,W SO THAT ORIGIN AT CTR OF WEB
CCC
         U=((PAR(4)+X(1))/2.)-50.
         V=((PAR(5)+X(2))/2.)-50.
         W=(PAR(6)+X(3))/2.
         THETAX=(ATAN((X(3)-PAR(3))/(X(2)-PAR(2))))*(180./3.14159)
         THETAY=(ATAN((PAR(3)-PAR(6))/(PAR(4)-PAR(1))))*(180./3.14159)
         PHI=(ATAN((PAR(5)-PAR(2))/(PAR(4)-PAR(1))))*(180./3.14159)
CCC
C   FIND A VECTOR PERP'R TO PLANE OF SECTION
C   IE. CROSS PROD OF CTR OF WEB-PT1 & CTR OF WEB-PT2
CCC
         VX=(PAR(2)-V-50.)*(PAR(6)-W)-(PAR(5)-V-50.)*(PAR(3)-W)
         VY=(PAR(4)-U-50.)*(PAR(3)-W)-(PAR(1)-U-50.)*(PAR(6)-W)
         VZ=(PAR(1)-U-50.)*(PAR(5)-V-50.)-(PAR(4)-U-50.)*(PAR(2)-V-50.)
         VL=SQRT(VX**2+VY**2+VZ**2)
CCC
C   MAKE VECTOR 50MM LONG (OUT TO PLANE OF LOAD PT)
```

```
CCC
        VX50=VX*50./VL
        VY50=VY*50./VL
        VZ50=VZ*50./VL
CCC
C   PAR 7,8,9 ARE LOCATION OF TIP OF V50 WRT ORIGIN   PT1
CCC
        PAR(7)=U+50.+VX50
        PAR(8)=V+50.+VY50
        PAR(9)=W+VZ50
CCC
C   PAR 17,18,19 ARE DISTS FROM PT OF APPLICATION OF LOAD
C   TO PT1, PT2, AND TIP OF V50 RESPECTIVELY
CCC
        PAR(17)=(50.+E)**2+146.8**2+50.**2
        PAR(18)=(E-50.)**2+146.8**2+50.**2
        PAR(19)=E**2+96.8**2
CCC
C   CALCULATE LOCATION OF LOAD POINT
C   INITIAL ESTIMATES FOR LOAD PT
CCC
        X(1)=U+50.+E
        X(2)=V+150.
        X(3)=W
        CALL ZSCNT(FCN4,NSIG,N,ITMAX,PAR,X,FNORM,WK,IER)
CCC
C   FOR O/P SIGNS:
C      RH COORD SYSTEM
C      RH RULE POS
CCC
C   TRANSLATE TO COORD SYS W/ORIGIN   CTR OF WEB
CCC
        X(1)=X(1)-50.
        X(2)=X(2)-50.
CCC
C   FOLLOWING O/P - ORIGIN   CTR OF WEB
CCC
        WRITE(6,120)U,V,W,THETAX,THETAY,PHI,X(1),X(2),X(3)
120     FORMAT(/,'U=',F6.1,' MM     V=',F6.1,' MM     W=',F6.1,
       *' MM'/,'THETAX=',F6.2,' DEG     THETAY=',F6.2,' DEG     PHI='
       *,F6.2,' DEG',//'XC=',F6.1,'   YC=',F6.1,'   ZC=',F6.1/)
CCC
C   PL=LAT LOAD;PA=AXIAL LOAD;PC=LOAD IN CABLE
C   INITIAL LENGTH OF CABLE=4995 MM;LOAD TO END OF WEB=48 MM
CCC
        PL=-LOAD*((X(1)-0.)/(4995.+STROKE-X(2)+96.8))
        PA=-LOAD*((X(3)-48.)/(4995.+STROKE-X(2)+96.8))
        PC=SQRT(PL**2+PA**2+LOAD**2)
CCC
C   NOM VALUES NEGLECT 2ND ORDER EFFECTS
CCC
        MXNOM=-LOAD*LB/1000.
        TNOM=LOAD*E/1000.
        MX=-(LOAD*(LB-48.+X(3))-PA*X(2))/1000.
        MY=(PL*(LB-48.+X(3))-PA*X(1))/1000.
        T=(LOAD*X(1)-PL*X(2))/1000.
        LC=SQRT((4995.+STROKE-X(2)+96.8)**2+(X(1)-0.)**2
      *+(X(3)-48.)**2)
        WRITE(6,130)LOAD,PL,PA,PC,LC,MXNOM,MX,MY,TNOM,T
130     FORMAT('PV=',F6.2,' KN   PL=',F6.2,
       *' KN   PA=',F6.2,' KN   PC=',F6.2,' KN   LC=',F7.1,' MM'
       */'MXNOM=',F6.2,' KN*M   MX=',F6.2,' KN*M   MY=',F6.2,' KN*M'
       */'TNOM=',F6.2,' KN*M   T=',F6.2,' KN*M'//)
CCC
C   IF   END OF DATA FILE, STOP
```

```
CCC
        IF(LSN.EQ.NR)GO TO 1000
        GO TO 10
150     L=L+1
        GO TO 28
1000    STOP
        END

        SUBROUTINE FCN1(X,F,N,PAR)
        REAL X(3),F(3),PAR(20)
CCC
C   INTEGER NUMBERS REPRESENT INITIAL LVDT LENGTHS IN MM
CCC
        F(1)=(X(1)+1508.)**2+X(2)**2+X(3)**2-(PAR(11)+1508.)**2
        F(2)=X(1)**2+(X(2)+898.)**2+X(3)**2-(PAR(12)+898.)**2
        F(3)=X(1)**2+X(2)**2+(1348.-X(3))**2-(PAR(13)+1348.)**2
        RETURN
        END
        SUBROUTINE FCN2(X,F,N,PAR)
        REAL X(3),F(3),PAR(20)
        F(1)=(X(1)-100.)**2+(X(2)+895.)**2+X(3)**2-(PAR(14)+895.)**2
        F(2)=(X(1)-100.)**2+X(2)**2+(1349.-X(3))**2-(PAR(15)+1349.)**2
        F(3)=(X(1)-PAR(1))**2+(X(2)-PAR(2))**2+(X(3)-PAR(3))**2-10000.
        RETURN
        END
        SUBROUTINE FCN3(X,F,N,PAR)
        REAL X(3),F(3),PAR(20)
        F(1)=(X(1)+1508.)**2+(X(2)-100.)**2+X(3)**2-(PAR(16)+
       *1508.)**2
        F(2)=(X(1)-PAR(4))**2+(X(2)-PAR(5))**2+(X(3)-PAR(6))**2-20000.
        F(3)=(X(1)-PAR(1))**2+(X(2)-PAR(2))**2+(X(3)-PAR(3))**2-10000.
        RETURN
        END
        SUBROUTINE FCN4(X,F,N,PAR)
        REAL X(3),F(3),PAR(20)
        F(1)=(X(1)-PAR(1))**2+(X(2)-PAR(2))**2+(X(3)-PAR(3))**2-PAR(17)
        F(2)=(X(1)-PAR(4))**2+(X(2)-PAR(5))**2+(X(3)-PAR(6))**2-PAR(18)
        F(3)=(X(1)-PAR(7))**2+(X(2)-PAR(8))**2+(X(3)-PAR(9))**2-PAR(19)
        RETURN
        END
```

B.2 Program *FEDEFL*

```
CCCCCCCCCCCCCCCCCCC
CCCCCCCCCCCCCCCCCCC
CC
CC   Program   "FEDEFL"
CC
CC   Function:   to calculate deflections and rotations at fixed end and
CC                    those at the free end due to rigid body movement.
CC
CCCCCCCCCCCCCCCCCCC
CCCCCCCCCCCCCCCCCCC
CC
         REAL  LOAD,D(6)
C   CDEG=CONV FACTOR: RAD -> DEG
         CDEG=180./3.14159
         WRITE(6,2)
2        FORMAT('THIS PROGRAM CALCULATES DEFL & ROT AT THE FIXED END',/
        *'AND THE INDUCED DEFL & ROT AT THE FREE END',//
        *'***NOTE THAT DEFL ARE IN MM, AND ROT ARE IN DEGREES***'/)
C   M=COUNTER;LSN=LOAD SET NO.;NLC=NO.LOG.CHAN.;NSR=NO.SETS READ.
         M=0
5        READ(5,6)LSN,NLC,NSR
6        FORMAT(3I8)
         IF(M.GT.0)GO TO 8
C   EXECUTED IN FIRST CYCLE ONLY
         NR=NSR
         M=M+1
8        READ(5,10)LOAD,(D(J),J=1,6)
10       FORMAT(5E15.6/2E15.6)
         WRITE(6,15)LOAD,LSN
15       FORMAT(//' MTS LOAD=',F7.3,' KN',/1X,19('*')/,'(LSN=',I2,')'/)
         U=D(6)
         V=(D(1)+D(2))/2.
         W=-(D(3)+D(4))/2.
         THX=(ATAN((D(5)+W)/152.4))*CDEG
         THY=(ATAN((D(4)-D(3))/152.4))*CDEG
         PHI=(ATAN((D(2)-D(1))/222.))*CDEG
         UFREE=U+950.*SIN(THY/CDEG)
         VFREE=V-950.*SIN(THX/CDEG)
         WFREE=W
         WRITE(6,50)U,V,W,THX,THY,PHI,UFREE,VFREE,WFREE
50       FORMAT('U=',E9.3,'   V=',E9.3,'   W=',E9.3,/
        *'THX=',E9.3,'   THY=',E9.3,'   PHI=',E9.3,/
        *'UFREE=',E9.3,'   VFREE=',E9.3,'   WFREE=',E9.3)
         IF(LSN.EQ.NR)GO TO 1000
         GO TO 5
1000    STOP
         END
```

B.3 Program *GAUGE*

```
CCCCCCCCCCCCCCCCCCC
CCCCCCCCCCCCCCCCCCC
CC
CC   Program   "GAUGE"
CC
CC   Function:   to calculate stresses from strains based on mean
CC                    stress-strain curve.
CC
CCCCCCCCCCCCCCCCCCC
CCCCCCCCCCCCCCCCCCC
CC
         REAL  LOAD,STRAIN(15),SIGMA(15)
         E=203027.
         EST=5840.
         SIGY=320.6
C   M=COUNTER;LSN=LOAD  SET  NO.;NLC=NO.LOG.CHAN.;NSR=NO.SETS  READ.
         M=0
5        READ(5,6)LSN,NLC,NSR
6        FORMAT(3I8)
         IF(M.GT.0)GO  TO  8
C   EXECUTED  IN  FIRST  CYCLE  ONLY
         NR=NSR
         M=M+1
8        READ(5,10)LOAD,(STRAIN(J),J=1,15)
10       FORMAT(5E15.6/5E15.6/5E15.6/E15.6)
         WRITE(6,15)LOAD,LSN
15       FORMAT(//' MTS  LOAD=',F7.3,'  KN',/1X,19('*')/,'(LSN=',I2,')'/)
         DO  180  I=1,15
         EPS=STRAIN(I)
         CALL  STRESS  (EPS,SIG,E,EST,SIGY)
         SIGMA(I)=SIG
180     WRITE(6,200)I,SIGMA(I),STRAIN(I)
200     FORMAT('GAUGE  #',I2,':    ',
        *'STRESS  =',F7.1,'  MPA     STRAIN  =',E11.4)
         IF(LSN.EQ.NR)GO  TO  1000
         GO  TO  5
1000    STOP
         END

         SUBROUTINE  STRESS  (EPS,SIG,E,EST,SIGY)
C   WORK  WITH  POS  NUMBERS
         AEPS=ABS(EPS)
C   TRI-LINEAR  STRESS-STRAIN  CURVE
         IF(AEPS.LE.0.00158)SIG=AEPS*E
         IF(AEPS.GT.0.00158.AND.AEPS.LE.0.0116)SIG=SIGY
         IF(AEPS.GT.0.0116)SIG=SIGY+(AEPS-0.0116)*EST
C   ULT  STRESS=471  MPA
         IF(SIG.GT.471.)SIG=471.
C   COMPRESSIVE  STRESSES  NEG
         IF(EPS.LT.0.)SIG=-SIG
         RETURN
         END
```

B.4 Program *ROSETTE*

```
CCCCCCCCCCCCCCCCCCC
CCCCCCCCCCCCCCCCCCC
CC
CC   Program   "ROSETTE"
CC
CC   Function:   to calculate normal and shear stresses from strains based on
CC                    mean stress-strain curve.
CC
CCCCCCCCCCCCCCCCCCC
CCCCCCCCCCCCCCCCCCC
CC
         INTEGER  ROSET(10)
         REAL  NORMAL(10),SHEAR(10),LOAD,STRAIN(45)
         E=203027.
         G=E/2.6
         EST=5840.
         SIGY=320.6
C   M=COUNTER;LSN=LOAD  SET  NO.;NLC=NO.LOG.CHAN.;NSR=NO.SETS  READ.
         M=0
5        READ(5,6)LSN,NLC,NSR
6        FORMAT(3I8)
         IF(M.GT.0)GO  TO  8
C   EXECUTED  IN  FIRST  CYCLE  ONLY
         NR=NSR
         M=M+1
8        READ(5,10)LOAD,(STRAIN(L),L=16,42)
10       FORMAT(5E15.6/5E15.6/5E15.6/5E15.6/5E15.6/3E15.6)
         WRITE(6,15)LOAD,LSN
15       FORMAT(//'  MTS  LOAD=',F7.3,'  KN',/1X,19('*')/,'(LSN=',I2,')'/)
         J=16
         JJ=1
18       JP1=J+1
         JP2=J+2
         GAMZX=2.*STRAIN(JP1)-STRAIN(J)-STRAIN(JP2)
         SROOT=SQRT(((STRAIN(J)-STRAIN(JP2))/2.)**2+(GAMZX/2.)**2)
         EPS1=(STRAIN(J)+STRAIN(JP2))/2.+SROOT
         EPS2=(STRAIN(J)+STRAIN(JP2))/2.-SROOT
         IF(STRAIN(J).EQ.0..AND.STRAIN(JP2).EQ.0.)GO  TO  23
         THETAP=0.5*ATAN(GAMZX/(STRAIN(J)-STRAIN(JP2)))*(180./3.14159)
         GO  TO  25
23       THETAP=0.
25       GAM12=SQRT((STRAIN(J)-STRAIN(JP2))**2+GAMZX**2)
         DO  150  I=1,5
         IF(I.NE.1)GO  TO  50
         EPS=STRAIN(J)
         CALL  STRESS  (EPS,SIG,E,EST,SIGY)
         SIGZ=SIG
         GO  TO  150
50       IF(I.NE.2)GO  TO  60
         EPS=STRAIN(JP1)
         CALL  STRESS  (EPS,SIG,E,EST,SIGY)
         SIG45=SIG
         GO  TO  150
60       IF(I.NE.3)GO  TO  70
         EPS=STRAIN(JP2)
         CALL  STRESS  (EPS,SIG,E,EST,SIGY)
         SIGX=SIG
         GO  TO  150
70       IF(I.NE.4)GO  TO  80
         EPS=EPS1
         CALL  STRESS  (EPS,SIG,E,EST,SIGY)
         SIG1=SIG
         GO  TO  150
```

```
80      EPS=EPS2
        CALL STRESS (EPS,SIG,E,EST,SIGY)
        SIG2=SIG
150     CONTINUE
        TAUZX=GAMZX*G
        IF(TAUZX.GT.185.1)TAUZX=185.1
        IF(TAUZX.LT.-185.1)TAUZX=-185.1
        TAU12=GAM12*G
        IF(TAU12.GT.185.1)TAU12=185.1
        IF(TAU12.LT.-185.1)TAU12=-185.1
        WRITE(6,200)J,SIGZ,SIG45,SIGX,SIG1,SIG2,TAUZX,TAU12,THETAP
200     FORMAT('##ROSETTE ',I2,'##',/
       *'SIGZ  =',F7.1,' MPA'/,
       *'SIG45=',F7.1,' MPA'/,
       *'SIGX  =',F7.1,' MPA'/,
       *'SIG1  =',F7.1,' MPA'/,
       *'SIG2  =',F7.1,' MPA'/,
       *'TAUZX=',F7.1,' MPA'/,
       *'TAU12=',F7.1,' MPA'/,'THETAP=',F6.1,' DEGREES'/)
        NORMAL(JJ)=SIGZ
        SHEAR(JJ)=TAUZX
        ROSET(JJ)=J
        IF(J.EQ.40)GO TO 500
        J=J+3
        JJ=JJ+1
        GO TO 18
500     WRITE(6,550)
550     FORMAT('SUMMARY',/7('-'))
        DO 700 K=1,9
        WRITE(6,600)ROSET(K),NORMAL(K),SHEAR(K)
600     FORMAT('ROSETTE ',I2,' -- NORMAL STRESS=',F7.1,
       *' MPA   &   SHEAR STRESS=',F7.1,' MPA')
700     CONTINUE
        IF(LSN.EQ.NR)GO TO 1000
        GO TO 5
1000    STOP
        END

        SUBROUTINE STRESS (EPS,SIG,E,EST,SIGY)
C   WORK WITH POS NUMBERS
        AEPS=ABS(EPS)
C   TRI-LINEAR STRESS-STRAIN CURVE
        IF(AEPS.LE.0.00158)SIG=AEPS*E
        IF(AEPS.GT.0.00158.AND.AEPS.LE.0.0116)SIG=SIGY
        IF(AEPS.GT.0.0116)SIG=SIGY+(AEPS-0.0116)*EST
C   ULT STRESS=471 MPA
        IF(SIG.GT.471.)SIG=471.
C   COMPRESSIVE STRESSES NEG
        IF(EPS.LT.0.)SIG=-SIG
        RETURN
        END
```

APPENDIX C - COMPUTER PROGRAM *MTINT*

```
CCCCCCCCCCCCCCCCCCC
CCCCCCCCCCCCCCCCCCC
CC
CC   Program   "MTINT"
CC
CC
CC   GENERATION OF MOMENT-TORQUE INTERACTION
CC   DIAGRAMS FOR I-SHAPED STEEL BEAMS
CC
CC   Note:   I/P unit 4 (SECDATA) refers to a data file (not listed)
CC             with properties of all I-shaped beams tabulated in
CC             the CISC handbook (CISC, 1984).
CC             O/P unit 7 is for input to a plotting program.
CC
CC      M/Mp vs T/(Tsh+Twp)
CC      M/Mp vs T/(Tshu+Twu)
CC
CCCCCCCCCCCCCCCCCCC
CCCCCCCCCCCCCCCCCCC
CC
         DIMENSION STSHP(5)
         REAL L,M,MF,MM,MP,MMP,L1,L2,LWIDTH
         INTEGER EC,A,ZX,ZXEXP
         CALL FTNCMD('ASSIGN 4=SECDATA',16)
         WRITE(6,10)
    10  FORMAT(/'GENERATION OF MOMENT-TORQUE INTERACTION'/
        *'DIAGRAM FOR I-SHAPED STEEL BEAMS'/)
         WRITE(7,12)
    12  FORMAT('0.0,0.2,1.0,12.7'/,'0.0,0.2,1.0,12.7')
    15  READ(5,20)A
    20  FORMAT(I2)
         IF(A.EQ.0)GO TO 1000
         NN=0
         READ(5,25)J
    25  FORMAT(I2)
         IF(J.EQ.1)GO TO 27
         READ(5,28)B,D,T,W,L,EC,LT,X
    28  FORMAT(5F7.1,2I2,F7.1)
         GO TO 32
    27  READ(5,30)STSHP(1),STSHP(2),STSHP(3),L,EC,LT,X
    30  FORMAT(3A4,F7.1,2I2,F7.1)
    32  READ(5,35)N
    35  FORMAT(I3)
         WRITE(7,37)N
    37  FORMAT(I3,',5,0,1,1,0.1,1')
         IF(J.EQ.2)GO TO 38
C
C   READ IN SECTION PROPERTIES
C
         CALL RREAD(STSHP,ZX,ZXEXP,ADEPTH,BDEPTH,LWIDTH,RWIDTH,T,W)
         D=ADEPTH+BDEPTH
         B=LWIDTH+RWIDTH
    38  L1=0.653*L
         L2=0.586*L
         B1=B/2.
         MP=(W*(D/2.-T)**2)+(B*T*(D-T))
C
C   CALCULATE ST. VENANT (SAND HEAP) TORSION
C
         CALL STV(T,B,W,D,TSH)
C
C   CALCULATE WARPING TORSION DEPENDING ON
```

```
C   LOAD TYPE AND END CONDITIONS
C
         TWP1=B**2*T*(D-T)
         IF(LT.NE.1.OR.EC.NE.1)GO TO 40
         TWP=TWP1/L
         GO TO 85
    40   IF(LT.NE.1.OR.EC.NE.2)GO TO 45
         TWP=TWP1*3./(2.*L)
         GO TO 85
    45   IF(LT.NE.1.OR.EC.NE.3)GO TO 50
         TWP=TWP1*5./(4.*L)
         GO TO 85
    50   IF(LT.NE.1.OR.EC.NE.4)GO TO 55
         TWP=TWP1/(2.*L)
         GO TO 85
    55   IF(LT.NE.2.OR.EC.NE.1)GO TO 60
         TWP=TWP1/(4.*X)
         GO TO 85
    60   IF(LT.NE.2.OR.EC.NE.2)GO TO 65
         TWP=TWP1*(2.+L/X)/(4.*L)
         GO TO 85
    65   IF(LT.NE.2.OR.EC.NE.3)GO TO 75
         IF(X.LT.L1)GO TO 68
         TWP=TWP1/(4.*(L-X))
         GO TO 85
    68   IF(X.LE.L2)GO TO 70
         TWP=TWP1*(-X**2+2.*L*X+2.*L**2)/(4.*X**2*(3.*L-X))
         GO TO 85
    70   TWP=TWP1*(2.*L**2+2.*L*X-X**2)/(4.*L*X*(2.*L-X))
         GO TO 85
    75   TWP=TWP1/(4.*X)
C
C   CALCULATE TOTAL PLASTIC TORQUE WITHOUT MOMENT
C
    85   TP=TWP+TSH
         IF(J.EQ.2)GO TO 87
         WRITE(6,86)STSHP(1),STSHP(2),STSHP(3)
    86   FORMAT(/,75('-'),//'SECTION =',3A4)
         GO TO 89
    87   WRITE(6,88)B,D,T,W
    88   FORMAT(/,75('-'),//'B =',F7.1,' MM'/,'D =',F7.1,' MM'/,
        *'T =',F7.1,' MM'/,'W =',F7.1,' MM')
    89   WRITE(6,90)L,EC,LT,X
    90   FORMAT('LENGTH = ',F7.1,' MM'/,
        *'END CONDITION CODE = ',I2/,'LOAD TYPE CODE = ',I2/,
        *'DISTANCE FROM LOAD TO SUPPORT WITH FEWEST DEGREES OF',
        *' FREEDOM = ',F7.1,' MM'/)
         WRITE(6,92)MP,TSH,TWP,TP
    92   FORMAT('PLASTIC MOMENT/SIGMA YIELD =',E9.4,' MM**3'/,
        *'SAND HEAP TORSION/SIGMA YIELD =',E9.4,' MM**3'/,
        *'WARPING PLASTIC TORSION/SIGMA YIELD =',E9.4,' MM**3'/,
        *'TOTAL PLASTIC TORSION/SIGMA YIELD =',E9.4,' MM**3'/)
C
C   IF ENTERING MOMENTS EXECUTE SECOND HALF OF PROGRAM
C   IF ENTERING TORSION EXECUTE FIRST HALF OF PROGRAM
C
         IF(A.EQ.2)GO TO 500
    94   READ(5,95)TTP
    95   FORMAT(F6.3)
         NN=NN+1
         TOR=TP*TTP
         VF=(TOR-TSH)/(D-T)
C
C   TO ELIMINATE ROUND OFF ERRORS IN LOCATING POINT
C   WHERE WARPING TORSION BEGINS TO ACT
```

```
C
      TOR1=TOR-TSH
      TOR2=TOR/1000.
      IF(TOR1.LT.TOR2)VF=0.
C
      IF(VF.LE.0.)GO TO 360
C
C   CALCULATE FLANGE MOMENTS DEPENDING ON
C   LOAD TYPE AND END CONDITIONS
C
      IF(LT.NE.1.OR.EC.NE.1)GO TO 100
      MF=VF*L/4.
      GO TO 350
  100 IF(LT.NE.1.OR.EC.NE.2)GO TO 120
      MF=VF*L/6.
      GO TO 350
  120 IF(LT.NE.1.OR.EC.NE.3)GO TO 140
      MF=VF*L/5.
      GO TO 350
  140 IF(LT.NE.1.OR.EC.NE.4)GO TO 160
      MF=VF*L/2.
      GO TO 350
  160 IF(LT.NE.2.OR.EC.NE.1)GO TO 180
      MF=VF*X
      GO TO 350
  180 IF(LT.NE.2.OR.EC.NE.2)GO TO 200
      MF=(VF*X*L)/(L+2.*X)
      GO TO 350
  200 IF(LT.NE.2.OR.EC.NE.3)GO TO 280
      IF(X.LT.L1)GO TO 220
      MF=VF*(L-X)
      GO TO 350
  220 IF(X.LE.L2)GO TO 240
      MF=(VF*X**2*(3.*L-X))/(-X**2+2.*L*X+2.*L**2)
      GO TO 350
  240 MF=VF*L*X*(2.*L-X)/(2.*L**2+2.*L*X-X**2)
      GO TO 350
  280 IF(LT.NE.2.OR.EC.NE.4)GO TO 990
      MF=VF*X
  350 CALL MOMENT(T,B,MF,D,W,MP,MMP,B1)
      GO TO 400
  360 MMP=1.0
  400 WRITE(6,410)TTP,MMP
  410 FORMAT('TORQUE/FULLY PLASTIC TORQUE =',F6.3,5X,
     *'MOMENT/FULLY PLASTIC MOMENT =',F6.3)
      WRITE(7,415)TTP,MMP
  415 FORMAT(F5.3,',',F5.3)
      IF(NN.EQ.N)GO TO 15
  420 GO TO 94
  500 READ(5,510)MMP
  510 FORMAT(F6.3)
      NN=NN+1
      M=MP*MMP
      MM=B/2.-(M-W*(D/2.-T)**2)/(2.*T*(D-T))
      IF(MM.GE.B1)GO TO 800
      IF(MM.LE.0.)MM=0.
      MF=MM*T*(B-MM)
C
C   CALCULATE FLANGE SHEARS DEPENDING ON
C   LOAD TYPE AND END CONDITIONS
C
      IF(LT.NE.1.OR.EC.NE.1)GO TO 600
      VF=MF*4./L
      GO TO 850
  600 IF(LT.NE.1.OR.EC.NE.2)GO TO 620
```

```
      VF=MF*6./L
      GO TO 850
  620 IF(LT.NE.1.OR.EC.NE.3)GO TO 640
      VF=MF*5./L
      GO TO 850
  640 IF(LT.NE.1.OR.EC.NE.4)GO TO 660
      VF=MF*2./L
      GO TO 850
  660 IF(LT.NE.2.OR.EC.NE.1)GO TO 680
      VF=MF/X
      GO TO 850
  680 IF(LT.NE.2.OR.EC.NE.2)GO TO 700
      VF=MF*(L+2.*X)/(L*X)
      GO TO 850
  700 IF(LT.NE.2.OR.EC.NE.3)GO TO 780
      IF(X.LT.L1)GO TO 720
      VF=MF/(L-X)
      GO TO 850
  720 IF(X.LE.L2)GO TO 740
      VF=MF*(-X**2+2.*L*X+2.*L**2)/((X**2)*(3.*L-X))
      GO TO 850
  740 VF=MF*(2.*L**2+2.*L*X-X**2)/(L*X*(2.*L-X))
      GO TO 850
  780 IF(LT.NE.2.OR.EC.NE.4)GO TO 990
      VF=MF/X
      GO TO 850
  800 TTP=1.0
      GO TO 900
  850 CALL TORQUE(VF,D,T,TSH,TTP,TP)
  900 WRITE(6,910)MMP,TTP
  910 FORMAT('MOMENT/FULLY PLASTIC MOMENT =',F6.3,5X,
     *'TORQUE/FULLY PLASTIC TORQUE =',F6.3)
      WRITE(7,950)TTP,MMP
  950 FORMAT(F5.3,',',F5.3)
      IF(NN.EQ.N)GO TO 15
      GO TO 500
  990 WRITE(6,995)
  995 FORMAT('ERROR IN LOAD TYPE OR END CONDITION CODE')
 1000 STOP
      END
C
C
C   SUBROUTINE FOR CALCULATING MOMENT/FULLY PLASTIC MOMENT
C   FROM FLANGE MOMENT
C
C
      SUBROUTINE MOMENT(T,B,MF,D,W,MP,MMP,B1)
      REAL MF,MM,MP,MMP
      R=(T*B)**2-4.*T*MF
      IF(R.LT.0.)GO TO 200
      R1=SQRT(R)
      MM=(R1+T*B)/(2.*T)
      IF(MM.LE.B1)GO TO 100
      MM=(T*B-R1)/(2.*T)
  100 IF(MM.LT.0.)GO TO 300
      M=(((B-2.*MM)*T)*(D-T))+((D/2.-T)**2)*W
      MMP=M/MP
      GO TO 1000
  200 WRITE(6,250)
  250 FORMAT('ERROR IN T, B, OR MF')
      STOP
  300 WRITE(6,350)
  350 FORMAT('ERROR IN DATA - NEGATIVE TORQUE OBTAINED')
      STOP
 1000 RETURN
```

```
      END
C
C
C   SUBROUTINE TO CALCULATE TORQUE/FULLY PLASTIC TORQUE
C   FROM FLANGE SHEAR
C
C
      SUBROUTINE TORQUE(VF,D,T,TSH,TTP,TP)
      TOR=VF*(D-T)+TSH
      TTP=TOR/TP
      RETURN
      END
C
C
C   SUBROUTINE TO CALCULATE SAND HEAP TORSION
C
C
      SUBROUTINE STV(T,B,W,D,TSH)
      HF=0.5*T/SQRT(3.)
      VF=HF*(T**2/3.+(B-T)*T/2.)
      HW=W/(2.*SQRT(3.))
      VW=HW*W*(D-2.*T)/2.+HW*W**2/6.
      TSH=2.*(2.*VF+VW)
      RETURN
      END
C
C   SUBROUTINE TO READ IN SECTION PROPERTIES
C
      SUBROUTINE RREAD(STSHP,ZX,ZXEXP,ADEPTH,BDEPTH,LWIDTH,RWIDTH,T,W)
      INTEGER BLANK1,BLANK2,COUNTR,CSAREA,CW,CWEXP,DEPTH,DUMY,
     &          DEPTH,SEC,SECT,SHAPE,SST1,SST2,STSHP,SX,SXEXP,SY,
     &          SYEXP,TYPE1,USAGE,USE,YES,ZX,ZXEXP,ZY,ZYEXP
C
      REAL LWIDTH
      DIMENSION SECT(5),SST1(10),SST2(10),STSHP(5)
      REWIND 4
      III = 0
 3500 CONTINUE


      II = 0
      III = III + 1
 4000 CONTINUE
      II = II + 1
      READ(4,20)BLANK1,SECT(1),SECT(2),SECT(3)
   20 FORMAT(I2,3A4)
C
      IF(STSHP(1).NE.SECT(1))GO TO 3500
      IF(STSHP(2).NE.SECT(2))GO TO 3500
      IF(STSHP(3).NE.SECT(3))GO TO 3500
C
C
      BACKSPACE 4
CCCCCCCCCCCCCCCCCCCCCCCCCCCCCCCCCCCCCCCCCCCCCCCCCCCCCCCCCCCCCCCCCCCC
C
C      Next, all of the geometric data for the standard steel shape
C      is read into storage.  Depending on the variables ID and
C      BLANK1, one of four possible READ routes is followed.
C
C
      IF(BLANK1.EQ.0)GO TO 5200
      IF(BLANK1.EQ.1)GO TO 5600
C
CCCCCCCCCCCCCCCCCCCCCCCCCCCCCCCCCCCCCCCCCCCCCCCCCCCCCCCCCCCCCCCCCCCC
C
```

```
 5200  READ(4,22)BLANK1,SECT(1),SECT(2),SECT(3),
      &              COUNTR,ID,SHAPE,USE,
      &              CSAREA,MASS,IX,IXEXP,SX,SXEXP,ZX,ZXEXP,IY,IYEXP,
      &              SY,SYEXP,ZY,ZYEXP,JJ,JEXP,CW,CWEXP,SST1(1),SST1(2),
      &              SST1(3),SST1(4)
    22  FORMAT(I2,3A4,A1,2I2,I1,2I6,I3,I2,I3,I2,I3,I2,I3,I2,I3,I2,I3,
      &           I2,I3,I2,I3,I2,4A2)
C
        READ(4,30)DEPTH,ADEPTH,BDEPTH,LWIDTH,RWIDTH,T,W,RADMIN,RADMAX,
      &               KK,K1,SUAREA,BLANK2,SST2(1),SST2(2),SST2(3),SST2(4)
    30  FORMAT(I5,8F5.1,2I5,F5.2,I12,4A2)
        RMASS = 0.0
        RETURN
C
CCCCCCCCCCCCCCCCCCCCCCCCCCCCCCCCCCCCCCCCCCCCCCCCCCCCCCCCCCCCCCCCCCCCCCCCCCC
C
 5600  READ(4,50)BLANK1,SECT(1),SECT(2),SECT(3),
      &              COUNTR,ID,SHAPE,USE,
      &              CSAREA,RMASS,IX,IXEXP,SX,SXEXP,ZX,ZXEXP,IY,IYEXP,
      &              SY,SYEXP,ZY,ZYEXP,JJ,JEXP,CW,CWEXP,SST1(1),SST1(2),
      &              SST1(3),SST1(4)
    50  FORMAT(I2,3A4,A1,2I2,I1,I6,F6.4,I3,I2,I3,I2,I3,I2,I3,I2,I3,I2,I3,
      &           I2,I3,I2,I3,I2,4A2)
C
        READ(4,30)DEPTH,ADEPTH,BDEPTH,LWIDTH,RWIDTH,T,W,RADMIN,RADMAX,
      &               KK,K1,SUAREA,BLANK2,SST2(1),SST2(2),SST2(3),SST2(4)
        MASS = 0
        RETURN
C
CCCCCCCCCCCCCCCCCCCCCCCCCCCCCCCCCCCCCCCCCCCCCCCCCCCCCCCCCCCCCCCCCCCCCCCCCCC
C
        END
```